THERMODYNAMIC ANALYSIS OF SOLAR OPERATED COMBINED POWER AND EJECTOR REFRIGERATION CYCLE USING ECOFRIENDLY REFRIGERANTS

A Thesis submitted in partial fulfillment of the requirements for the award the degree of

DOCTOR OF PHILOSOPHY

IN

(MECHANICAL ENGINEERING)

By

DEVENDRA KUMAR GUPTA

(2K12/Ph.D.ME/10)

Under the Supervision of

Prof. RAJESH KUMAR

(Professor)

Mechanical Engineering Department

Delhi Technological University

Prof. NAVEEN KUMAR

(Professor)

Mechanical Engineering Department

Delhi Technological University

MECHANICAL ENGINEERING DEPARTMENT

DELHI TECHNOLOGICAL UNIVERSITY

Delhi- 110042, INDIA

OCTOBER, 2017

ACKNOWLEDGEMENTS

I express my deep gratitude to my supervisors Prof. Naveen Kumar, Professor, and Prof. Rajesh Kumar, Professor Department of Mechanical Engineering, Delhi Technological University, Delhi for assisting me in identifying and formulating the research problem. Despite their busy schedule, Prof. Naveen Kumar and Prof. Rajesh Kumar were always available for the advice and discussions. Their valuable comments and advice gave me the confidence to overcome the challenges in formulation of this PhD thesis work.

I express my special thanks to Prof. R. S. Mishra, Head of Mechanical Engineering Department, DTU, for their continuous inspiration and support during this research work. I would like to thank all the faculty members of DTU guiding me most of the occasion, resulting in successful completion of my PhD thesis work.

I would like to thank my friends, who have supported me through their encouragement, support and friendship during this period of thesis research work. I would like to thank to all those who directly and indirectly supported me in carrying out this thesis work successfully.

Last, but not the least by any means, in this auspicious moment, I shall forever remember the contribution of my elder brother, younger brother, sisters, wife and, daughter for their endless inspiration, support and guidance during entire period of the work with great patience and understanding.

Devendra Kumar Gupta
(2K12/Ph.D.ME/10)

DECLARATION

I hereby declare that the thesis entitled **"THERMODYNAMIC ANALYSIS OF SOLAR OPERATED COMBINED POWER AND EJECTOR REFRIGERATION CYCLE USING ECOFRIENDLY REFRIGERANTS"** is an original work carried out by me under the supervision of Prof. Naveen Kumar, Professor and Prof. Rajesh Kumar, Professor, Department of Mechanical Engineering, Delhi Technological University, Delhi. This thesis has been prepared in conformity with the rules and regulations of the Delhi Technological University, Delhi. The research work reported and results presented in the thesis have not been submitted either in part or full to any other university or institute for the award of any other degree or diploma.

Devendra Kumar Gupta
(2K12/Ph.D.ME/10)
Research Scholar
Mechanical Engineering Department
Delhi Technological University,
Delhi-110042

CERTIFICATE

This is to certify that the work embodied in the thesis entitled **"THERMODYNAMIC ANALYSIS OF SOLAR OPERATED COMBINED POWER AND EJECTOR REFRIGERATION CYCLE USING ECOFRIENDLY REFRIGERANTS"** by **Devendra Kumar Gupta, (Roll No: 2K12/Ph.D.ME/10)** in partial fulfillment of requirements for the award of Degree of **DOCTOR OF PHILOSOPHY in Mechanical Engineering**, is an authentic record of student's own work carried by him under our supervision.

This is also certified that this work has not been submitted to any other Institute or University for the award of any other diploma or degree.

Prof. RAJESH KUMAR
(Professor)
Mechanical Engineering Department
Delhi Technological University

Prof. NAVEEN KUMAR
(Professor)
Mechanical Engineering Department
Delhi Technological University

ABSTRACT

Development of innovative thermodynamic cycles is important for the efficient utilization of low-temperature heat sources such as solar, geothermal, and waste heat sources. This work is an investigation of a novel concept to produce power and cooling with the energy contained in low-temperature, thermal resources. Exergy destructions within the system and exergy losses to environment are investigated to determine thermodynamic inefficiencies in the system and to assist in guiding future improvements in the system.

In this study, thermodynamic analysis of a solar operated combined power and ejector refrigeration cycle has been carried out to evaluate the performance of the cycle using R141b refrigerants as working fluid and duratherm 600 oil as the heat transfer fluid, which produces cooling and power simultaneously. The effect of various parameters as the turbine inlet pressure (0.9MPa-1.3MPa), evaporator temperature (262K-270K), condenser temperature (297K-303K), and extraction ratio (0.2-0.8) on the performance of the cycle (the net power output, refrigeration output, first law efficiency and second law efficiency) along with the exergy destruction in its various components is evaluated. The results show that the exergy loss is biggest in central receiver and heliostat which is around 52.5% and 25% respectively. Exergy losses/destruction is observed in the HRVG, ejector, and turbine is 5.3%, 2.6% and 1.6% respectively, other components of the cycle is less than unity.

A Parametric study has been carried out to analyses the effect of some influenced parameters such as turbine expansion ratio, driving pressure ratio, and compression pressure ratio on the performance (entrainment ratio, net power output,

refrigeration output, first law and second law efficiency) of the solar driven combined power and ejector cooling cycle with ecofriendly refrigerants (R290, R152a, R134a, and R717) as working substance. It is observed that the turbine expansion ratio, driving pressure ratio, and compression pressure ratio have significant effect on the net power output, refrigeration output, entrainment ratio, first law efficiency and second law efficiency. The results also show that at high turbine expansion ratio the performance of R290 and R152a is better than that of other refrigerants, at high compression ratio the performance of R717 and R134a shows better than that of R290 and R152a, and at high driving pressure ratio R290 and R134a gives better performance. Therefore the performance of the system depends upon the type of refrigerant used and operating conditions.

Nowadays some of the refrigeration industries required double effect cooling along with power. In this context, an ejector organic Rankine cycle (EORC) integrated with a triple pressure level vapour absorption system (TPLAS) based on parabolic trough collector (PTC) solar field was thermodynamically analyzed. This cycle produces power and cooling effects at two evaporators at two different temperatures using single source of solar energy. This system meets out the demand of electricity, space air-conditioning and preservation of fruits & vegetables in cold storage. Results of exergy distribution show that 89.5% of the input exergy is destroyed/losses due to irreversibilities/losses from various components, 10.5% is available as exergy output.

There are many applications where simultaneously power and cooling at different temperatures is required. In this context, recently a PTC (parabolic trough

collector) field based double ejector organic cycle (DEORC) using refrigerant R141b as working fluid and Therminol VP1 as heat transfer fluid is presented and thermodynamically analyzed. This cycle produces power and cooling at two different temperatures by using single source of solar energy. Thermal storage tanks are also used to store the thermal energy from the Sun which provides the continuous power and cooling effect during insufficient solar radiation. Parametric analyses of DEORC and EORC show that inlet temperature and pressure of turbine at various extraction ratios has the significant effect on first law efficiency & second law efficiency and cooling to power ratio of this system. With the addition of ejector in EORC the first law efficiency increases from 11.43% to 11.85% while second law efficiency decreases from 10.44% to 9.785%.

TABLE OF CONTENTS

LIST OF FIGURES

LIST OF TABLES

NOMENCLATURES

A_p	Aperture area (m^2)
ABS	Absorber
C	Condenser
CSP	Concentrating solar power
DEORC	Double ejector organic Rankine cycle
E	Energy
EORC	Ejector organic Rankine cycle
ERC	Ejector refrigeration cycle
X	Exergy
EJ	Ejector
G1	Heat recovery vapor generator (HRVG)
G2	Generator of TPLAS
G_b	Solar beam radiation (SBR) (kWm^{-2})
h	Specific enthalpy ($kJ\ kg^{-1}$)
HE	Heat exchanger
HRVG	Heat recovery vapor generator
HTF	Heat transfer fluid (Therminol VP1)
HTV	High temperature vessel

I	Direct normal irradiance (kWm^{-2})
LTV	Low temperature vessel
Oil	Heat transfer oil (Duratherm600)
P	Pressure (MPa)
PTC	Parabolic trough collector
R	Extraction ratio
s	Specific entropy ($kJ\ kg^{-1}K^{-1}$)
System1	Ejector Organic Rankine cycle
System2	Ejector Organic Rankine cycle integrated with a triple pressure level vapour absorption system
T	Absolute temperature (K)
TES	Thermal energy storage
T_i	Inlet temperature of HTF to PTC field (K)
T_o	Outlet temperature of HTF from PTC field (K)
TPLAS	Triple pressure level absorption system
TV	Throttle valve
VARC	Vapour absorption refrigeration cycle
$\dot{E}$	Energy rate (kW)
$\dot{X}$	Exergy rate (kW)
$\dot{Q}$	Heat transfer rate (kW)
$\dot{Q}_E$	Refrigeration output in the evaporator (kW)

$\dot{Q}_{Solar}$	Solar energy input (kW)
$\dot{W}_{net}$	Work output/ net power output (kW)
$\dot{m}$	Mass flow rate (kg s^{-1})

Greek symbols

μ	Entrainment ratio
θ	Incidence angle
τ	$\text{Turbine expansion ratio} = \frac{\text{Turbine inlet pressure}}{\text{Turbine exit pressure}}$
σ	$\text{Driving pressure ratio} = \frac{\text{Turbine extraction pressure}}{\text{Ejector exit pressure}}$
ρ	Cooling to Power ratio
λ	$\text{Compression pressure ratio} = \frac{\text{Condenser pressure}}{\text{Evaporator pressure}}$
ε	Work to refrigeration ratio
ε_x	Work to exergetic refrigeration ratio
η_E	Energy efficiency/First law efficiency (%)
η_x	Exergy efficiency//Second law efficiency (%)

Subscript

CR	Central receiver
d	Diffuser
D	Destruction
E	Evaporator

$\mathbf{e}_1$	Evaporator 1
$\mathbf{e}_2$	Evaporator 2
f	Refrigerant fluid
m	Mixing chamber
n	Nozzle
n_1	Inlet of nozzle
n_2	Outlet of nozzle
P	Pump
p_f	Primary flow
s	Isentropic process
s_f	Secondary flow
T	Turbine
w	Water
1, 2, 3…… a, b, c ….	State points

CHAPTER 1

INTRODUCTION AND LITERATURE REVIEW

1.1 Introduction

Energy is a life blood of civilization and key for economic growth of every nation. The energy demand for producing power and cooling applications are increasing continuously due to increase in the energy requirements for industries, office campuses, institutions. In India, the increase in huge energy demand for industries, institutions, office complexes, commercial establishments etc. have resulted in higher consumption of conventional energy e.g. coal, fossil fuel [1,2], as well as increasing the greenhouse gas (GHG) emission and negative impact of climate change. To meet the higher energy demand, renewable energy sources like solar thermal energy is one of the best options to operate thermally driven power and cooling systems in place of conventional system [3]. The average intensity of Direct normal irradiation (DNI) received in most of the parts on India is 4-5.5 kWh/m^2/day [4]. Solar energy can play an important role in generating power and refrigeration without concerning the cost as it is free natural resources, clean widely available renewable energy. Posed menace for these types of solar assisted cooling techniques is its initial capital cost that is required for its installation, however its operational costs are quite lower than the conventional ones.

World now is severely striving to get a cleaner and healthier environment, for which the fossil fuels are intimidating danger, which directly relates human kind. The advent of technologies using solar energy is helping from the problems for the effects of fossil fuels. More and more minds of researchers are getting pooled and drained towards the search of solar driven cooling technologies like - solar ejector refrigeration, and solar driven combined power cycles [5, 6].

Recently, modification in the elementary technology for CSP has been done worldwide that convert the solar energy to high temperature heat for power production [7, 8, and 9]. The development of CSP and its influence over the market in global scenario is suffering for the very fact that the solar irradiation is not constant, it

fluctuates throughout the day. So there comes the difference in the value of calculated power output to the actual output. Researchers did find that this particular problem can be tackled or rather the performance of the CSP could be elevated by the use of Thermal Energy Storage systems (TES). This system stores the thermal energy from sun throughout the day and releases the same stored energy when there is hardly or no sunshine.

Vapour compression system has its impact directly on the decaying of the protective layer of ozone which is having irreparable loss to the mankind and to the planet earth. The depletion of the ozone layer is manoeuvring us to a mammoth recurring effect of global warming, which probably everyone on this planet needs to give a thought. These conditions exigently drive the advent of cooling techniques through solar radiation like solar air conditioning/ refrigeration systems. These systems rather use the refrigerants having lesser ODP and GWP [10, 11].Conventional vapour compression systems has a major disadvantage of its moving parts (frictional losses & need for lubricating it), whereas the ejector system suffice all the conditions that are not preceded by the vapour compression system. It also has certain merits in terms of low operating, installation and maintenance cost. It also comes with a promising usage of new and wide range of eco-friendly refrigerants. In addition these systems are heat operated. Therefore combined power and cooling cycles can be operated by low temperature heat sources like waste heat from industries, solar heat etc. An ejector cooling system can be made a practicable and economically feasible option by using of low temperature heat sources. Similarly vapour absorption refrigeration system has unique advantages of being operated on solar heat and on refrigerants having zero ODP and GWP as well as of high reliability and simplicity.

Energy utilization is improved with the use of combined power and refrigeration cycles, which produce power and cooling simultaneously. Fuel consumption is reduced in these cycles as compared to the separate power and cooling generation cycles [12]. In such a way the efficiency of the system improves when both cooling and power are required.

The research work pre-cursorily dedicates to the immaculate severity of losing all the natural fossil fuels and its detrimental impact on environmental health. In the **second chapter** of the thesis, the solar operated ejector cooling and power cycle using R141b is thermodynamically analyzed.

A Parametric study has been conducted to analyse the effect of some constraints on the performance of the solar operated ejector cooling and power cycle with ecofriendly refrigerants (R290, R152a, R134a, and R717) as working substance in the **third chapter** of the thesis. The proposed cycle produces both power and cooling simultaneously using single source of solar energy.

Most of the refrigeration industries required double effect cooling along with power. In this context, an ejector organic Rankine cycle (EORC) integrated with a triple pressure level vapour absorption system (TPLAS) based on parabolic trough collector (PTC) solar field is proposed and thermodynamically analyzed in the **fourth chapter** of the thesis. The proposed cycle now uses a single heat source probably a solar concentrator heating arrangement, and with the utilization of the same it could now give us power and cooling at two different evaporators and different temperatures. This system meets out the demand of electricity, space air-conditioning and preservation of fruits & vegetables in cold storage. The performance of EORC and proposed system is also compared on the basis of energy and exergy methodology.

There are many applications where simultaneously power and cooling at different temperatures is required. In this context, recently a PTC (parabolic trough collector) field based double ejector organic cycle (DEORC) using refrigerant R141b as working fluid and Therminol VP1 as heat transfer fluid is presented and thermodynamically analyzed in the **fifth chapter** of the thesis. The solar irradiation is not constant it fluctuates, hence some method is needed to be charted out which can store the thermal energy from sun while the value of radiant energy is at its peak, and then can be utilized back when the energy falling on the concentrator is not enough, thus the usage of thermal storage found its way in my system as well. The performance of EORC and DEORC is also compared on the basis of energy and

exergy methodology. The proposed system can be considered as dual-evaporator cooling system which provides wide range of cooling along with power.

It is well known that the method used for evaluating the performance of energy conversion system is 1^{st} law of thermodynamic analysis, which is based upon the energy balance methodology for the components. First law analyses have no provision for computing the quality of heat and also cannot account for the work lost in the process. Due to the energy crisis, attempt for efficiency improvement have directed to revamp or reconsider this method by which power and cooling systems are analyzed, thus the performance estimation of a thermodynamic system based on 1^{st} law methodology is insufficient, and more significant estimation must include second law methodology. 2^{nd} law (exergy) analyses identify the system components that are accountable for losses and hence it provides the ranking among the components, which assist to select the component of the system that should be repaired or changed first to improve the performance.

1.2 Literature review

As the depletion of conventional energy sources is going on and due to the use of fossil fuel for producing the power causes the emissions of green-house gases like CO_2, CO, NOx etc. which results in global warming. More woes are being added by our conventional cooling systems which emit refrigerant gases like CFCs which are high in GWP & ODP.

Since the last few decades scientists did carry out enormous research on the alternative technologies which can be a simile to our natural fossil fuels and also to cut down on greenhouse effect by actually reducing the carbon emission. Solar energy also affects the convective ambience creating currents that fuels the air to be wind; hence the wind energy is a derivative of crude solar energy. Not only on winds, it also affects the formation of tides and we could then materialize the energy as tidal energy [13].

The advantage of solar energy than other form of energy is that it is freely available, clean, and environmental friendly. High capacity of thermal energy can be

transferred to the heat transfer fluid using solar thermal technologies like - solar power tower, paraboloid dish, parabolic trough collector and linear Fresnel reflectors. Parabolic trough collector has operation temperature range of 60^0C to 300^0C, paraboloid dish has operation temperature range of 100^0C to 500^0C and solar power tower (heliostat field) has operation temperature range of 150^0C to 2000^0C as cited by Kalogirou [14]. Many researchers have [15-20] deliberated different kinds of solar thermal collector and their findings show that using high temperature solar collector is advantageous in terms of power generation and efficiency.

PTCs are generally oriented in North-South direction and tracking the sun from East-West focusing solar energy on a receiver. They concentrate the solar radiation flux 30-80 times and increase the temperature of HTF (synthetic oil or molten salt) approximately up to 300^0C. The high temperature HTF transfers the heat from the solar field to heat recovery vapour generator (HRVG) of a conventional Rankine cycle, to generate high pressure steam. The high pressure and high temperature steam expands in a steam turbine, which produces power/electricity [21]. Major applications of PTC are found in solar electric generating systems (SEGS). Power plant based on PTC has been installed at southern California with an installed capacity of 354MW [22]. For experimental purposes an installed capacity of power 1.2 MW by the collector has been installed at Plataforma Solar de Almeria (PSA) in Southern Spain [23]. Mokheimer et al. [24] developed a simulation model to evaluate the optical and thermal efficiencies of parabolic trough collector's solar field and also carried out the cost analysis. Their findings showed that the maximum optical efficiency that can be reached is 73.5% in Dhahran and the specific cost for a PTC field per unit aperture area can be reduced approximately 46%. Barbero et al. [25] presented a new approach for the prediction of thermal efficiency in solar receivers. Two simplifications can be made based on this approach to obtain much simpler equations that describe collector performance for the majority of solar technologies. Tyagi et al. [26] conducted the exergy analysis of PTC for different mass flow rates of heat transfer fluid. Their result shows that for a given value of solar intensity, the exergy output, exergetic and thermal efficiencies had been found to be the increasing function of mass flow rates. An analysis of exergy has been presented in Padilla et al.

[27], which shows that the solar irradiance has the effect on the performance of PTC. The exergy efficiency has a relation with the inlet temperature of the heat transfer fluid. If the inlet temperature of the heat transfers fluid entering the collector increases, then there will be an increase of exergy efficiency but it also causes a decrease in the energy efficiency. The performance of CSP varies heavily due to the variation of intensity of solar radiation throughout the day. It will be good in a clear bright sky but could hamper the performance during overcast situations. So with the above limitations it is not feasible to use CSP alone for running of the power plants. Thermal energy storage (TES) systems facilitate to enhance the working of CSP technology. Amalgamating the CSP with the TES is a new face for the present scenario and helping us to penetrate the global market with higher power outputs and efficiencies [28–30]. Properly designed combination of CSP and TES can demonstrate working of the system continuously for 24 hours allowing short transient buffers to longer-term night time storage [31, 32]. Feasibility studies of using two tank molten salt storage for parabolic trough solar plants are shown in Herrmann et al. [33]. Their finding predominantly states that for the continuous operation cycle of solar thermal power plant, TES could actually reduce the cost of electricity. Analysis of the PTC coupled with organic Rankine cycle is done for the optimization of the system in terms of energy and finances in Tzivanidis et al. [34].Their studies reveals the suitability of cyclohexane to operate PTC to produce 1MW.

The performance of parabolic trough solar thermal power plants depends on the type of heat transfer fluid (HTF) which flows through the receiver that concludes not only the working temperature range of the solar field but also other engineering aspects like thermal storage and material selection [35]. Montes et al. [36] developed a thermodynamic model to evaluate collector performance using various heat transfer fluid (oil, molten salt, and water/steam). Generation of steam in direct methods proves out to be more efficient than using oil and molten salt systems.

Rigorous research has gone into for converting heat into useful work or electricity, and the researchers have found organic Rankine Cycle to be more significantly efficient over others [37, 38]. The heat source for this type of cycle could be accessed from any of the sources like solar radiation, biomass combustion,

geothermal heat or industrial waste heat. Organic Rankine cycles (ORC) employ an organic fluid (refrigerants or hydrocarbons) occurring at a lower temperature as compared to the vapour steam used in the steam power cycle. Saitoh et al. [39], Kane et al. [40] and Yagoub et al. [41] proposed and deliberate different micro- ORCs designed for electricity generation. Prigmore et al. [42] investigated cooling systems coupled with Rankine engines. Wei et al. [43], Zhang et al. [44], Roy et al. [45], Yamamoto et al. [46], Madhawa Hettiarachchi et al. [47], Nguyen et al. [48], Drescher et al. [49], Quoilin [50] and Hung [51] studied and analyzed the performance of ORCs for waste heat recovery.

The performance and economics of an organic Rankine cycle plant depends on the working fluid used [52]. This justifies the literature dedicated to fluids selection for different heat recovery applications from which properties of good fluids can be summarized [53-64]:

- Vapor saturation curve with zero or positive slope
- High latent heat of vaporization
- High density
- High specific heat
- More critical parameters (temperature, pressure)
- Low viscosity,
- High thermal conductivity
- Stable at high temperature
- Noncorrosive
- High energetic/exergetic efficiency
- Nontoxic and non-flammable
- Low ODP, low GWP
- Low cost and good availability

Gupta et al. [65] carried out energy and exergy analysis of a direct steam generation (DSG) solar-thermal power plant. Their result shows that maximum exergy losses occur in the solar collector field. Kaska [66] carried out energy and exergy analysis of an organic Rankine cycle for power generation from waste heat

recovery in steel industry using actual plant data. Jung et al. [67] investigated the feasibility of transforming refinery waste heat-to-power in an organic Rankine cycle using R123, R134a, R245fa, butane, pentane, a mixture of butane and pentane, a mixture of 40% isobutane and 50% butane on a mole basis. Deethayat et al. [68] investigated the performance of a 50 kW organic Rankine cycle (ORC) with internal heat exchanger (IHE) using R245fa/R152a zeotropic refrigerant as working fluid with various compositions. Their results show that reduction of R245fa composition reduces the irreversibilities at the evaporator and the condenser. Mohammad et al. [69] carried out design and experimental investigation of a 1 kW organic Rankine cycle system using R245fa as working fluid for low grade waste heat recovery from steam and observed that the maximum thermal efficiency was 5.75%.

Yuandan et al. [70] studied the performance of an organic Rankine cycle using zeotropic mixture fluids (R227ea/R245fa, Butane/ R245fa, and RC318/ R245fa) and compared with corresponding pure fluids. Their findings show that the cycle efficiency, exergy efficiency and net power output increases when the temperature of cooling water is near the temperature glide of zeotropic mixture in the condenser. Dong et al. [71] investigated the performance of low temperature organic Rankine cycle (ORC) using pure fluids and zeotropic mixtures as working fluids through pinch analysis method. Their results show that Using mixtures as working fluid, an increase in cycle efficiency of up to 17.96% is observed comparing with using their pure constituents. Li et al. [72] conducted an experimental investigation for conversion of low-grade heat energy into power in a small-scale organic Rankine cycle (ORC) using R245fa as working fluid. The results show that at constant heat source parameters (temperature and flow rate), the power output and cycle efficiency increased with lower cooling water temperatures. Wang et al. [73] developed a computer program to compare the first and second law efficiencies, and turbine size factor with increase in turbine inlet temperature for an organic Rankine cycle (ORC) using hydrofluoroethers including HFE7000, HFE7100 and HFE7500 as working fluids. Their findings show that HFE7000 produces the maximum thermodynamic efficiencies and has the lowest turbine size factor comparing with HFE7100 and HFE7500. Therefore, HFE7000 can be suggested to be used as working fluid in ORC to convert low-grade heat into power.

The refrigeration has many applications in human life for cooling and air-conditioning, conservation of vegetables, fruits, pharmaceutical products, maintaining environmental conditions etc. The vapour compression refrigeration cycle is used frequently that utilized electricity which will be produced from fossil fuels. For the design and growth of solar energy conversion systems like ejector refrigeration, a detailed knowledge of available solar radiation is required. The use of the solar energy as the heat source for ejector refrigeration and absorption refrigeration system has studies by the many researchers.

The ejector is the heart of the ejector cooling system, which increases the pressure without consuming mechanical energy directly. Due to this the ejector is a simple and safer device than a compressor or a pump which can increase pressure.

The basic principle of the ejector cycle was introduced by Keenan et al. [74] based on gas dynamics, and then developed by Huang et al. [75] and Ouzzaneet et al. [76]. Research has been extensively performed to understand and improve the performance of steam jet systems [77-82]. However, steam jet systems suffer the disadvantages of very low COP value and being unable to generate refrigeration below 0oC. Therefore, halocarbon compounds, organic compound, and an azeotrope have been used in ejector refrigeration systems and their performances are compared [83]. Cizungu et al. [84] carried out the Performance comparison of vapour jet refrigeration system with environment friendly working fluids (R123, R134a, R152a and R717) for the same ejector geometry. Their findings show that the entrainment ratio and the system efficiency (COP) depend mainly on the ejector geometry and the compression ratio. Selvaraju et al. [85] shows the effect of thermodynamic parameters on performance of vapor ejector refrigeration system with environment friendly refrigerants like, R134a, R152a, R290, R600a, and R717. Dahmani et al. [86] formulated a model of simple ejector refrigeration systems for a particular combination of fixed cooling load with fixed temperatures of the external fluids entering the generator, the condenser and the evaporator temperature.

Low operating , maintenance & installation cost with lesser moving parts are some of the basic reasons why ejector cycles are drawing good attention, but costs us

in terms of efficiency and COP [87-91]. Pridasawas et al. [92] determined the irreversibility in each component of solar operated ejector refrigeration system and find out that the maximum irreversibility occurred in solar collector and ejector. Ejector based cooling system is attractive technology due to the absence of mechanical compressor and CFC which leads to energy efficient and environmental friendly production of cooling from solar energy [93-95].

In the last decades, remarkable numbers of studies have been carried out by many researchers to explore different aspects of absorption refrigeration system [96]. Vapour absorption refrigeration system is becoming more important because it can be run by low temperature heat source such as waste heat, solar heat, biomass or geothermal energy and on refrigerants having zero ODP and GWP [97]. Since the system is characterized by low COP and economic constraints. With the above mentioned constraints, an efficient and optimum operating range should be found. The possible operating conditions of solar absorption refrigeration system was being thermodynamically analyses in Shwartz et al. [98] It was found that the system is actually beneficial for domestic uses. A mathematical simulation of a water ammonia system was being done and then being implemented and optimized by Sun [99]. A thermodynamically optimized design of water ammonia and lithium bromide- water absorption systems was being presented by Sun [100]. Maximum performance of the system can be derived using their results. Different binary mixtures were being thermodynamically analyzed by Sun in their absorption system [101]. Solar absorption system using LiBr-H_2O was being simulated by Atmaca et al. [102]. A correlation has been drawn between hot water inlet temperature, COP and surface area of absorption through their findings. The finding that shows that the total exergy destruction is greater in NH_3-H_2O than LiBr-H_2O has been examined by Khaliq et al. [103]. The major contributor of the exergy destruction has been found to occur in generator and absorber and it is also stated that increase in temperature of the absorber can actually contribute in increasing the exergetic efficiency. Numerous analyses have been examined for exergy investigation of absorption refrigeration system [104–106]. The method of rational efficiency (exergetic efficiency) analysis is more complicated than energy efficiency analysis [107]. It is a novel methodology permitted us to

compare different energy system's performance. Moreover, both the methods are utilized. Energy analysis provides an initial investigation and exergy analysis should be used as a more detailed examination of ARS [108]. Modi et al. [109] carried out the energy and exergy analyses of a single effect lithium bromide absorption refrigeration system. They observed that COP and exergy efficiency increases with the increase in generator temperature (75^0C to 110^0C) and the maximum exergy destruction occurs in the generator & followed by the absorber.

For efficient utilization of solar energy, a combined power and refrigeration cycle has been analyses to improve the overall efficiency of the system. Xu et al. [110] proposes a cycle that combines the absorption cooling with The Rankine cycle .Padilla et al. [111] evaluate the effects of generator pressure, ammonia concentration, turbine efficiency and heat source temperature on the performance of the cogeneration cycle. Their findings shown that the turbine efficiency had significant effect on the network and cooling output of the cycle. Thermodynamic analysis of a combined power and cooling cycle using solar energy as heat source has been analyses by Hasan et al. [112]. The maximum second law efficiency of the cycle was found 65.8% at the source temperature of 420 K. Tamm et al. [113] investigated an ammonia–water based power and cooling thermodynamic cycle analytically and experimentally. Their analysis showed that the losses in the system can be reduced over wide range of operational parameters. Vidal et al. [114] have done the exergy analysis of a combined power and refrigeration cycle using ammonia–water mixture as the working substance. The second law efficiency of the combined cycle was found to be 53%. Cogeneration of power and refrigeration using ammonia water had been proposed by Zhang et al. [115]. Efficiencies of energy and exergies have been found to be in the zone of 25 % and 50.9% respectively. Liu and Zhang [116] projected and analyzed a novel ammonia–water combined cycle for the production of power and cooling. The performance of the cycle had been evaluated on the basis of exergy efficiency and the results were found to have the efficiency of around 58%. A condenser and evaporator were introduced between the rectifier and the second absorber. Thus fluid will go through a phase change in the cooler to produce more refrigeration capacity. Whereas Zheng et al [117] proposed a co-generative plant producing power and refrigeration,

on the basis of Kalina cycle. The modification has been done by using a rectifier for better ammonia water concentration, in place of an earlier used flash tank in Kalina cycle. To get more cooling capacity, a condenser and an evaporator has been introduced in between the existing rectifier and secondary absorber, and virtue to that this will make the fluid go phase change in cooler for more refrigeration capacity. Zhang and Lior [118] projected a new combined refrigeration and power system. The system operates in a parallel combined cycle mode with an ammonia–water Rankine cycle and an ammonia refrigeration cycle, interconnected by absorption, separation and heat transfer processes. Thermodynamic parameters were being analysed on the efficiencies of both exergy and energy. A combined system has been developed by Zhang and Lior [119] to give both power and refrigeration effect using ammonia water as working substance for higher operating efficiencies. A cycle with the combination of power and refrigeration system employing Rankine and absorption cycles has been carried out by Wang et al. [120]. Wang et al. [121] carried out thermodynamic analysis of a new combined cooling and power system using ammonia–water mixture by using low grade heat sources. Exergy destruction study was conducted to identify the exergy distribution in the various components of the system. The result shows that the major exergy destruction takes place in the heat exchangers.

Most of the researchers have been concentrate their efforts on combined Rankine with absorption refrigeration cycle. The use of the ejector refrigeration cycle with the combination of power is given a little attention. A computer program has also been generated by Alexis [122], that analyzes the performance parameters of combined cycles. Ejector system has been found to be more economical than the absorption system. A combined power and ejector cooling cycle was proposed by Zheng et al. [123] using R245fa as the working fluid. The analysis shows that while we increase the temperatures of generator from 335 K to 415 K , the energy efficiency is found to increase from 15.8% to 38% and on the other side the exergy efficiency increased from 45.2% to 57.2%.The generating temperature cannot be increased beyond a limit due to increase in turbine size. Rashidi et al. [124] developed a computer program for a combined power and ejector cooling cycle using R123 as the

working fluid to determine the effects of various operating parameters on the performance of the cycle. Their results show that the first and second law efficiency increase with the increase in evaporator temperature, and maximum exergy losses occurs in the boiler and ejectors. In addition to this, there is increase in first law efficiency and decrease in second law efficiency with increase in turbine inlet pressure. Habibzadesh et al. [125] investigated the performance of a combined power and ejector refrigeration cycle from thermodynamic point of view and determine the optimum values of the turbine and pump inlet pressures which minimize the total thermal conductance of the cycle for the working fluid considered. Chen et al. [126] analyses a combined power and ejector cooling system using low grade energy as heat source. The system performance were compared for five working fluid (HFE7100, HFE7000, methanol, ethanol, water) at a source temperature of 120^0C, evaporator temperature of 10^0C and condenser temperature of 35^0C. Methanol shown the highest efficiency (19.50%) followed by ethanol and water (17.30%). Their results also shown that the heat source temperature, condenser temperature and evaporator temperature have significant effect on the power output, ejector entrainment ratio and thermal efficiency of the system. An energy and exergy analyses of combined power and ejector refrigeration cycles was reported by Wang et al., Dai et al., Agrawal et al. and Khaliq [127-130] which shows that the maximum irreversibility/exergy loss occurs in heat addition process followed by the ejector and turbine.

In order to enhanced the use of the concentrating solar energy for their potential in decreasing fossil fuel consumption and alleviating environmental complications, a solar operated combined power and ejector refrigeration cycle has been proposed by using R141b refrigerants for simultaneous production of cooling and power, and thermodynamically analyzed in the **second chapter** of the thesis.

A parametric study has been conducted to investigates the effect of some influenced parameters on the performance of the solar driven combined power and ejector cooling cycle with ecofriendly refrigerants (R290, R152a, R134a, and R717) as working substance in the **third chapter** of the thesis. This combined cycle can produce both power and refrigeration output simultaneously using single source of solar energy.

In order to improve the performance of single effect absorption refrigeration system, a combined ejector-absorption refrigeration cycle is proposed and examined by few of the researchers. Wang et al. [131], Goktun [132], Eames et al. [133], Levy et al. [134], and Sozen et al. [135] proposed ejector-absorption refrigeration cycles to improve the performance of single stage absorption refrigeration cycle. Sozen et al. [136] highlighted the prospects for utilization of solar driven ejector– absorption cooling in Turkey and observed that there is a great potential of solar cooling system for domestic heating and cooling applications. Alexis [137] carried out the exergy analysis of an ejector-absorption refrigeration system for cooling applications using LiBr–H_2O. Their result showed that the exergy destruction in ejector is highest (37.81%) and that of pump is lowest (0.3%) at 30^0C ambient temperature, 150^0C generator temperature, 5^0C evaporator temperature and at mass entrainment ratio of 0.5. Hong et al. [138] proposed a novel triple pressure level absorption refrigeration cycle. Their results have shown that the COP of the proposed cycle is 30% more than that of a single effect absorption refrigeration cycle for specific conditions. Verda et al. [139] develop a mathematical model of a triple pressure level absorption refrigeration cycle using ammonia-lithium nitrate solution as working fluid. Simulation results concluded that with the use of the ejector, the absorption pressure becomes higher than the evaporation pressure and increase the cooling capacity. The above reported studies on combined ejector-absorption refrigeration system uses only single evaporator which produces cooling only at single point in the system. Recently, in refrigeration industry the use of efficient dual-evaporator refrigeration systems has been paid a lot of attention. These systems sound even more interesting when they are a combination of different kinds of conventional refrigeration systems for simultaneously production of power and producing cooling effects at two different temperatures in the system by using low temperature heat source. In this context, an ejector organic Rankine cycle (EORC) integrated with a triple pressure level vapour absorption system (TPLAS) based on parabolic trough collector (PTC) solar field is proposed and thermodynamically analyzed in the **fourth chapter** of the thesis. This cycle produces power and cooling effects at two evaporators at two different temperatures in this system by using single source of solar energy. This system meets out the demand of electricity, space air-conditioning and preservation of fruits &

vegetables in cold storage. The performance of EORC and proposed system is also compared on the basis of energy and exergy approach.

At the exit of heat recovery vapor generator of combined power and ejector cooling cycle, a great amount of thermal energy is waste which causes the reduction in performance of the system. To recover some of the thermal energy from the exit, a PTC (parabolic trough collector) field based double ejector organic cycle (DEORC) using refrigerant R141b as working fluid and Therminol VP1 as heat transfer fluid is presented and thermodynamically analyzed in the **fifth chapter** of the thesis. The proposed cycle produces power and cooling at two different temperatures by using single source of solar energy. Thermal storage tanks are also used to store the thermal energy from the Sun which provides the continuous power and cooling effect during insufficient solar radiation. The performance of EORC and DEORC is also compared on the basis of energy and exergy approach. The proposed system can be accounted as dual-evaporator refrigeration system which provides wide range of cooling along with power.

1.3 Research Gap

Based on the literature survey following outcomes are identified:

- A lot of researchers focused their work on combined power and vapor absorption refrigeration cycle, but very few concentrate their work on the combination of organic Rankine cycle and ejector refrigeration cycle.
- Most of the research work has been done for the performance estimation of the combined power and ejector cooling cycle based on the 1^{st} law of thermodynamics but very few concentrate on the 2^{nd} law of thermodynamics for performance estimation.
- Research work has been done to analyze the combined power and cooling cycle using solar energy as heat source without using thermal energy storage (TES), which provides power and cooling on sunshine hour only. But the research contribution on solar driven combined power and cooling cycle with thermal energy storage (TES) is not available in the literature.

1.4 Objective of the research work

The abundance of solar energy in the nature proves to be beneficial for designing a system which stands out to be an eco-friendly design. Amongst all the researches that are going on for a sustainable design, solar assisted technology shares the maximum of it. In the proposed research thesis the use of solar energy has been utilized for production of power and cooling simultaneously and this work could prove to be great for those areas where there is no lack of solar radiation but need of cooling is foremost priority. Modification, manipulation and innovation in the basic thermodynamic cycles, can reduce the extent of usage of fossil fuels by using the solar energy to its near full potential.

This work of thesis targets and then analyzes the irreversibilities / exergy destruction and losses while designing the various components of a solar assisted combined power and ejector cooling cycle, PTC field based ejector organic Rankine cycle integrated with a triple pressure level vapour absorption system, and a PTC field based double ejector organic Rankine cycle (DEORC) using the concept of exergy and entropy generation analysis viz:

- Comparison of the performance of the cycles for various ecofriendly refrigerants.
- To reduce the fossil fuel consumption by using low grade solar heat.
- For all the above mentioned cycles, efficiencies of the energy and exergy have been determined and moreover the exergy destruction/ losses has also been derived analytically for all the components present in the said system.
- Irreversibility is the key for the parameters of performance to deviate from the ideal. So the identification of the irreversibility issues has been done to explain the deviation of performance by putting light on the parameters like exergy destruction and entropy generation.
- Effect of main thermodynamic operating constraints on the performance of the proposed multi-generation thermodynamic cycles/systems.

In this work, the concept of entropy generation and exergy analysis has been applied to power and cooling cycles. An attempt has been made to visualize the

deviation between ideal and actual performance of the various multi-generation thermodynamic cycles/systems. This can guide researcher, engineers, decision makers, educators and designers in the evaluation of existing real systems and design of future energy systems.

1.5 Methodology

1.5.1 Introduction

Inefficiencies or the deviations of the process parameters can be taken care by in depth analysis of exergy values of the process points that is purely based on second law of classical thermodynamics.

1.5.2 Limitation of First law analysis

- It solely targets overall system performance.
- Internal losses are not monitored by the energy balance equations.
- It is inefficient in identifying the probable causes of losses in the system which hampers the overall performance.
- The quantification of the performance deterioration is not being identified by the first law.
- Inadequacy of information about the system is the major drawback of this law.

1.5.3 Second law analysis

2^{nd} law approach, is applied for the analysis of thermodynamic cycles of power and cooling. This methodology is expected to provide a complete thermodynamic view of the given systems with a view to provide guidance for performance improvement.

The relation between heat and work and also for determining the overall system efficiencies the laws of energy conservation and first law of thermodynamics paves the path. Whereas the quantification of the relation between work and heat in terms of irreversibility is being taken care by the second law. Exergy is characterized as the most extreme conceivable reversible work reachable in conveying the condition of the system to equilibrium with that of the environment. To analyze the process deviations thermodynamically, exergy analysis turns out to be a valuable device. The

investigation relates the possibility of improvement for the process or systems that has been considered for the analysis.

The total exergy associated with the work obtainable by bringing a stream of matter from its initial state to a state that is in thermal and mechanical equilibrium with the environment.

Mathematically,

$$\dot{X} = \dot{m}[(h - h_0) - T_0(s - s_0)] \tag{1.1}$$

The destruction of the exergy states the exergy lost in the ambient is not to be gained back by the system or process e.g. due to system irreversibilities. Entropy generation over a control volume is given by the Bejan [145].

$$\dot{S}_{gen} = \frac{dS}{dt} - \sum_{i=0}^{n} \frac{\dot{Q}_i}{T_i} - \sum_{in} \dot{m} + \sum_{out} \dot{m} \geq 0 \tag{1.2}$$

The relation among the exergy destruction and entropy generation is given by Gouy-Stodola theorem.

$$\dot{X}_D = T_0 \dot{S}_{gen} \tag{1.3}$$

Application of this equation helps in to evaluate the thermodynamic losses take place in different components of power and refrigeration system due to entropy generation via heat transfer and fluid flow, and minimizing these losses results in the effective exploitation of input source of energy for the generation of power and cooling simultaneously. This analysis pin points the component which is much responsible to deteriorate the performance of the system due to which a deviation is observed between its ideal and actual performance.

The advantages of exergy analysis are:

- Can analyze thermodynamically the points which are responsible for the energy downpour from the system.
- Complex thermal systems can easily be analyzed by the 2nd law.

- Can exclusively be utilized to distinguish and to expel the inconsistencies of the procedure parameters.
- Provide ranking among the component.
- Process improvements can deeply be sighted and analyzed by the exergy calculations.
- Guide to reduce sources of inefficiency in existing system and evaluate system economics.
- Operating conditions can be analyzed and optimized with this analysis.
- It rather saves time and costs that would have occurred to conduct many experiments to acutely analyze the process parameters deviation.
- More useful for process enhancement and plant development.

1.5.4 Energy equations for thermodynamic analysis of ejector

The formula for the entrainment ratio has been reported at Dai et al. [128].

$$\mu = \sqrt{\eta_n \eta_m \eta_d \left(h_{pf,n1} - h_{pf,2s}\right)/\left(h_{mf,ds} - h_{mf,m}\right)} - 1 \tag{1.4}$$

The properties of the refrigerants used in the ejector cycle are taken from REFPROP 6.01[140].

Nozzle, mixing chamber and the diffuser are the main components of any ejector system.

The conservation of energy for the adiabatic and steady flow of a nozzle section is given by:

$$\dot{m}_{pf} h_{pf,n2} + \frac{\dot{m}_{pf} u_{pf,n2}^2}{2} = \dot{m}_{pf} h_{pf,n1} + \frac{\dot{m}_{pf} u_{pf,n1}^2}{2} \tag{1.5}$$

$$\eta_n = \frac{h_{pf,n1} - h_{pf,n2}}{h_{pf,n1} - h_{pf,n2s}} \tag{1.6}$$

The conservation of momentum in the mixing section is given by:

$$\dot{m}_{pf}u_{pf,n2} + \dot{m}_{sf}u_{sf,n2} = (\dot{m}_{pf} + \dot{m}_{sf})u_{mf,m,s} \quad (1.7)$$

The energy equation for a diffuser is given by:

$$\frac{(u_{mf,m}^2 - u_{mf,d,s}^2)}{2} = h_{mf,d,s} - h_{mf,m} \quad (1.8)$$

The efficiency of a diffuser is given by:

$$\eta_d = \frac{h_{mf,d,s} - h_{mf,m}}{h_{mf,d} - h_{mf,m}} \quad (1.9)$$

1.5.5 Energy and exergy equations for thermodynamic analysis of Heliostat and Central Receiver

The elementary equations derived for the heliostat and central receiver is reported at Xu et al. [141] and Yao et al. [142],

$$\dot{Q}_{Solar} = A_p G_b \quad (1.10)$$

Where, A_p is the aperture area and G_b is the solar beam radiation respectively.

$$\dot{Q}_{Solar} = \dot{Q}_{CR} + \dot{Q}_{lost,heliostate} \quad (1.11)$$

1st law efficiency (energy efficiency) of Heliostat is reported as

$$\eta_{E,\ heliostat} = \frac{\dot{Q}_{CR}}{\dot{Q}_{Solar}} \quad (1.12)$$

For Central Receiver (CR): The solar tower has central receiver normally installed at the top which receive a part of solar energy that transfer to the oil (Duratherm600) and remaining get lost to the atmosphere according to Li et al. [143].

$$\dot{Q}_{CR} = \dot{Q}_{oil} + \dot{Q}_{lost,CR} \tag{1.13}$$

1st law efficiency of CR is reported as

$$\eta_{E,\ CR} = \frac{\dot{Q}_{oil}}{\dot{Q}_{CR}} \tag{1.14}$$

The elementary equations of exergy destruction rate in the heliostat and central receiver are given below:

For Heliostat:

$$\dot{X}_{Solar} = \dot{X}_{CR} + \dot{X}_{lost,heliostat} \tag{1.15}$$

2nd law efficiency of heliostat is reported as

$$\eta_{X,\ heliostat} = \frac{\dot{X}_{CR}}{\dot{X}_{Solar}} \tag{1.16}$$

For Central Receiver (CR):

$$\dot{X}_{CR} = \dot{X}_{oil} + \dot{X}_{lost,CR} \tag{1.17}$$

2nd law efficiency of CR is reported as

$$\eta_{X,\ CR} = \frac{\dot{X}_{oil}}{\dot{X}_{CR}} \tag{1.18}$$

1.6 Organization of thesis

The introduction, literature review and methodology used is presented in **Chapter 1** of the thesis. The literature review thoroughly reviews the research efforts made on organic Rankine cycle, ejector cooling cycle, absorption cooling cycle and combined cooling and power cycle.

Chapter 2 describes the solar derived combined power and ejector cooling cycle which produces power and cooling simultaneously. The equation used to calculate the first and second law efficiency along with irreversibility in different parts of the proposed cycle has been presented. The thermodynamic analysis of the cycle has been done on the bases of first and second law approach. The impact of most affected parameters (turbine inlet pressure, evaporator temperature, condenser temperature, extraction ratio, and direct normal radiation per unit area) has been seen on the 1^{st} law and 2^{nd} law efficiency of the proposed cycle alongside the exergy destruction in its different parts.

Chapter 3 depicts the parametric investigation of combined power and ejector cooling cycle with ecofriendly refrigerants such as R290, R152a, R134a, and R717. The impact of most affected parameters, for example, turbine expansion ratio, driving pressure ratio, and compression pressure ratio on the entrainment ratio, net power output, refrigeration output, 1^{st} law and 2^{nd} law efficiency of the proposed cycle have been studied. The performance comparison of the cycle using various environmentally benign fluids is also studied.

Chapter 4 presents the performance analysis of PTC field based ejector organic Rankine cycle integrated with a triple pressure level vapour absorption system. The Proposed system consists of ejector organic Rankine cycle integrated with a triple pressure level vapour absorption system based on parabolic trough collector (PTC) solar field. The proposed system produces power and refrigeration output at different temperatures simultaneously. Thermodynamic investigation was directed to find the impact of different outline parameters, for example, DNI, turbine inlet pressure, turbine extraction pressure, and ejector evaporator temperature on the performance of proposed system and furthermore compared with the performance of

ejector organic Rankine cycle Evaluation for irreversibility of individual parts of the cycle prompts conceivable measures for performance improvement.

Chapter 5 deals with thermodynamic evaluation of PTC based organic Rankine cycle for power & cooling. The thermodynamic evaluation is done to assess the performance of PTC field based EORC & DEORC system which produces power and cooling simultaneously utilizing refrigerant R141b as working fluid and Therminol VP1 as heat transfer fluid. Thermal energy storage tanks are used to store the PTC heat, which provides the continuous net power output and cooling during insufficient solar radiation. Parametric investigations of EORC and DEORC demonstrate that inlet temperature and pressure of turbine at different extraction ratios has the noteworthy impact on 1^{st} law and 2^{nd} law efficiency and cooling to power ratio of this system.

Chapter 6 summarizes overall conclusions of the result which will be obtained in the above study and a little effort will be made to search out a domain for further research in the proposed area of interest.

CHAPTER 2

SOLAR OPERATED EJECTOR COOLING AND POWER CYCLE

2.1 Introduction:

In this chapter, a combined Rankine and ejector refrigeration cycle is proposed for the production of power and refrigeration output utilizing duratherm 600 oil as the heat exchange fluid. Thermodynamic investigation has been done to observe the impact of parameters on the performance of the combined cycle. The impact of various parameters as the turbine inlet pressure, evaporator temperature, condenser temperature, and extraction ratio on the performance of the cycle (the net power output, refrigeration output, 1^{st} law efficiency and 2^{nd} law efficiency) along with the exergy destruction in its various components is evaluated.

2.2 Working of proposed cycle:

Fig. 2.1 shows the solar operated combined Rankine and ejector refrigeration cycle. It consists of a turbine (T) and an ejector (EJ) which produces power and cooling respectively. Solar energy is utilized to heat the HTF (duratherm fluid 600) (1) with the help of heliostat and central receiver. Heat transfer fluid is utilized to superheat the high pressure refrigerant in the HRVG. Superheated refrigerant vapor (4) expands in the turbine. Extracted vapor (5) flows into the ejector nozzle and entrains secondary vapor (13) from the evaporator, mixes in mixing chamber of the ejector. The ejector exit stream (6) mixes with the turbine exhaust (14) and is cooled in the heat exchanger (7-8), and then enters into the condenser (C). Saturated liquid (9) from condenser then enters into throttle valve (11) and pump (10). The high pressure liquid flows into the heat exchanger (15-3) and then converted into superheated vapor (4) in the HRVG. The saturated liquid (11) expands to the evaporator pressure (11-12) in the throttle valve and vaporized in the evaporator (12-13) to produce refrigeration effect.

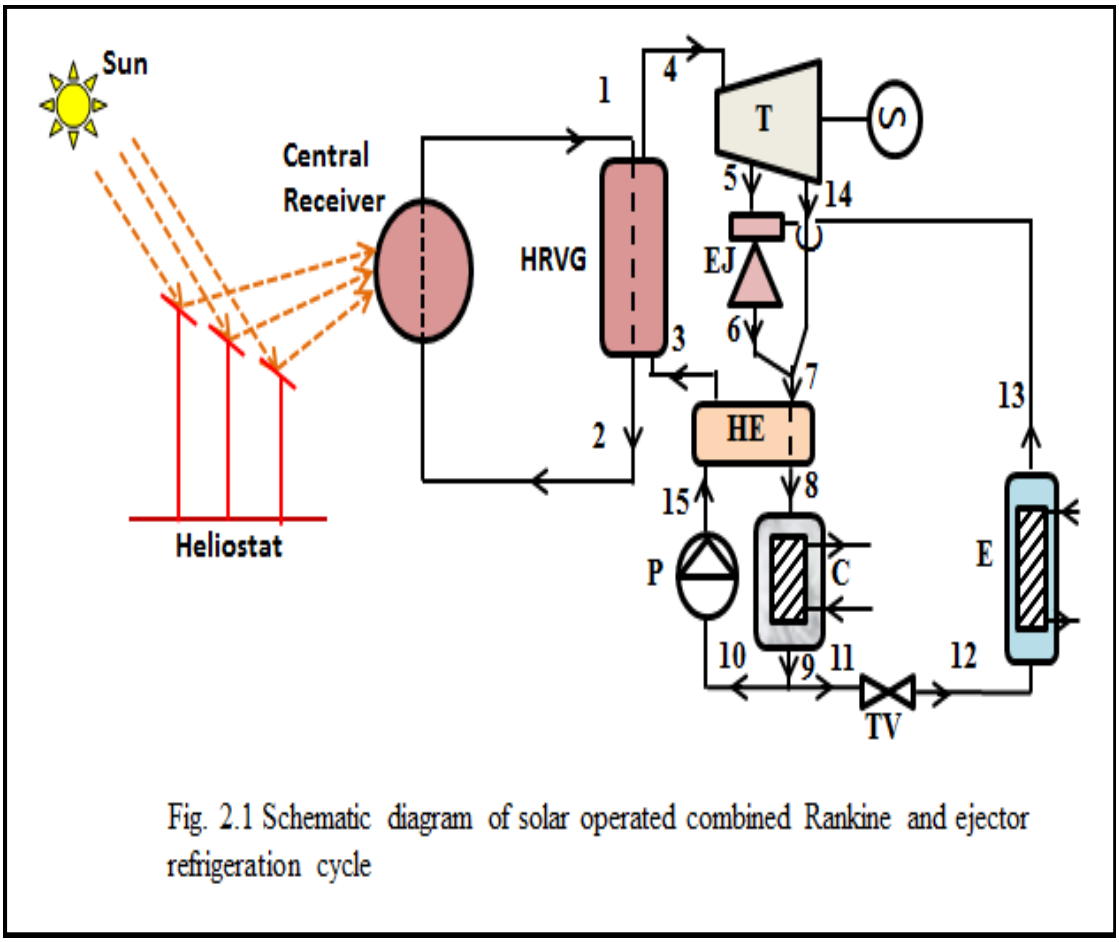

Fig. 2.1 Schematic diagram of solar operated combined Rankine and ejector refrigeration cycle

For the investigation, the specifications of the combined Rankine and ejector refrigeration cycle are given in Table 2.1.

Table 2.1: Key parameters considered for the analysis [127-130].

Ambient temperature (K)	298
Ambient pressure (bar)	1.0135
Pressure at the inlet of the turbine (bar)	9-13
Turbine inlet temperature (K)	423
Extraction ratio	0.2-0.8
Turbine extraction pressure (bar)	2.5
Turbine efficiency	0.85
Pump efficiency	0.70
Condenser temperature (K)	297-303
Evaporator temperature (K)	262-270
Water temperature inlet to evaporator (K)	298
Water temperature outlet to evaporator (K)	278
Solar beam radiation (kW/m^2)	0.8-0.9
Apparent Sun temperature (K)	4500
Heliostat aperture area (m^2)	3000
Oil temperature inlet to CR (K)	373
Oil temperature inlet to HRVG (K)	433
Heat recovery vapour generator efficiency	1.00
Pinch point temperature difference (℃)	10.0

Efficiency of the nozzle	0.90
Mixing efficiency	0.85
Efficiency of the diffuser	0.85
1st law efficiency of heliostat field	0.75
1st law efficiency of central receiver	0.90
2nd law efficiency of heliostat field	0.75
2nd law efficiency of central receiver	0.30

2.3 First and second law analysis of proposed cycle:

2.3.1 First law efficiency (η_E)

1st law/energy efficiency (η_E) can be characterized as the proportion of the net power output ($\dot{W}_{net}$) and refrigeration output in the evaporator ($\dot{Q}_E$) to the input solar energy.

The 1st law efficiency of the proposed cycle is given by

$$\eta_E = \frac{\dot{W}_{net} + \dot{Q}_E}{\dot{Q}_{Solar}} \tag{2.1}$$

2.3.2 Energy balance for components of the proposed cycle

For HRVG:

$$\dot{m}_{oil}(h_1 - h_2) = \dot{m}_f(h_4 - h_3) \tag{2.2}$$

For Turbine (T):

$$\dot{W}_T = \dot{m}_f(h_4 - h_5) + \dot{m}_f(1 - R)(h_5 - h_{14}) \tag{2.3}$$

Where extraction ratio (R) is reported as

$$R = \frac{\dot{m}_{pf}}{\dot{m}_f} = \frac{\dot{m}_5}{\dot{m}_4} \tag{2.4}$$

For Ejector (EJ):

$$\dot{m}_{pf}h_5 + \dot{m}_{sf}h_{13} = h_6(\dot{m}_{pf} + \dot{m}_{sf}) \tag{2.5}$$

For heat exchanger (HE):

$$\dot{m}_7(h_7 - h_8) = \dot{m}_f(h_3 - h_{15}) \tag{2.6}$$

$$\dot{m}_f = \dot{m}_{pf} + (1 - R)\dot{m}_f \tag{2.7}$$

$$\dot{m}_7 = \dot{m}_{pf} + \dot{m}_{sf} + (1 - R)\dot{m}_f \tag{2.8}$$

For Condenser (C):

$$\dot{Q}_c = \dot{m}_f(1 + \mu)(h_8 - h_9) \tag{2.9}$$

Where entrainment ratio (μ) is reported as

$$\mu = \frac{\dot{m}_{13}}{\dot{m}_5} \tag{2.10}$$

For Pump (P):

$$\dot{W}_p = \dot{m}_f(h_{15} - h_{10}) \tag{2.11}$$

$$\dot{W}_{net} = \dot{W}_T - \dot{W}_p \tag{2.12}$$

For Throttle Valve (TV):

$$h_{11} = h_{12} \tag{2.13}$$

For Evaporator (E):

$$\dot{Q}_E = \dot{m}_f R\mu(h_{13} - h_{12}) = \dot{m}_w(h_a - h_b) \quad (2.14)$$

2.3.3 Second law efficiency (η_X)

2nd law/exergy efficiency (η_X) of proposed cycle reported as

$$\eta_X = \frac{\dot{W}_{net} + \dot{X}_E}{\dot{X}_{Solar}} \quad (2.15)$$

Where, $\dot{X}_E$is the exergy of refrigeration output in the evaporator, $\dot{X}_{Solar}$ is incoming exergy,

$$\dot{X}_E = \dot{m}_{sf}[(h_{12} - h_{13}) - T_0(s_{12} - s_{13})] \quad (2.16)$$

$$\dot{X}_{Solar} = \dot{Q}_{Solar}\left(1 - \frac{T_0}{T_{Solar}}\right) \quad (2.17)$$

Where T_{Solar} is the apparent sun temperature.

2.3.4 Exergy destruction rate in the components of proposed cycle

The elementary equations of exergy destruction rate in the components of proposed cycle are written as follows:

For heat recovery vapor generator (HRVG):

$$\dot{X}_{D,HRVG} = T_0[\dot{m}_{oil}(s_2 - s_1) + \dot{m}_f(s_4 - s_3)] \quad (2.18)$$

For Turbine (T):

$$\dot{X}_{D,T} = T_0\dot{m}_f[Rs_5 + (1 - R)s_{14} - s_4] \quad (2.19)$$

For Ejector (EJ):

$$\dot{X}_{D,EJ} = T_0 \dot{m}_f R[(1+\mu)s_6 - s_5 - \mu s_{13}] \quad (2.20)$$

For heat exchanger (HE):

$$\dot{X}_{D,HE} = T_0[\dot{m}_7(s_8 - s_7) + \dot{m}_f(s_3 - s_{15})] \quad (2.21)$$

For Condenser (C):

$$\dot{X}_{D,C} = \dot{m}_f(1+\mu)[(h_8 - h_9) - T_0(s_8 - s_9)] \quad (2.22)$$

For Pump (P):

$$\dot{X}_{D,P} = T_0 \dot{m}_f(s_{15} - s_{10}) \quad (2.23)$$

For Throttle Valve (TV):

$$\dot{X}_{D,TV} = T_0 \dot{m}_f R\mu(s_{12} - s_{11}) \quad (2.24)$$

For Evaporator (E):

$$\dot{X}_{D,E} = T_0[\dot{m}_f R\mu(s_{13} - s_{12}) + \dot{m}_w(s_b - s_a)] \quad (2.25)$$

2.4 Result and discussion:

A thermodynamic analysis has been done to recognize the impact of some constraints on the **performance** of the solar driven combined power and refrigeration cycle. Following constraints have been chosen in the typical range of its operation; turbine inlet pressure (0.9MPa-1.3MPa), evaporator temperature (262K-270K), condenser temperature (297K-303K), and extraction ratio (0.2-0.8). The constraints under consideration are changed over a given typical range while valuations of other constraints are kept consistent.

Energy balance approach is applied to find out the energy distribution of solar heat source. While exergy balance methodology is applied to find out the exergy

destruction in every part of the system. The energy and exergy distribution of each component of the system is made non-dimensional by communicating it as the percentage of energy and exergy of solar heat source respectively. The thermodynamic properties of refrigerant (R141b) were calculated by REFPROP 6.01[140]. So as to distinguish, the reasons for deviation, between the energy performance (1st law) and exergy performance (2nd law) of the proposed cycle which generate the power and cooling at the same time, the energy and exergy distribution of the cycle is shown in Figs. 2.2 -2.3. The sum of the energy input at the solar field (100%) and at the evaporator (4.19%) in the form of cooling is equal to 104.19%. The sum of the energy output is equal to the net power output (10.62%) and energy lost to the environment (93.57%) through heliostat, central receiver and condenser from the system which is equal to the total energy input to the system [146].

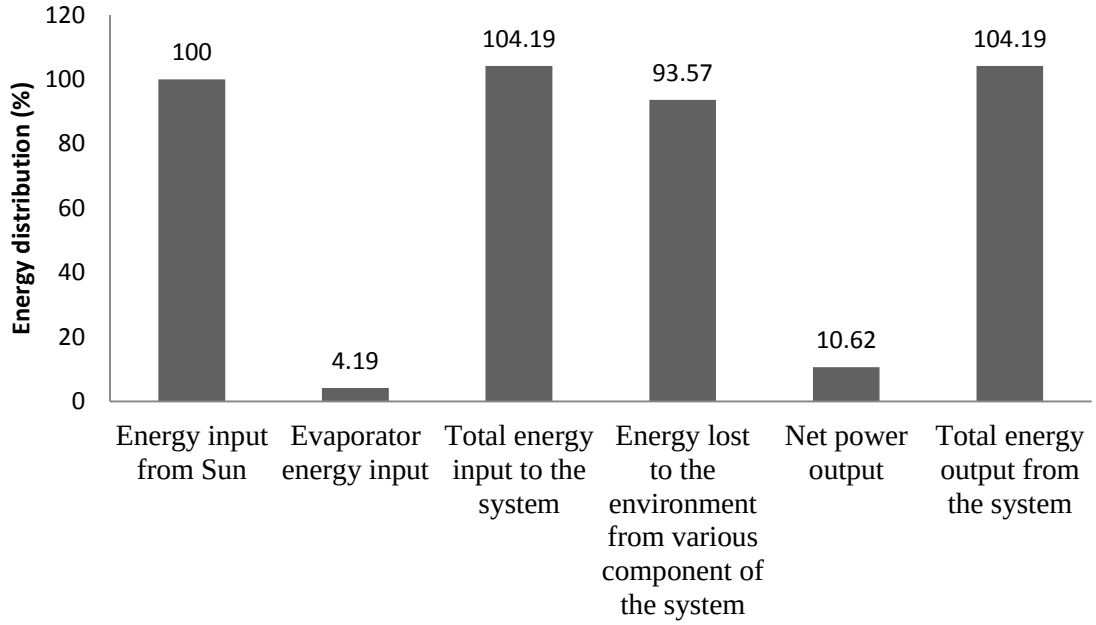

Fig. 2.2 Energy distribution in solar operated combined Rankine and ejector refrigeration cycle

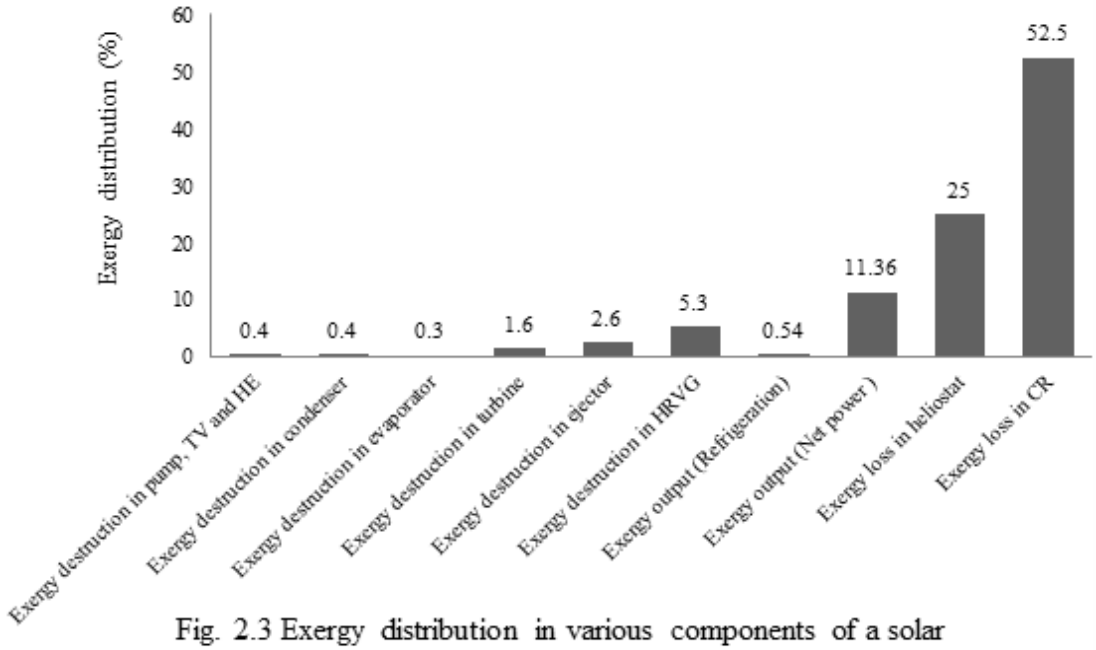

Fig. 2.3 Exergy distribution in various components of a solar operated combined Rankine and ejector refrigeration cycle

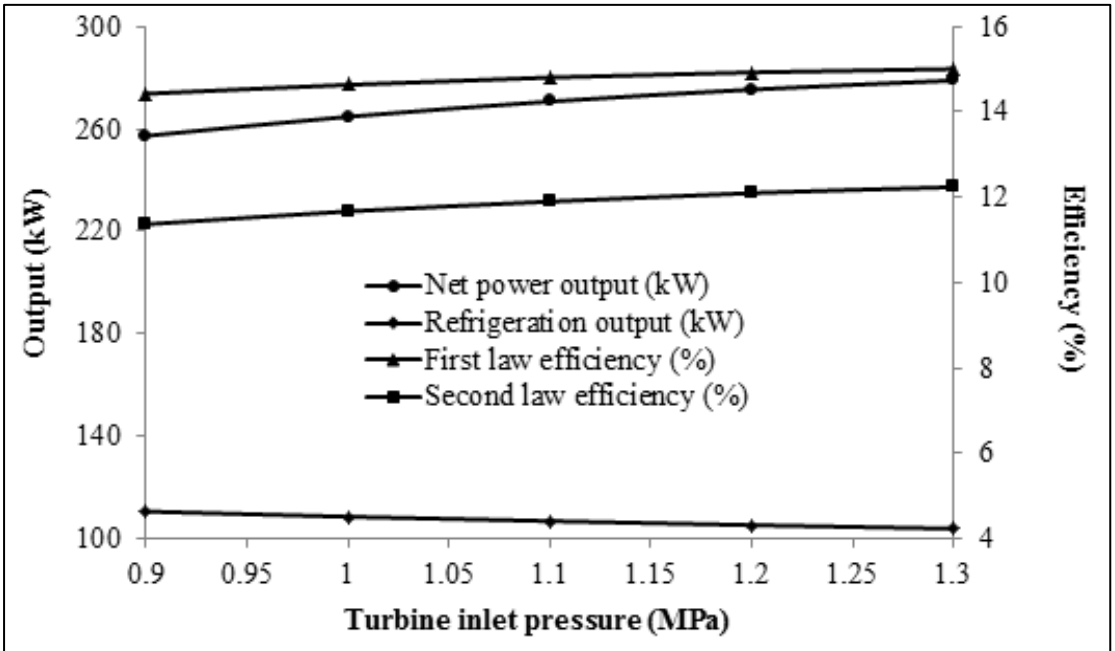

Fig. 2.4 Variation of net power output, refrigeration output, first law efficiency and second law efficiency with turbine inlet pressure

Fig. 2.4 demonstrates the change of net power output, refrigeration output, first law efficiency and second law efficiency with turbine inlet pressure. It is observed that the net power output increases as the turbine inlet pressure increases.

This is due to increase in the enthalpy drop across the turbine as the pressure ratio over the turbine increases. It is also observed that the refrigeration output decreases as the pressure at the inlet of the turbine increases. Increase in turbine inlet pressure causes decrease in turbine extraction temperature (T5) with constant extraction pressure, which is the inlet temperature of primary flow stream to the ejector. The decrease in temperature of primary flow stream reduces the velocity of stream leaving the nozzle in the ejector. This results in decrease of the entrainment ratio in the ejector which reduces the mass flow rate of secondary flow coming from the evaporator. The rate of increase in net power output is more as compare to decrease in refrigeration output thus the combined effect is to increase in first law efficiency with increase in turbine inlet pressure. In addition, second law efficiency increases with increase in turbine inlet pressure as net power output increases.

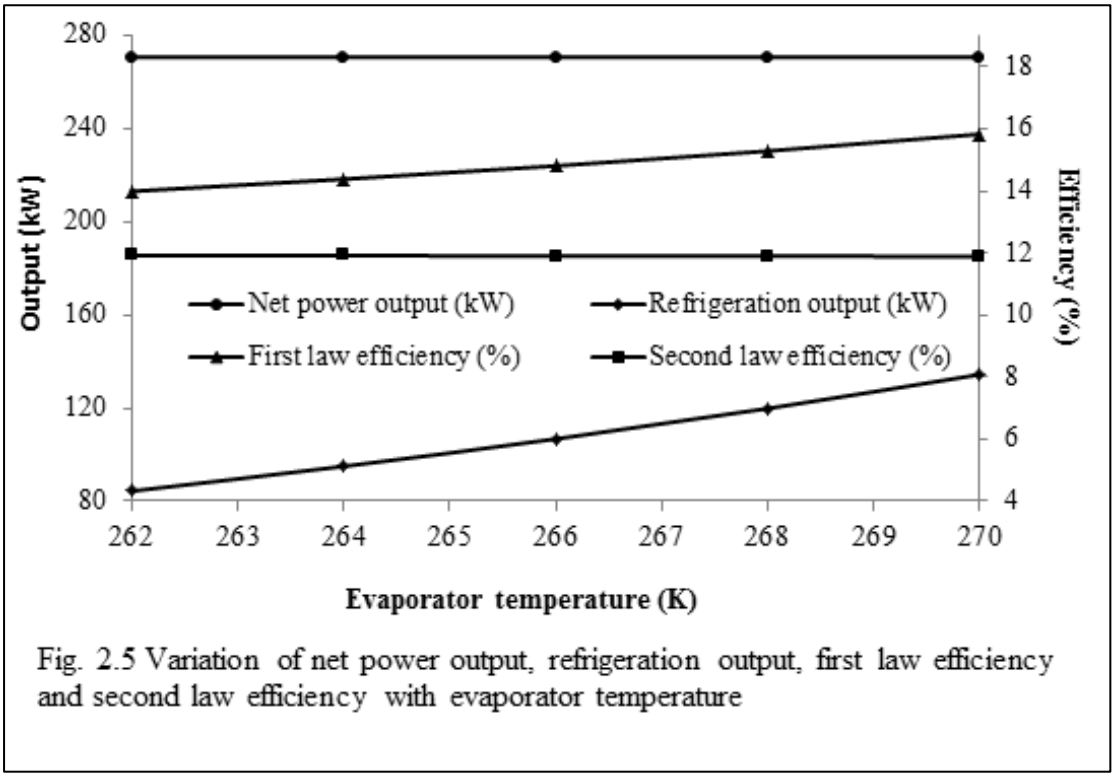

Fig. 2.5 Variation of net power output, refrigeration output, first law efficiency and second law efficiency with evaporator temperature

Fig. 2.5 demonstrates the change of net power output, refrigeration output, first law efficiency and second law efficiency with evaporator temperature. The net power output remains constant with increase in evaporator temperature as the

condition of refrigerant at the entry and exit of the turbine remain same. The refrigeration output and consequently mass flow rate of secondary flow increases with increase in evaporator temperature. Further there is increase in first law efficiency as refrigeration output increases with increase in evaporator temperature whereas there is small decrease in second law efficiency because the exergy of refrigeration output decreases.

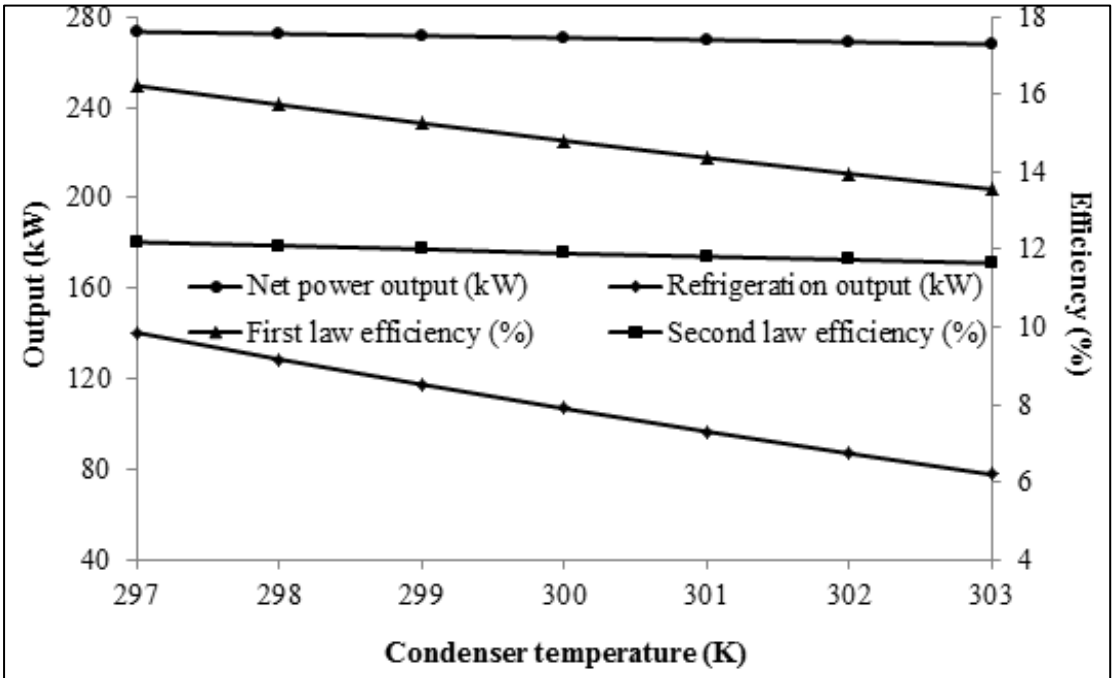

Fig. 2.6 Variation of net power output, refrigeration output, first law efficiency and second law efficiency with condenser temperature

Fig. 2.6 demonstrates the change of net power output, refrigeration output, first law efficiency and second law efficiency with condenser temperature. It is observed that there is decrease in net power output as the condenser temperature increases because the turbine back pressure increases which affects turbine power output. It can also be seen that the refrigeration output decreases as the condenser temperature increases because there is decrease in entrainment ratio which reduces the secondary flow in the evaporator, resulting in a decrease for the refrigeration output.

It also observed that there is decrease in 1st law and 2nd law efficiency with increasing condenser temperature.

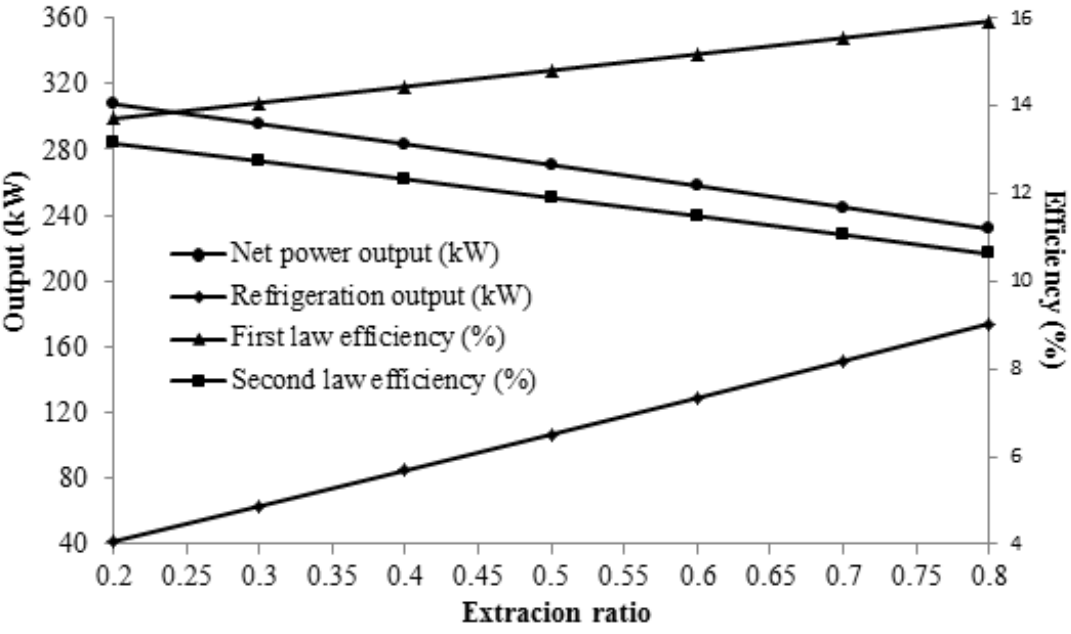

Fig. 2.7 Variation of net power output, refrigeration output, first law efficiency and second law efficiency with extraction ratio

Fig. 2.7 shows the variation of net power output, refrigeration output, first law efficiency and second law efficiency with extraction ratio. It is observed that the net power output decreases and the refrigeration output increases as the extraction ratio increases. It is also found out that there is increase in 1st law efficiency and decrease in 2nd law efficiency with increase in the extraction ratio.

2.5 Summary:

A solar driven combined Rankine and ejector refrigeration cycle is proposed for the generation of power and refrigeration output. Thermodynamic analysis has been done to distinguish the impacts of various parameters like turbine inlet pressure, condenser temperature, evaporator temperature, and extraction ratio on the performance of the proposed cycle. The conclusions of the present investigation can be concise as follows:

- Out of 100% energy (solar heat source) provided to the system around 14.81% is available as useful energy output (i.e. 10.62% net power output and 4.19% refrigeration output), 93.57% is lost to the atmosphere.

- About 11.90% of the total input exergy is accessible as an exergy output (11.36% of exergy related with the net power output, and 0.54% exergy associated with the refrigeration output), and 88.1% of the input (solar heat) exergy is destructed and lost due to irreversibilities.

- The percentage of exergy loss is biggest in central receiver and heliostat which is around 52.5% and 25% respectively.

- The second law efficiency of around 11.90% for solar operated combined Rankine and ejector refrigeration cycle is obtained which is lower than its first law efficiency of 14.81%.

Results got in the present examination might be used by the architects and researchers for a reasonable thermodynamic plan of solar operated combined Rankine and ejector cooling cycle.

CHAPTER 3

EJECTOR COOLING AND POWER CYCLE WITH VARIOUS ECOFRIENDLY REFRIGERANTS

3.1 Introduction:

A parametric study is done to examine the performance of a solar driven combined power and ejector cooling system using various ecofriendly refrigerants (R290, R152a, R134a, and R717). The effect of most influenced parameters such as turbine expansion ratio, driving pressure ratio, and compression pressure ratio on the entrainment ratio, net power output, refrigeration output, 1^{st} law and 2^{nd} law efficiency of the proposed cycle have been studied. The performance comparison of the cycle using various environmentally benign fluids is also studied.

3.2 System description:

Fig. 3.1 shows the solar operated combined power and ejector cooling system. It consists of an extraction turbine (ET) and an ejector (EJ) which produces power and cooling respectively. Solar energy is used to heat the heat transfer fluid (duratherm fluid 600) (14) with the help of heliostat and central receiver. Heat transfer fluid is used to superheat the high pressure refrigerant in the HRVG. Superheated refrigerant vapor (1) expands in the extraction turbine. Extracted vapor (2) flows into the ejector nozzle and entrains secondary vapor (13) from the evaporator, mixes in mixing chamber of the ejector. The ejector exit stream (4) mixes with the extraction turbine exhaust (3) and is cooled in the heat exchanger (5-6), and then enters into the condenser (C). Saturated liquid (7) from condenser then enters into throttle valve (11) and pump (8). The high pressure liquid flows into the heat exchanger (9-10) and then converted into superheated vapor (1) in the HRVG. The saturated liquid (11) expands to the evaporator pressure (11-12) in the throttle valve and vaporized in the evaporator (12-13) to produce refrigeration effect.

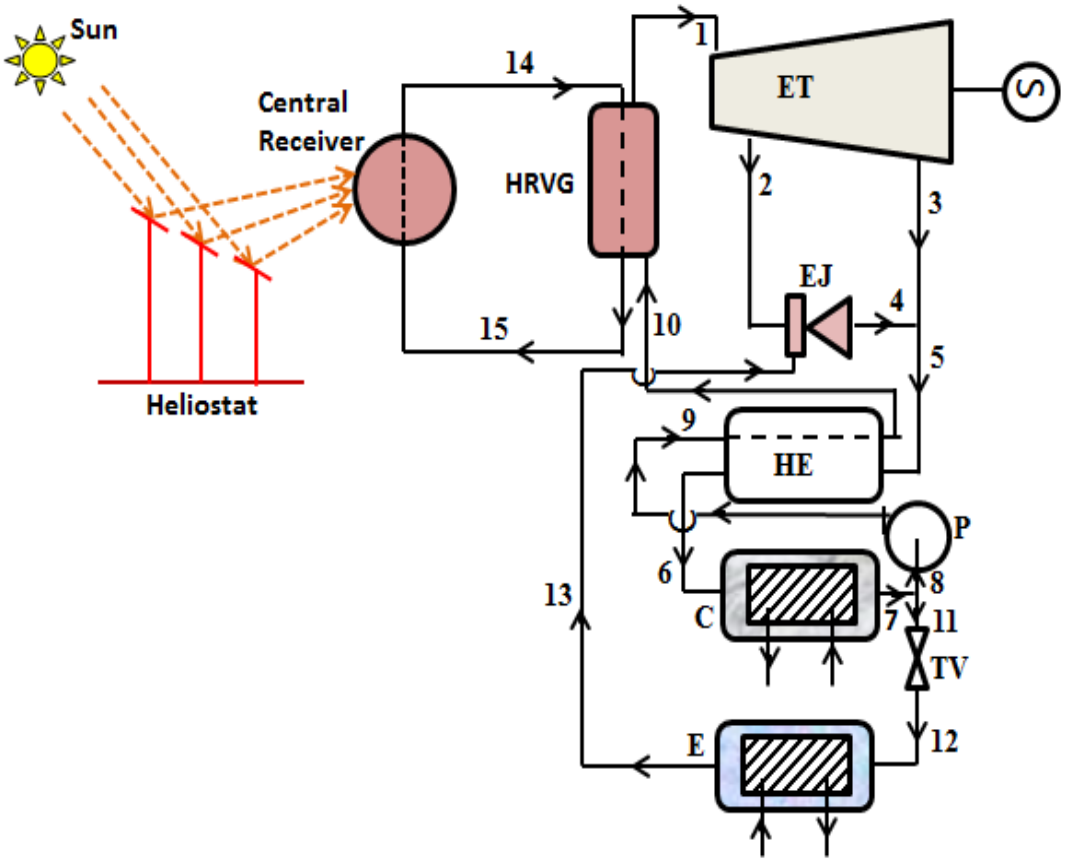

Fig. 3.1 Solar operated combined power and ejector cooling cycle

3.3 Properties of refrigerants

Properties of various ecofriendly refrigerants are given in Table 3.1.

Table 3.1: Properties of ecofriendly refrigerants [84, 86]

Refrigerant	Chemical Formula	Critical Pressure (bar)	Critical Temperature (^{0}C)	NBP (^{0}C)	ODP	GWP
R717	NH3	113.4	133	-33.6	0	<<1
R134a	C2H2F4	40.59	101	-26.4	0	420
R141b	C2H3Cl2F1	46.4	210.2	32.1	0.11	725
R152a	C2H4F2	45.2	113.3	-24.3	0	47
R290	C3H8	42.54	96.8	-42.07	0	3
R600a	C4H10	36.47	135	-11.73	0	3

3.4 Thermodynamic analysis:

First law/energy efficiency (η_E) can be characterized as the proportion of the net power output ($\dot{W}_{net}$) and refrigeration output in the evaporator ($\dot{Q}_E$) to the input solar energy.

$$\eta_E = \frac{\dot{W}_{net} + \dot{Q}_E}{\dot{Q}_{Solar}} = \frac{(\dot{W}_T - \dot{W}_p) + \dot{Q}_E}{A_p G_b} \quad (3.1)$$

Where refrigeration output in the evaporator:

$$\dot{Q}_E = \dot{m}_f E_r \mu (h_{13} - h_{12}) = \dot{m}_w (h_a - h_b) \quad (3.2)$$

Turbine output:

$$\dot{W}_T = \dot{m}_f (h_1 - h_2) + \dot{m}_f (1 - R)(h_2 - h_3) \quad (3.3)$$

$$\dot{m}_f = \dot{m}_{pf} + (1 - R)\dot{m}_f \quad (3.4)$$

Pump work:

$$\dot{W}_p = \dot{m}_f(h_9 - h_8) \tag{3.5}$$

A_p and G_b are the aperture area and solar beam radiation respectively.

Extraction ratio:

$$R = \frac{\dot{m}_{pf}}{\dot{m}_f} = \frac{\dot{m}_2}{\dot{m}_1} \tag{3.6}$$

Entrainment ratio:

$$\mu = \frac{\dot{m}_{13}}{\dot{m}_2} = \frac{\dot{m}_{sf}}{\dot{m}_{pf}} \tag{3.7}$$

Turbine expansion ratio:

$$\tau = \frac{\text{Turbine inlet pressure}}{\text{Turbine exit pressure}} \tag{3.8}$$

Driving pressure ratio:

$$\sigma = \frac{\text{Turbine extraction pressure}}{\text{Ejector exit pressure}} \tag{3.9}$$

Compression pressure ratio:

$$\lambda = \frac{\text{Condeser pressure}}{\text{Evaporator preessure}} \tag{3.10}$$

The second law efficiency (η_X)of proposed system may be reported as

$$\eta_X = \frac{\dot{W}_{net} + \dot{E}_E}{\dot{X}_{Solar}} \tag{3.11}$$

3.5 Parameters consider for operation of proposed system:

Main Parameters consider for operation of proposed system and the range of turbine expansion ratio (τ), driving pressure ratio (σ), compression pressure ratio (λ) at constant condenser pressure for various ecofriendly refrigerants are given in Table 3.2.

Table 3.2: Main Parameters consider for operation of the proposed system [125,127].

Particulars	**R290**	**R152a**	**R134a**	**R717**
Turbine expansion ratio (τ)	3.02-3.62	3.0-4.75	3.75-4.65	3.0-4.25
Driving pressure ratio (σ)	2.3-4.1	2.5-3.9	2.7-3.8	2.5-4.1
Compression pressure ratio (λ)	2.272-4.316	2.423-4.605	2.802-5.138	2.458-4.245
Ambient Temperature (K)	298	298	298	298
Ambient pressure (bar)	1.01325	1.01325	1.01325	1.01325
Turbine inlet Temperature (K)	393	393	393	393
Extraction ratio	0.5	0.5	0.5	0.5
Turbine efficiency (%)	85	85	85	85
Pump efficiency (%)	70	70	70	70
Condenser temperature (K)	303	303	303	303
Evaporator temperature (K)	273	273	273	273
Water temperature inlet to evaporator (K)	299	299	299	299
Water temperature outlet to evaporator (K)	283	283	283	283
Apparent temperature of the Sun (K)	4500	4500	4500	4500
Heliostat aperture area (m^2)	3000	3000	3000	3000

Solar beam radiation (kWm^{-2})	0.85	0.85	0.85	0.85
Oil temperature inlet to CR (K)	363	363	363	363
Oil temperature inlet to HRVG (K)	403	403	403	403
HRVG efficiency (%)	100	100	100	100
Pinch point temperature difference (℃)	10.0	10.0	10.0	10.0
Nozzle efficiency (%)	90	90	90	90
Mixing efficiency (%)	85	85	85	85
Diffuser efficiency (%)	85	85	85	85
1^{st} law efficiency of heliostat field (%)	75	75	75	75
1^{st} law efficiency of CR (%)	90	90	90	90
2^{nd} law efficiency of heliostat field (%)	75	75	75	75
2^{nd} law efficiency of CR	varied	varied	varied	varied

3.6 Result and discussion:

A parametric study has been done to examine the impact of some influenced parameters on the performance of a solar driven combined power and ejector cooling system.

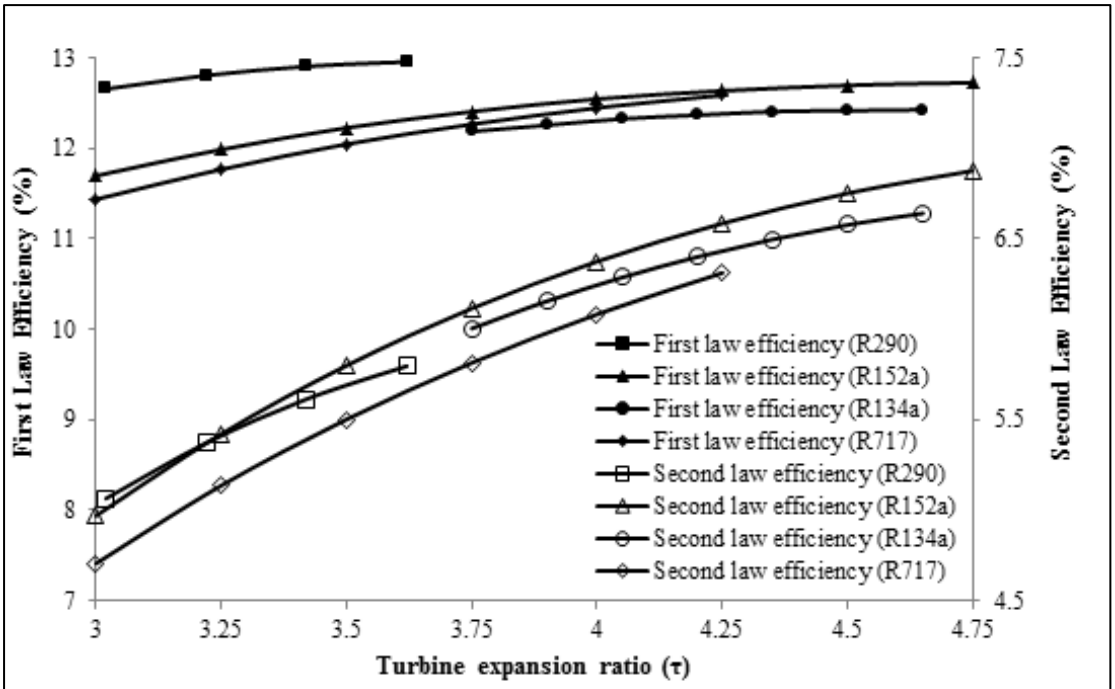

Fig. 3.2 Effect of turbine expansion ratio on First and Second law efficiency of the cycle

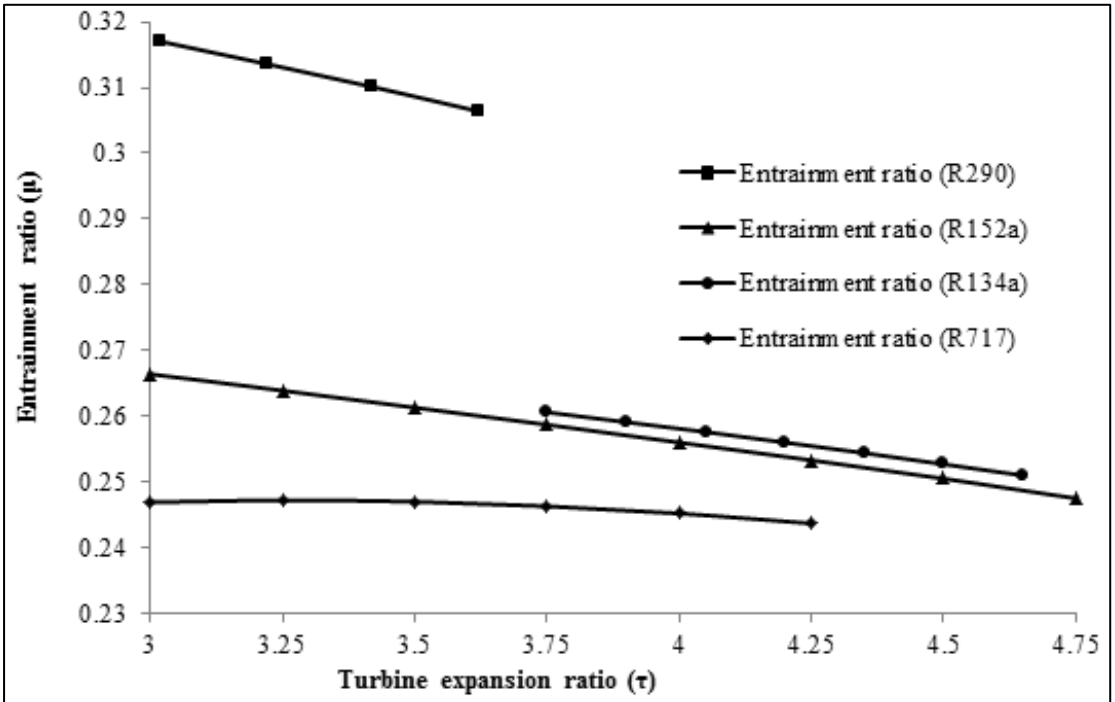

Fig. 3.3 Effect of turbine expansion ratio on entrainment

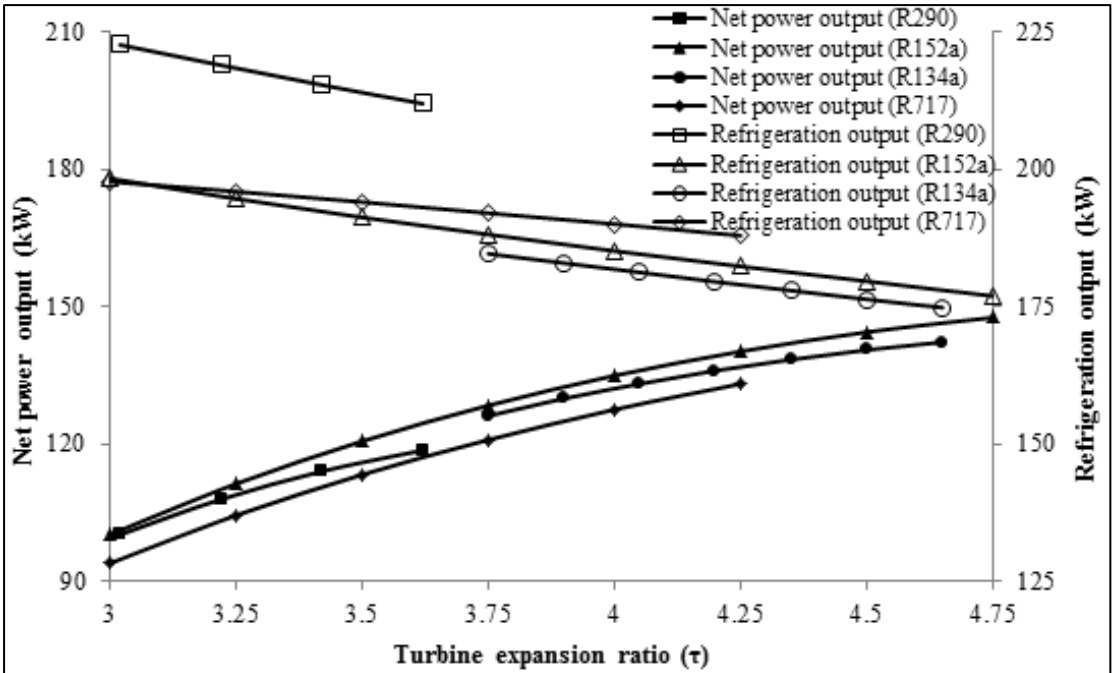

Fig. 3.4 Effect of turbine expansion ratio on net power output and refrigeration output of the cycle

Fig. 3.2, 3.3 and 3.4 show the effect of variation of turbine expansion ratio (τ) for constant turbine extraction pressure, condenser pressure and evaporator pressure on first law efficiency and second law efficiency , entrainment ratio, net power output and refrigeration output for various eco-friendly refrigerants (R290, R152a, R134a, and R717). As turbine expansion ratio (τ) increases keeping the condenser pressure constant, enthalpy change across the turbine increases which results in increase in net power output. At the same time, refrigeration output decreases because at high turbine expansion ratio the turbine extraction temperature (T_2) decreases. The increase in turbine power output is more than the decrease in refrigeration output brings about in increase in first law efficiency. A similar trend is also observed for the second law efficiency because the turbine power output increases and exergy of refrigeration output decreases with the increase in turbine expansion ratio. With the increase in turbine expansion ratio (τ), there is decrease in turbine extraction temperature (T_2). This decrease in turbine extraction temperature results in decrease in enthalpy drop in the nozzle of the ejector which causes the reduction of the velocity of primary flow at the exit of the nozzle in the ejector i.e. the entrainment ratio decreases. As stated

earlier when turbine expansion ratio increases, the enthalpy change across the turbine increases which results in increase in net power output. At the same time refrigeration output decreases because at high turbine expansion ratio the turbine extraction temperature decreases.

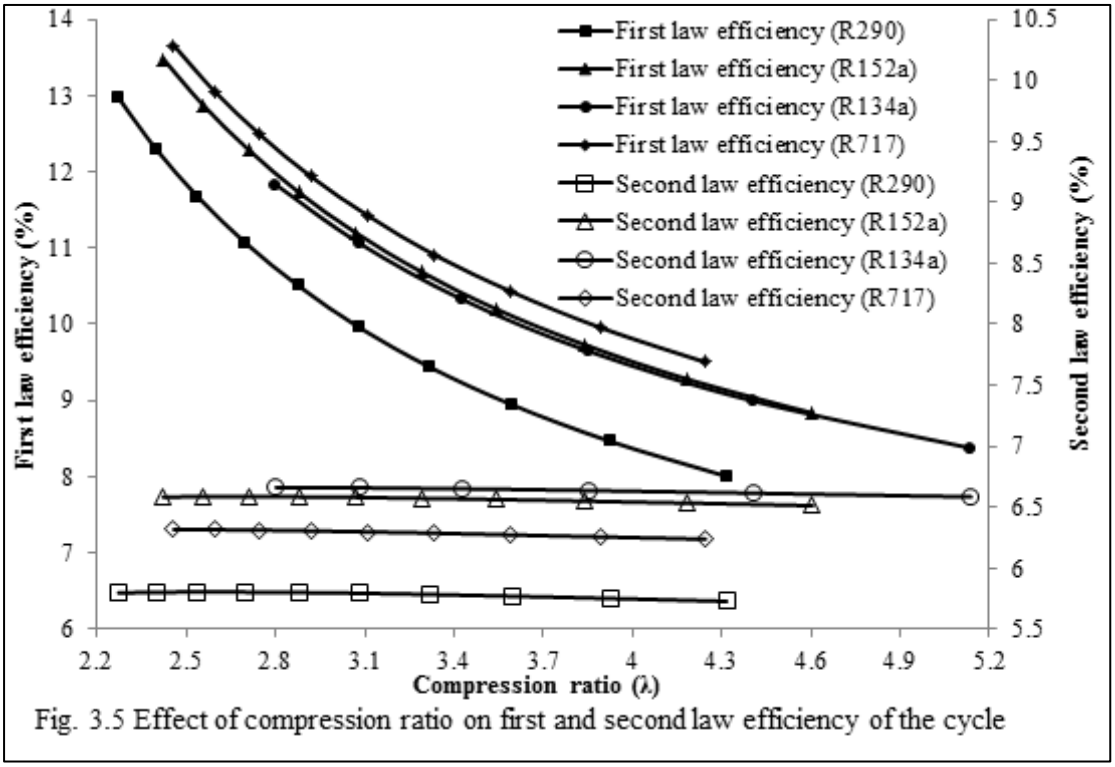

Fig. 3.5 Effect of compression ratio on first and second law efficiency of the cycle

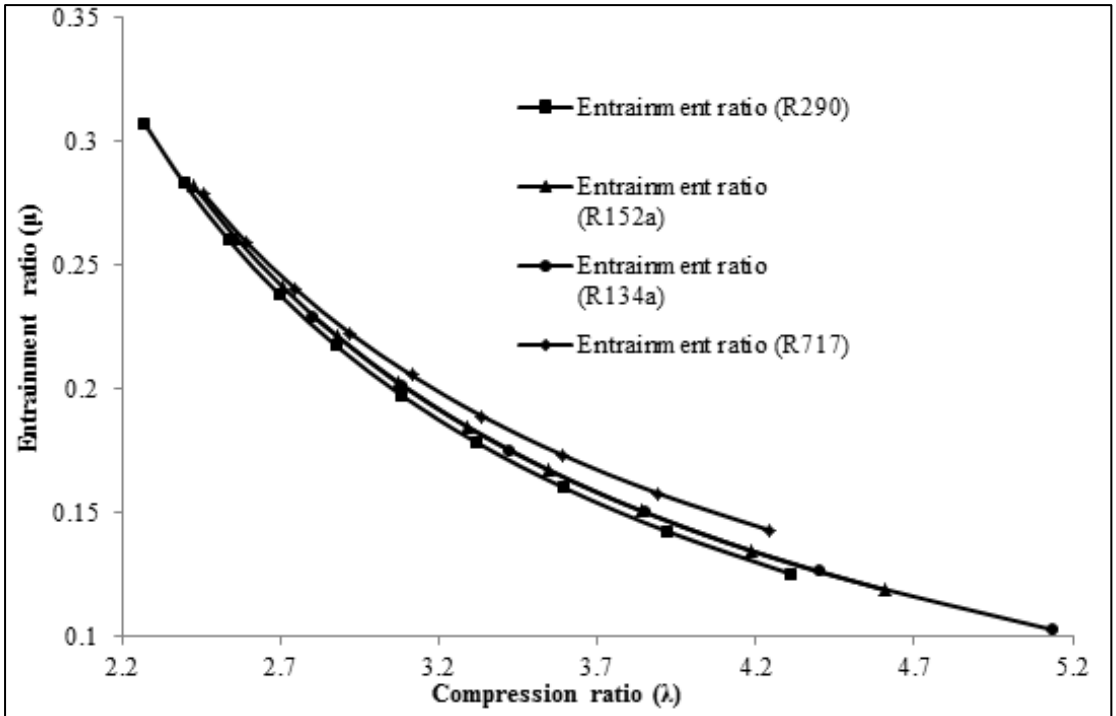

Fig. 3.6 Effect of compression ratio on entrainment ratio

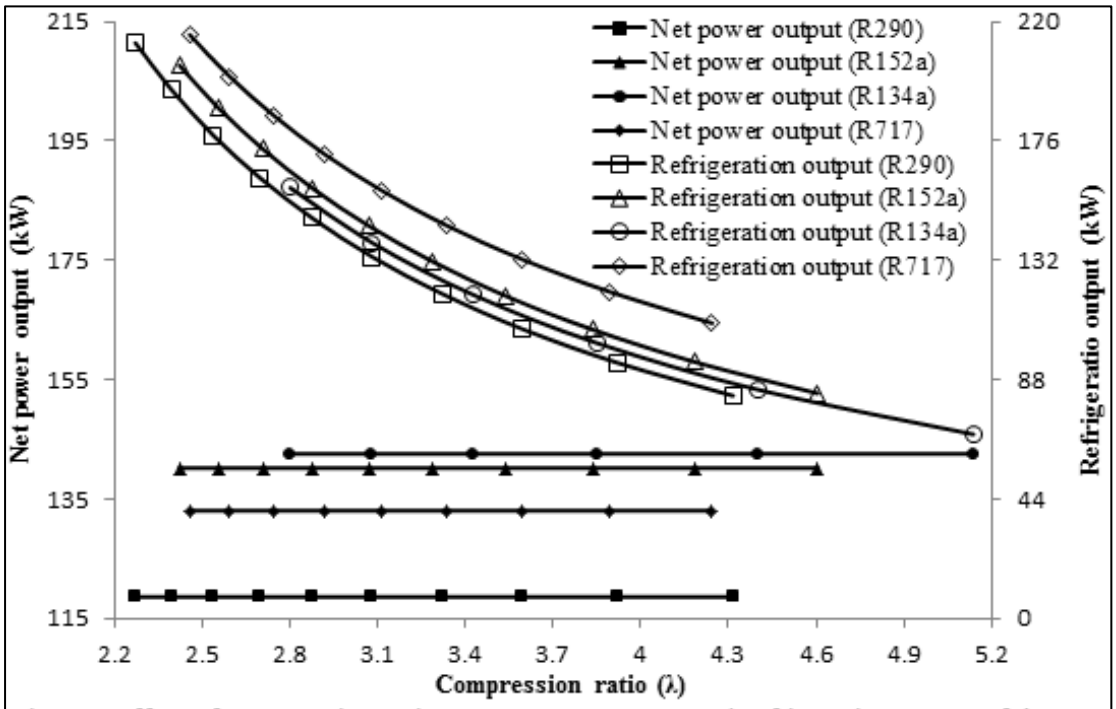

Fig. 3.7 Effect of compression ratio on net power output and refrigeration output of the cycle

Fig. 3.5, 3.6 and 3.7 show the effect of variation of compression ratio (λ) for constant turbine inlet pressure, turbine extraction pressure, and condenser pressure on first law efficiency and second law efficiency, entrainment ratio, net power output and refrigeration output for various eco-friendly refrigerants (R290, R152a, R134a, and R717). As the compression ratio increases at constant condenser pressure, evaporator temperature and entrainment ratio decreases. This causes the lower refrigeration output and first law efficiency. The exergy of refrigeration is combined effect of refrigeration output and evaporator temperature which results in almost constant second law efficiency. As the inlet and exit state in the turbine remain same so there is no change in net power output.

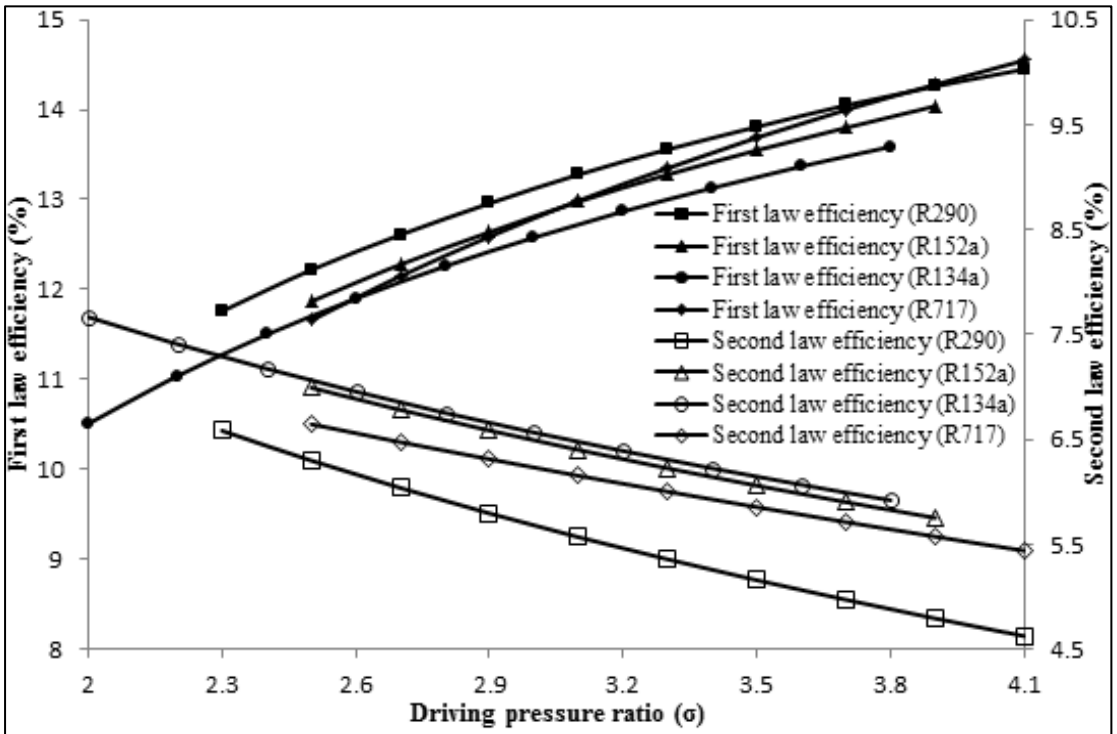

Fig. 3.8 Effect of driving pressure ratio on first and second law efficiency of the cycle

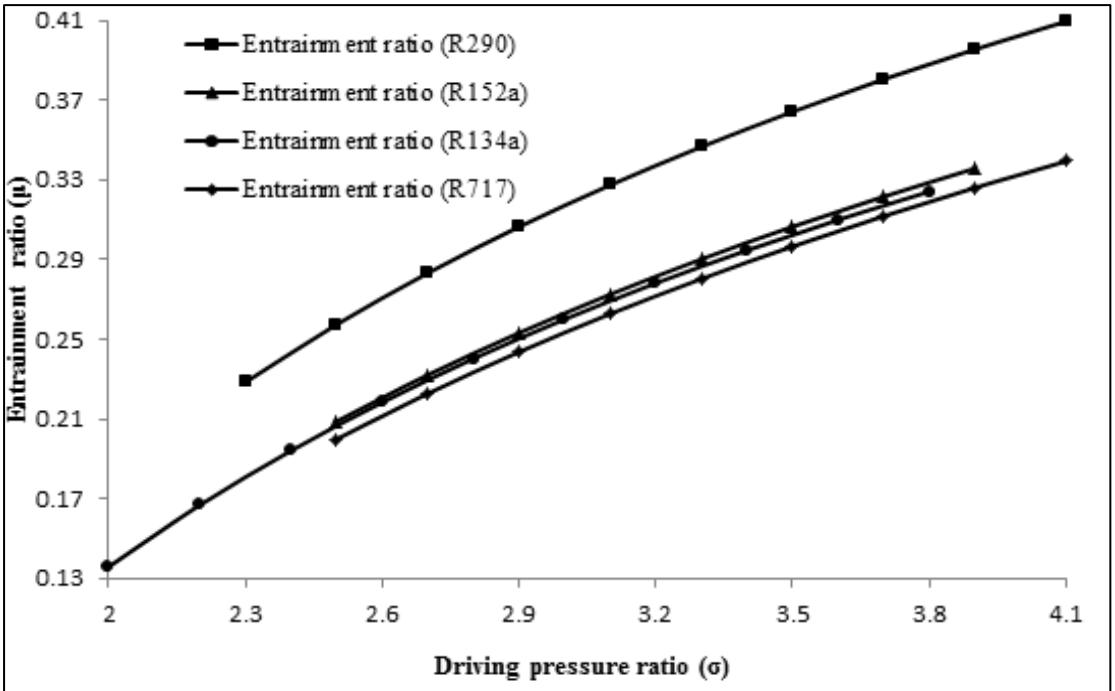

Fig. 3.9 Effect of driving pressure ratio on entrainment ratio

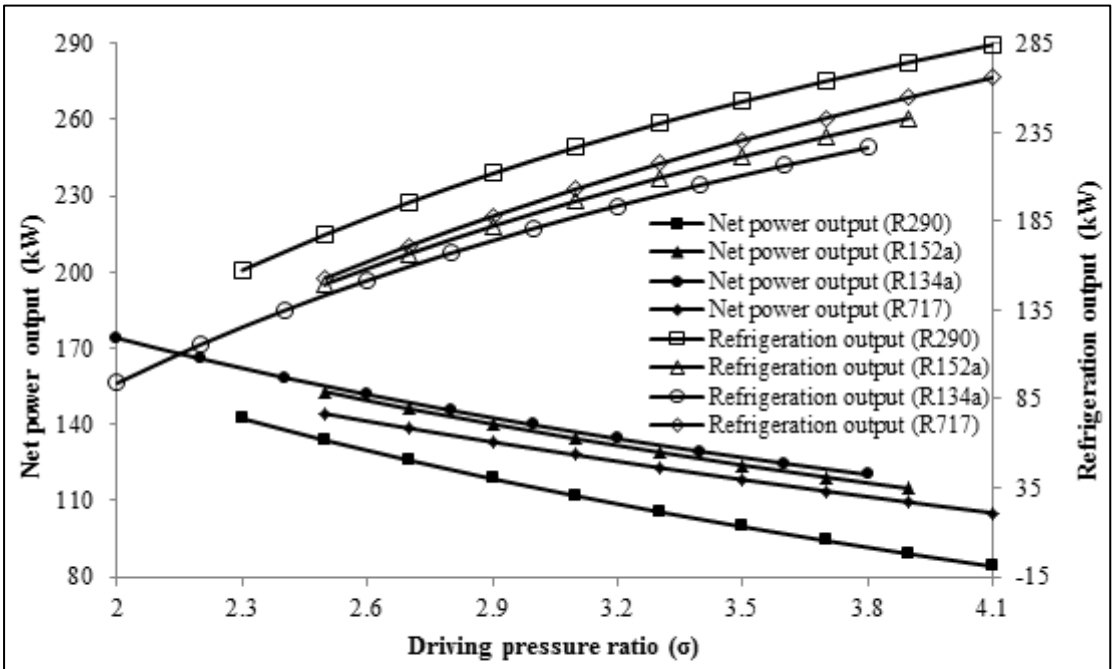

Fig. 3.10 Effect of driving pressure ratio on net power output and refrigeration output of the cycle

Fig. 3.8, 3.9 and 3.10 show the effect of driving pressure ratio (σ) for constant turbine inlet pressure, condenser pressure , and evaporator pressure on first law efficiency and second law efficiency, entrainment ratio, net power output and refrigeration output for various eco-friendly refrigerants (R290, R152a, R134a, and R717). As driving pressure ratio increases (or extraction pressure increases) net power output decreases. Due to higher driving pressure ratio, the ejector suck more secondary refrigerant from the evaporator at constant evaporator pressure resulting in increase in entrainment ratio, refrigeration output and exergy of refrigeration. Increase in the refrigeration output is more than the reduction in net power output causing in increase in first law efficiency and decrease in second law efficiency.

The performance of the system for various ecofriendly refrigerants at different turbine expansion ratio (τ), compression ratio (λ), driving pressure ratio (σ) is summarized in Table 3.3.

Table 3.3: Performance of the system for various ecofriendly refrigerants

	R290	**R152a**	**R134a**	**R717**
(η_E)	High η_E for high τ Low η_E for high λ High η_E for high σ		Low η_E for high τ Low η_E for high σ	High η_E for high λ
(η_X)	Low η_X for high λ Low η_X for high σ	High η_X for high τ	High η_X for high λ High η_X for high σ	Low η_X for high τ
$\dot{W}_{net}$	Low $\dot{W}_{net}$ for high λ Low $\dot{W}_{net}$ for high σ	High $\dot{W}_{net}$ for high τ	High $\dot{W}_{net}$for high λ High $\dot{W}_{net}$ for high σ	Low $\dot{W}_{net}$ for high τ
$\dot{Q}_E$	High $\dot{Q}_E$ for high τ Low $\dot{Q}_E$ for high λ High $\dot{Q}_E$for high σ		Low $\dot{Q}_E$ for high τ Low $\dot{Q}_E$ for high σ	High $\dot{Q}_E$ for high λ

3.7 Summary:

Present study deals with the solar operated combined power and an ejector refrigeration cycle with ecofriendly refrigerants as working substance. The effect of most influenced parameters such as turbine expansion ratio, driving pressure ratio, and compression pressure ratio has been observed on the performance (1^{st} law efficiency and 2^{nd} law efficiency, entrainment ratio, net power output and refrigeration output) of the proposed cycle.

From the above discussion, it can be concluded that

- As the turbine expansion ratio (τ) increases (3 to 4.75), net power output, first and second law efficiency increases while the entrainment ratio and refrigeration output decreases. First law efficiency is maximum (12.96%) for R290 at turbine expansion ratio of 3.62 (at compression ratio 2.274, driving pressure ratio 2.9) while second law efficiency is maximum (6.88%) for R152a at turbine expansion ratio of 4.75 (at compression ratio 2.613, driving pressure ratio 2.9). Beyond this turbine expansion ratio the working of the fluid is not feasible.
- As the compression ratio (λ) increases, entrainment ratio, refrigeration output and first law efficiency decreases, no change in net power output and second law efficiency is almost constant.
- As the driving pressure ratio (σ) increases (2 to 4.1), entrainment ratio, refrigeration output, and first law efficiency increases while second law efficiency and net power output decreases. First law efficiency is maximum (14.45%) for R290 at driving pressure ratio of 3.62 (at compression ratio 2.274, turbine expansion ratio 3.62) while second law efficiency is maximum (7.67%) for R134a at driving pressure ratio of 3.75 (at compression ratio 2.63, turbine expansion ratio 4.7). Beyond this driving pressure ratio the working of the fluid is not feasible.

Results got might be used by the architects and researchers for outline a solar operated combined power and ejector cooling cycle.

CHAPTER 4

EJECTOR ORGANIC RANKINE CYCLE INTEGRATED WITH A TRIPLE PRESSURE LEVEL VAPOUR ABSORPTION SYSTEM

4.1 Introduction:

The proposed multi-generation system consists of ejector organic Rankine cycle integrated with a triple pressure level absorption system (TPLAS) based on parabolic trough collector (PTC) solar field. The proposed system produces power and refrigeration output at two different temperatures simultaneously. Thermodynamic investigation is led to find the impact of different outline parameters such as solar beam radiation (SBR), turbine inlet pressure, turbine extraction pressure, and ejector evaporator temperature on the performance of proposed system (system2) and also compared with the performance of ejector organic Rankine cycle (system1). Assessment for irreversibility of individual parts of the cycle leads to possible measures for performance enhancement. To produce continuous output during insufficient solar radiation, oil tanks are provided between the PTC field and G2 as thermal energy storage. This cycle meets out the demand of electricity, space air-conditioning and preservation of fruits & vegetables in cold storage. This multi-generation cycle also meets out the varying demands of power and refrigeration by changing the turbine extraction pressure. The performance of EORC and proposed multi-generation cycle is also compared on the basis of energy and exergy methodology.

4.2 Working of proposed system:

The description for ejector organic Rankine cycle (system1) shown in Fig. 4.1 can be done on the same bases as of system2 in Fig. 4.2 mentioned below. Both the systems have fixed mass flow rate of HTF. Also the exit temperature of HTF from PTC at given SBR is considered to be same.

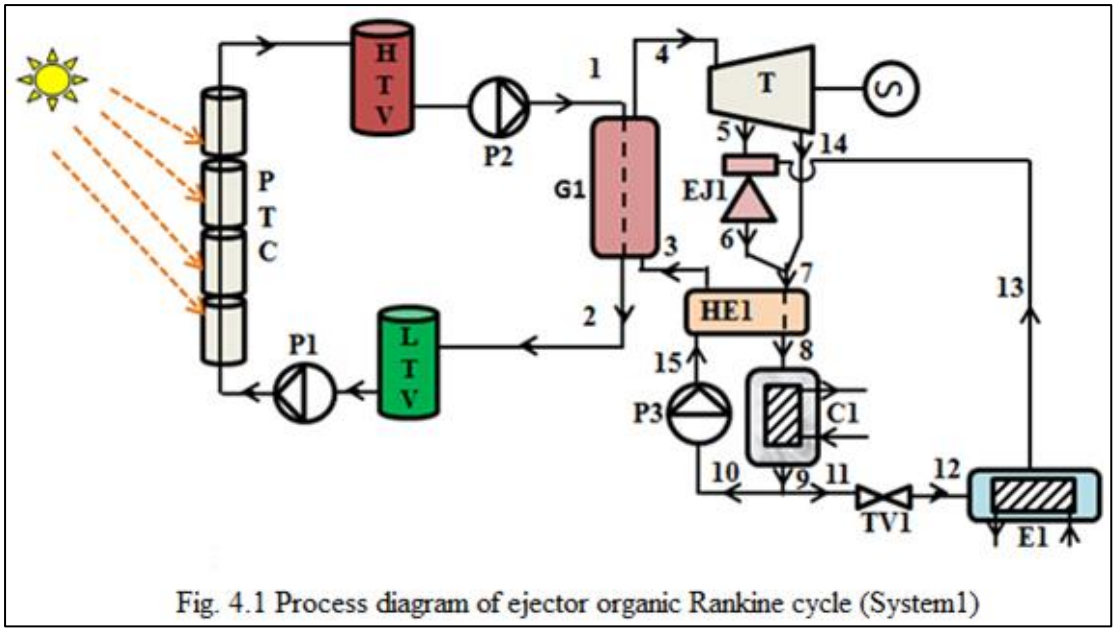

Fig. 4.1 Process diagram of ejector organic Rankine cycle (System1)

The proposed system consists of ejector organic Rankine cycle integrated with a triple pressure level vapour absorption system based on parabolic trough collector (PTC) solar field as shown in Fig. 4.2. Solar energy is used to heat the heat transfer fluid (Therminol VP1) (1) with the help of PTC field. Heat transfer fluid (HTF) enters the heat recovery vapor generator (G1) which is used to superheat the high pressure refrigerant and leaves at (2), which again enters the TPLAS generator (G2) to vaporize the water vapor from LiBr-H2O solution and return back to the PTC solar field (16). Superheated refrigerant vapor (4) expands in the turbine. After expansion up to the extraction pressure (Pext), refrigerant vapors are extracted (5) from turbine at extraction pressure and then flows into the nozzle of the ejector. The primary refrigerant vapour from the nozzle of the ejector, entrains the secondary refrigerant vapor (13) from the evaporator (E1) mixes in mixing chamber of the ejector (EJ1). The ejector exit stream (6) mixes with the turbine exhaust stream (14) and is cooled in the heat exchanger (HE1) (7-8) by transferring the heat to the refrigerant (15-3) and enters into the condenser (C1). Saturated liquid refrigerant (9) from condenser enters into throttle valve (TV1) (11) and pump (P3) (10). The high pressure liquid refrigerant (15) from pump (P3) flows into the heat exchanger (HE1) (15-3) is preheated and then converted into superheated refrigerant vapor (4) in the heat recovery vapor generator (G1). The saturated liquid refrigerant (11) expands to the evaporator pressure (11-12) in the throttle valve (TV1) and vaporized in the evaporator (E1) (12-13) to produce

refrigeration effect. The water vapor (23) leaving from the TPLAS generator (G2) is condensed in the condenser (C2) and leaves as saturated water (24) which further cools in the liquid vapor heat exchanger (HE3) (24-25) then it expands in throttle valve (TV2) to the evaporator pressure (25-26) and vaporized in the evaporator (E2) (26-27) to produce refrigeration effect. The refrigerant water vapor coming from the evaporator (E2) is preheated in the HE3 (27-28). The LiBr-H2O solution (20) from the TPLAS generator (G2) enters into the heat exchanger (HE2) and cools to (21). The solution (21) flows into the ejector nozzle and it entrains secondary water vapor (28) from the heat exchanger (HE3) and mixes in mixing chamber of the ejector (EJ2). The exit of the ejector flows in the absorber (ABS) (22) and leaves as rich solution (17), which passes through pump (P5) (17-18) and heat exchanger (HE2) (18-19) and finally enters the TPLAS generator (G2).

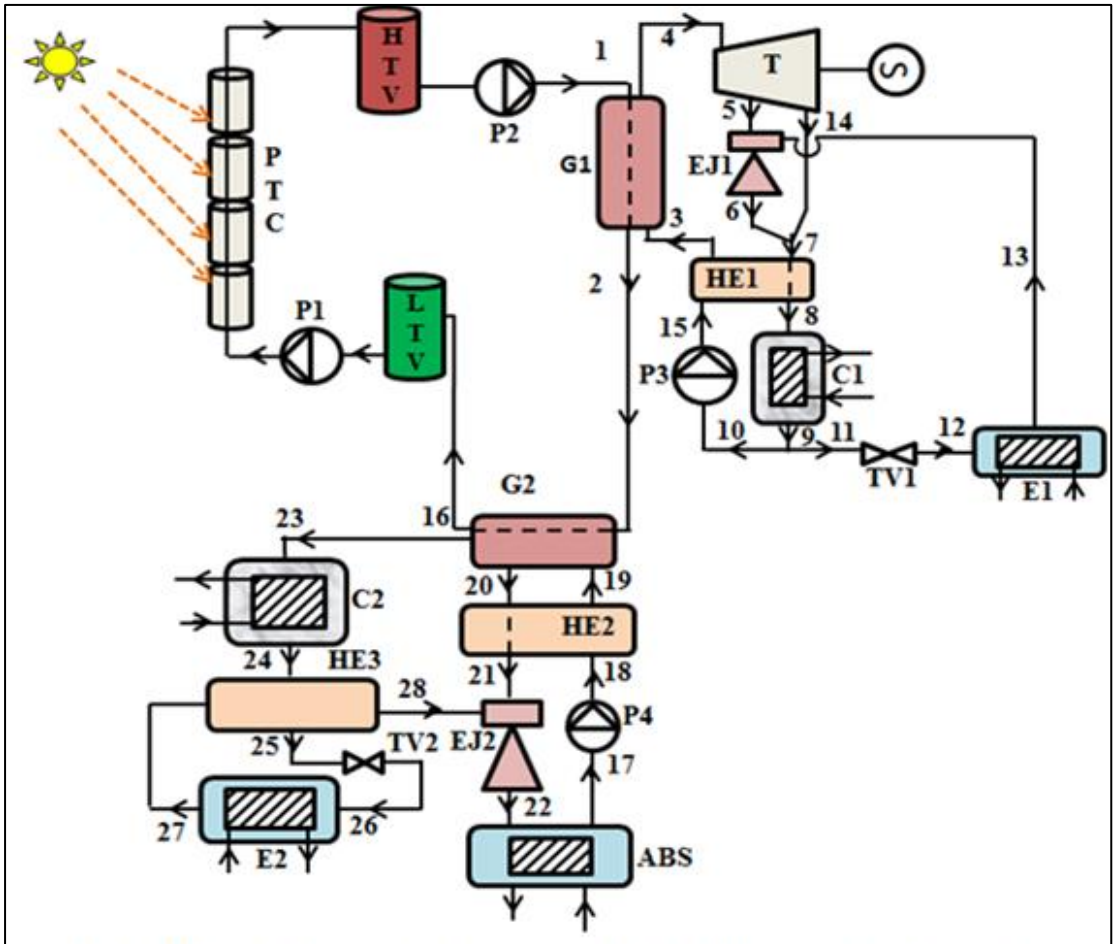

Fig. 4.2 Process diagram of ejector organic Rankine cycle integrated with a triple pressure level vapour absorption system (System2)

For the thermodynamic analysis, the parameters considered for the operation of proposed system are depicted in Table 4.1.

Table 4.1: Main parameters considered for the analyses [127-130, 147].

Atmospheric temperature (^{0}C)	25
Atmospheric pressure (bar)	1.01325
Pressure at the inlet of the turbine (bar)	11
Extraction pressure (bar)	4
Extraction ratio	0.3
Efficiency of the turbine (%)	85
Efficiency of the pump (%)	80
Mass flow rate of HTF (kg/s)	22
Tracking mode for PTC field	Focal axis N-S horizontal and E-W tracking
Inlet temperature of HTF in PTC for system1 (^{0}C)	100
Inlet temperature of HTF in PTC for system2 (^{0}C)	90
Pinch point temperature difference (^{0}C)	10
Ejector evaporator temperature (^{0}C)	-5
Condenser temperature (^{0}C)	36
Solar beam radiation (W/m^2)	600
Aperture Area (m^2)	10000
TPLAS evaporator temperature (^{0}C)	10
TPLAS generator temperature (^{0}C)	85

4.3 Energy and exergy analysis of the proposed system:

In order to simulate the performance of the proposed system, the principle of mass and energy conservation are used. The mass and energy balance for a general steady flow system was given as

$$\sum_{in} \dot{m} = \sum_{out} \dot{m} \tag{4.1}$$

The rate of mass transfer into the system is $\sum_{in} \dot{m}$ and the rate of mass transfer out of the system is $\sum_{out} \dot{m}$

$$\dot{E}_{in} = \dot{E}_{out} \tag{4.2}$$

$$\dot{Q}_{in} + \dot{W}_{in} + \sum_{in} \dot{m}\left(h + \frac{C^2}{2} + gz\right) = \dot{Q}_{out} + \dot{W}_{out} + \sum_{out} \dot{m}\left(h + \frac{C^2}{2} + gz\right) \tag{4.3}$$

$$\dot{X}_{heat} - \dot{X}_{work} + \dot{X}_{mass,in} - \dot{X}_{mass,out} - \dot{X}_d = \Delta\dot{X} \tag{4.4}$$

$$\dot{X}_{heat} = \sum (1 - \frac{T_0}{T})\dot{Q} \tag{4.5}$$

$$\dot{X}_{work} = \dot{W} - p_0 dV \tag{4.6}$$

$$\dot{X}_{mass} = \dot{m}[(h - h_0) - T_0(s - s_0)] \tag{4.7}$$

4.3.1 Energy analysis

Solar energy received from the Sun

$$\dot{Q}_{Solar} = G_b A_p \tag{4.8}$$

where

G_b = I Cosθ = Solar beam radiation

I = Direct normal irradiance (Wm^{-2}),

A_p = Aperture area (m^2),

θ =Incidence angle.

Heat gain in the PTC field for ejector organic Rankine cycle (System1)

$$\dot{Q}_{gain} = \dot{m}_1(h_1 - h_2) = \eta_{E,\ PTC} G_b A_p = \dot{m}_4\ (h_4 - h_3) \tag{4.9}$$

where $\eta_{E,\ PTC}$ = Energy efficiency of PTC field

$$\eta_{E,\ PTC} = a - b\left[\frac{T_m - T_0}{G_b}\right] - c\left[\frac{(T_m - T_0)^2}{G_b}\right] \tag{4.10}$$

a = optical efficiency = 0.7, b = first order loss coefficient = 0.1, c = second order loss coefficient = 0, $T_m = \{(T_i+T_o)/2\}$ = mean temperature of HTF.

The energy efficiency of the system1 (η_{E1}) can be characterized as the proportion of the network output ($\dot{W}_{net}$) and refrigeration output in the ejector evaporator ($\dot{Q}_{e_1}$) to the solar energy input ($\dot{Q}_{Solar}$).

$$\eta_{E1} = \left(\dot{W}_{net} + \dot{Q}_{e_1}\right)/\dot{Q}_{Solar} \tag{4.11}$$

Turbine work output

$$\dot{W}_T = \dot{m}_4(h_4 - h_5) + \dot{m}_4(1 - R)(h_5 - h_{14}) \tag{4.12}$$

where extraction ratio (R) is reported as

$$R = \dot{m}_5/\dot{m}_4 \tag{4.13}$$

Pump work

$$\dot{W}_P = \dot{m}_4(h_{15} - h_{10}) \tag{4.14}$$

Work output

$$\dot{W}_{net} = \dot{W}_T - \dot{W}_P \tag{4.15}$$

Refrigeration output in ejector evaporator (E_1)

$$\dot{Q}_{e_1} = \dot{m}_5\mu_1(h_{13} - h_{12}) \tag{4.16}$$

Work to refrigeration ratio for system1

$$\varepsilon_1 = \dot{W}_{net}/\dot{Q}_{e_1} \tag{4.17}$$

Heat gain in the PTC field for ejector organic Rankine cycle integrated with triple pressure level vapour absorption system (system2)

$$\dot{Q}_{gain} = \dot{m}_1(h_1 - h_{16}) = \eta_{E,\ PTC} G_b A_p = \dot{m}_4\ (h_4 - h_3) + \dot{m}_{23} h_{23} + \dot{m}_{20} h_{20} - \dot{m}_{19} h_{19} \tag{4.18}$$

Solution circulation ratio of TPLAC

$$f = \dot{m}_{17}/\dot{m}_{28} \tag{4.19}$$

$$\text{Compression pressure ratio} = \frac{\text{Absorber pressure}}{\text{Evaporator pressure}} = \frac{p_{22}}{p_{26}} \tag{4.20}$$

The energy efficiency (η_{E2}) of the system2 characterized as the proportion of summation of the network output ($\dot{W}_{net}$) and total refrigeration output in the ejector evaporator E_1 ($\dot{Q}_{e_1}$) and TPLAS evaporator E_2 ($\dot{Q}_{e_2}$) to the solar energy input ($\dot{Q}_{Solar}$).

$$\eta_{E2} = \left(\dot{W}_{net} + \dot{Q}_{e_1} + \dot{Q}_{e_2}\right)/\dot{Q}_{Solar} \tag{4.21}$$

Refrigeration output in TPLAS evaporator (E_2)

$$\dot{Q}_{e_2} = \dot{m}_{26}(h_{27} - h_{26}) \tag{4.22}$$

Work to refrigeration ratio for system2

$$\varepsilon_2 = \dot{W}_{net}/\left(\dot{Q}_{e_1} + \dot{Q}_{e_2}\right) \tag{4.23}$$

Entrainment ratio for ejector (EJ_1)

$$\mu_1 = \dot{m}_{13}/\dot{m}_5 \tag{4.24}$$

Entrainment ratio for ejector (EJ_2)

$$\mu_2 = \dot{m}_{28}/\dot{m}_{21} \tag{4.25}$$

4.3.2 Exergy analysis

Exergy efficiency of PTC field is given by

$$\eta_{x,\ PTC} = \{\dot{m}(h_1 - h_{16}) - T_0(s_1 - s_{16})\}/G_b A_p \psi \tag{4.26}$$

Maximum useful work obtainable from sun radiation (ψ) is calculated from [144] that is given as

$$\psi = 1 - \frac{4}{3}\frac{T_0}{T_{solar}} + \frac{1}{3}\left(\frac{T_0}{T_{solar}}\right)^4 \tag{4.27}$$

The exergy efficiency (η_{x1}) of system1 may be reported as

$$\eta_{x1} = \left(\dot{W}_{net} + \dot{X}_{e_1}\right)/\dot{X}_{Solar} \tag{4.28}$$

where, $\dot{X}_{Solar}$ is exergy input associate with solar radiation falling on PTC field, $\dot{X}_{e_1}$ is the exergy associate with refrigeration output in the ejector evaporator (E_1),

$$\dot{X}_{e_1} = \dot{Q}_{e_1}\left[(T_0/T_{e_1}) - 1\right] \tag{4.29}$$

Work to exergetic refrigeration ratio for system1

$$\varepsilon_{x1} = \dot{W}_{net}/\dot{X}_{e_1} \tag{4.30}$$

The exergy efficiency (η_{x2}) of the system2 may be reported as

$$\eta_{x2} = \left(\dot{W}_{net} + \dot{X}_{e_1} + \dot{X}_{e_2}\right)/\dot{X}_{Solar} \tag{4.31}$$

Work to exergetic refrigeration ratio for system2

$$\varepsilon_{x2} = \dot{W}_{net}/\left(\dot{X}_{e_1} + \dot{X}_{e_2}\right) \tag{4.32}$$

$\dot{X}_{e_2}$ is the exergy associate with refrigeration output in the TPLAS evaporator (E_2)

$$\dot{X}_{e_2} = \dot{Q}_{e_2}\left[(T_0/T_{e_2}) - 1\right] \quad (4.33)$$

$$\dot{X}_{Solar} = G_b A_p \psi \quad 4.34)$$

4.4 Result and discussion:

Performance analysis of PTC field based ejector organic Rankine cycle integrated with a triple pressure level vapor absorption system (system2) has been carried out. A theoretical examination is directed to determine the impact of different design parameters, for example, SBR, turbine inlet pressure, turbine extraction pressure, and ejector evaporator temperature on the **performance** of system1 & system2. In this investigation, where a thermodynamic parameter is varied, the other parameters are kept steady as specified in Table 4.1.

Table 4.2 and 4.3 shows the thermodynamic state of each point for system1& system2.

Table 4.4 and 4.5 shows the distribution of energy & exergy in various components of system1 and system2.

Table 4.2 Results of simulation for system1

State points	P (kPa)	T (^{0}C)	ṁ (kg/s)	h (kJ/kg)	s (kJ/kgK)
1	1500	172	22	443.9	22.74
2	1400	100	22	258	12.71
3	1100	82.83	15.77	139.4	0.473
4	1100	162	15.77	398.7	1.128
5	400	127.8	4.731	375.8	1.138
6	116.1	108.7	5.479	362.9	1.19

7	116.1	98.08	16.52	353.6	1.165
8	116.1	36	16.52	298.3	1.001
9	116.1	36	16.52	80.31	0.2962
10	116.1	36	15.77	80.31	0.2962
11	116.1	36	0.7484	80.31	0.2962
12	22.28	-5	0.7484	80.31	0.3085
13	22.28	-5	0.7484	273.8	1.03
14	116.1	92.77	11.04	348.9	1.152
15	1100	37.05	15.77	81.55	0.3002

Table 4.3 Results of simulation for system2

State points	P (kPa)	T (^{0}C)	ṁ (kg/s)	h (kJ/kg)	s (kJ/kgK)
1	1500	162.2	22	418.5	21.47
2	1400	100	22	258	12.71
3	1100	75.52	13.66	130	0.4464
4	1100	152.2	13.66	388.5	1.104
5	400	117.6	4.098	366.3	1.114
6	116.1	99.58	4.736	354.9	1.169
7	116.1	88.35	14.3	345.1	1.142
8	116.1	36	14.3	298.9	1.003
9	116.1	36	14.3	80.31	0.2962

10	116.1	36	13.66	80.31	0.2962
11	116.1	36	0.6381	80.31	0.2962
12	22.28	-5	0.6381	80.31	0.3085
13	22.28	-5	0.6381	273.8	1.03
14	116.1	82.71	9.563	340.3	1.128
15	1100	37.05	13.66	81.55	0.3002
16	1300	90	22	232.2	11.17
17	1.474	36	1.137	75.83	0.2474
18	5.945	36	1.137	75.83	0.2474
19	5.945	70.41	1.137	150.7	0.4765
20	5.945	85	0.9347	214.2	0.4664
21	5.945	35.81	0.9347	123.1	0.1925
22	1.474	57.71	1.137	558.9	0.3182
23	5.945	85	0.2026	2659	8.61
24	5.945	36	0.2026	150.8	0.5185
25	5.945	24	0.2026	100.5	0.3527
26	1.228	10	0.2026	100.5	0.3577
27	1.228	10	0.2026	2519	8.899
28	1.228	36.82	0.2026	2569	9.064

Table 4.4 The distribution of energy in various components of system1 and system2

Term	Ejector organic Rankine cycle (system 1)		Ejector organic Rankine cycle integrated with a triple pressure level absorption system (system2)	
	Amount (kW)	**% of solar energy input**	**Amount (kW)**	**% of solar energy input**
Solar energy input	**6000**	**100**	**6000**	**100**
Ejector evaporator energy input	144.8	2.4	120	2
TPLAS evaporator energy input	____	____	492	8.2
Total energy input to the system	**6144.8**	**102.4**	**6612**	**110.2**
Work output	638.5	10.6	534	8.9
Energy lost to the environment from various component of the system	5506.3	91.8	6078	101.3
Total energy output from the system	**6144.8**	**102.4**	**6612**	**110.2**

Table 4.5 The distribution of exergy in various components of system1 and system2

Term	Ejector organic Rankine cycle (system 1)		Ejector organic Rankine cycle integrated with a triple pressure level absorption system (system2)	
	Amount (kW)	% of exergy input	Amount (kW)	% of exergy input
Exergy input	5470	100	5470	100
Exergy output:				
Work output	640	11.7	534	9.76
Ejector exergetic refrigeration output	16.4	0.3	14.22	0.26
TPLAS exergetic refrigeration output	____	____	26.26	0.48
Total exergy output	656.4	12	574.48	10.50
Exergy destruction/ losses:				
HRVG	136.2	2.49	90.8	1.66
Turbine	94.63	1.73	81.37	1.49
Ejector 1	119.25	2.18	92.98	1.7
Condenser 1	12.58	0.23	11.47	0.21
Pump	16.41	0.3	16.21	0.3

Heat exchanger	16.41	0.3	15.47	0.28
Throttle valve	2.7	0.05	2.735	0.05
Evaporator 1	1.094	0.02	2.07	0.04
TPLAS Generator	——	——	101.4	1.85
Condenser 2	——	——	20.24	0.37
Absorber	——	——	19.14	0.35
Parabolic trough collector	4414.29	80.7	4441.64	81.2
Total Exergy destruction/loss	4813.60	88	4895.52	89.50
Sum of total exergy output and Total Exergy destruction/loss	**5470**	**100 (12+88)**	**5470**	**100 (10.5+89.5)**

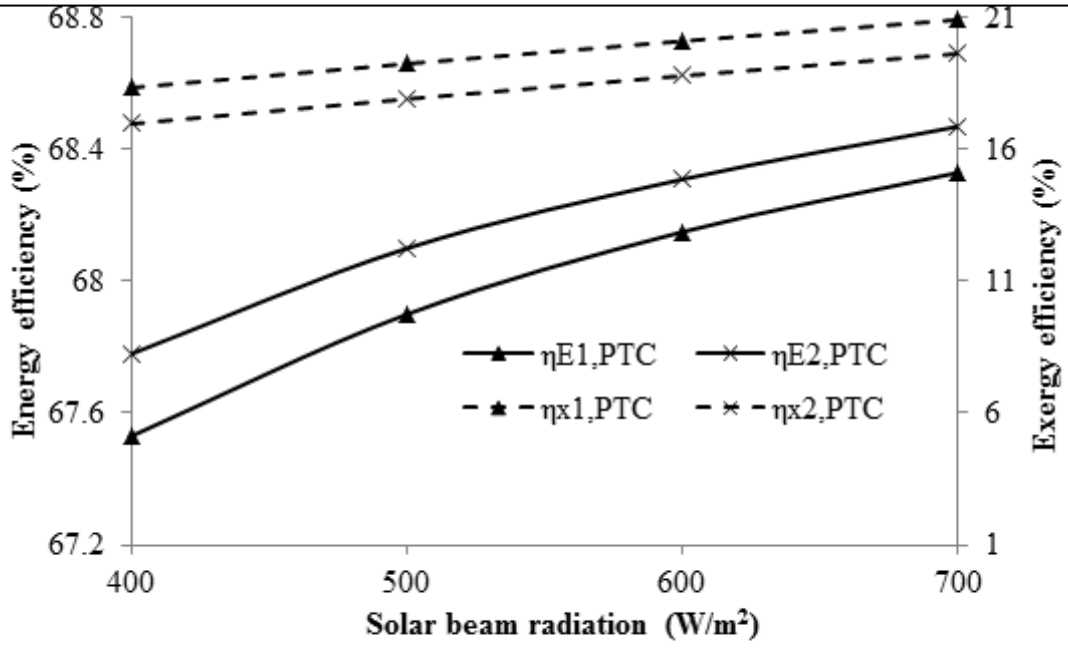

Fig. 4.3. Variation of energy and exergy efficiencies of PTC field for system1 and system2 with the change in SBR

The change of energy and exergy efficiencies of PTC field for system1 and system2 with the change in SBR is shown in Fig. 4.3. It is evident from Fig. 4.3 and equations (4.10 and 4.26) that the energy and exergy efficiencies of PTC field increases with increase in the value of SBR for both the systems because the outlet temperature of HTF (T_o) from PTC field and the amount of heat transferred to the HTF increases at fixed mass flow rate and inlet temperature of HTF (T_i) to the PTC field. It is clear from equation (4.10) that the mean temperature of HTF (T_m) for system1 is higher than system2, therefore the energy efficiency for system2 is greater than for that of system1 at the same SBR. It is also clear that the exergy efficiency of system1 is more as that of system2 because mean temperature of heat addition is greater so the exergy efficiency is greater.

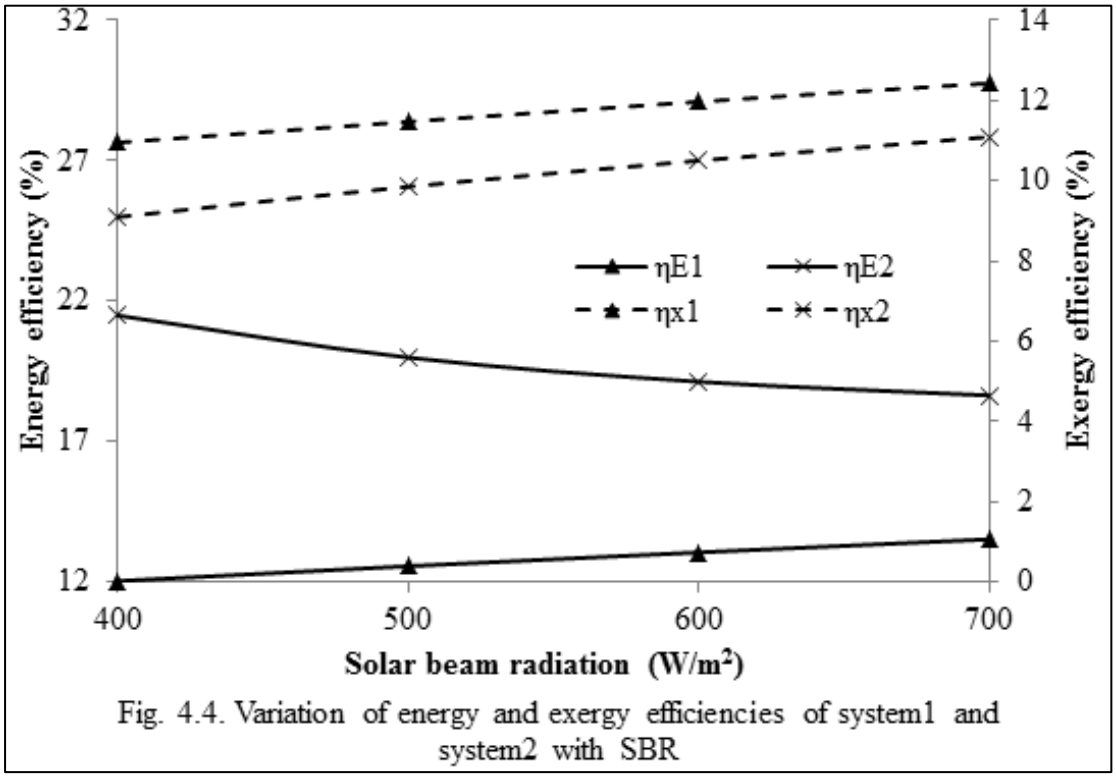

Fig. 4.4. Variation of energy and exergy efficiencies of system1 and system2 with SBR

The change of energy and exergy efficiencies for system1 and system2 with SBR is displayed in Fig. 4.4. As SBR increases, the turbine inlet temperature increases which results in greater work output. Also the temperature of working fluid at the extraction point (5) of turbine is higher at higher SBR which results in

entrainment of more refrigerant from ejector evaporator (13). This leads to greater refrigeration output at the evaporator of the ejector. So, this increase in work output and refrigeration output increases the energy and exergy efficiency of system1 with increase in SBR. It is also found that with the addition of TPLAS in system1, the energy efficiency of system2 increases considerably but decreases with the increase in SBR. This is because of the way that with the increase in SBR, work output, ejector refrigeration output increases, and TPLAS refrigeration output remain constant but solar energy input increases significantly. This leads to decrease in energy efficiency of system2 with increase in SBR. Exergy efficiency of system2 is lesser than that of system1 due to the reduction of work output at the same SBR. Exergy efficiency of system2 increases because the work output & exergy of ejector refrigeration output increases, while exergy of TPLAS refrigeration output remain constant with increase in SBR.

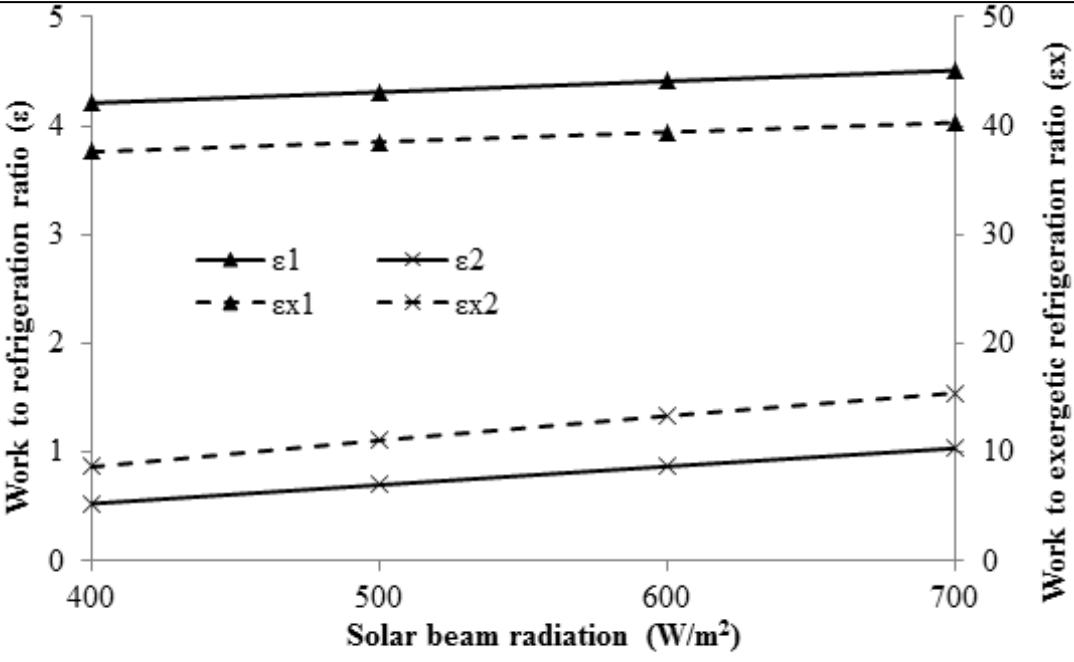

Fig. 4.5. Variation of work to refrigeration ratio and work to exergetic refrigeration ratio of system1 and system2 with SBR

The variation of work to refrigeration ratio (ε) and work to exergetic refrigeration ratio (ε_x) with SBR is shown in Fig. 4.5 for system1and system2. Both work to refrigeration ratio and work to exergetic refrigeration ratio increases with

increase in SBR as the enhancement of work output is better than that of both the refrigeration and exergetic refrigeration output for system1 and system2. Work to refrigeration ratio (ε) and work to exergetic refrigeration ratio (ε_x) at the same SBR for system1 is higher than that of system2 because of the enhancement of refrigeration output ($Q_{e1}+Q_{e2}$) & exergetic refrigeration output ($E_{e1}+E_{e2}$) and reduction in work output. Work to refrigeration ratio (ε) varies from 4.2 to 4.5 for system1 and 0.53 to 1.04 for system2 and work to exergetic refrigeration ratio (ε_x) varies from 37.6 to 40.3 for system1 and 8.7 to 15.4 for system2 with the SBR variation from 400 to 700 W/m^2.

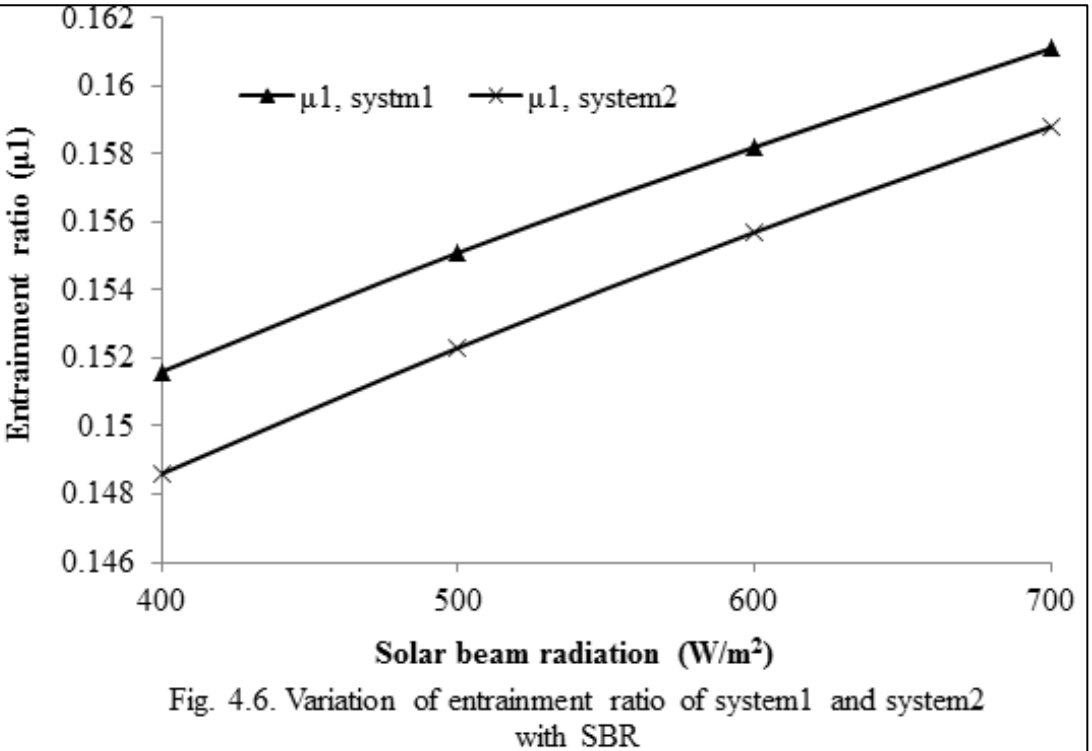

Fig. 4.6. Variation of entrainment ratio of system1 and system2 with SBR

The change of entrainment ratio (μ1) with SBR is shown in Fig. 4.6 for system1 and system2. As SBR increases, the temperature at the inlet of the turbine increases resulting in the increase in the temperature of working fluid at the extraction point (5) of turbine. This increases the exit velocity of working fluid from the ejector nozzle which leads to the entrainment of more refrigerant from ejector evaporator. Therefore entrainment ratio for system1 and system2 increases with increase in SBR.

Entrainment ratio for system1 is higher than that of system2 because turbine inlet temperature is more in system1 as compared to system2.

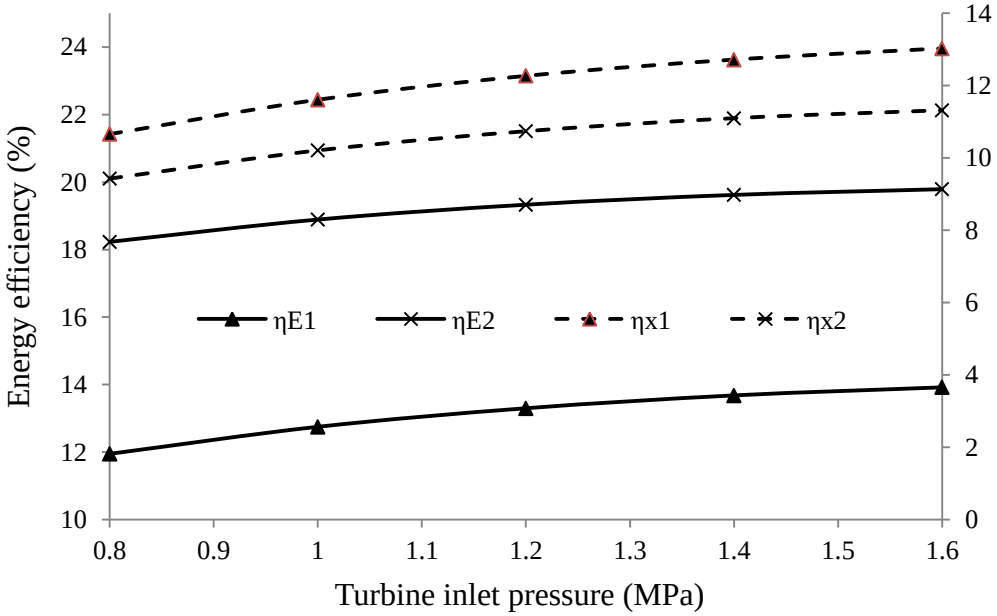

Fig. 4.7. Variation of energy and exergy efficiencies of system1 and system2 with turbine inlet pressure

The change of energy and exergy efficiencies with turbine inlet pressure is shown in Fig. 4.7 for system1and system2. Increasing trend of work output with increase in turbine inlet pressure is observed because of high enthalpy drop for high pressure ratio. This also results in low turbine extraction temperature (5). This low turbine extraction temperature diminishes the primary stream velocity in ejector bringing about reduction of entrainment of secondary vapor which decreases the refrigeration output at ejector evaporator (Q_{e1}). The refrigeration output at TPLAS does not change because of the same working conditions across TPLAS with variation in turbine inlet pressure. The combined effect of work output and refrigeration output (s) on the performance of system1 and system2 is to increase in energy efficiency with increase in turbine inlet pressure. Similar trend is found for exergy efficiency.

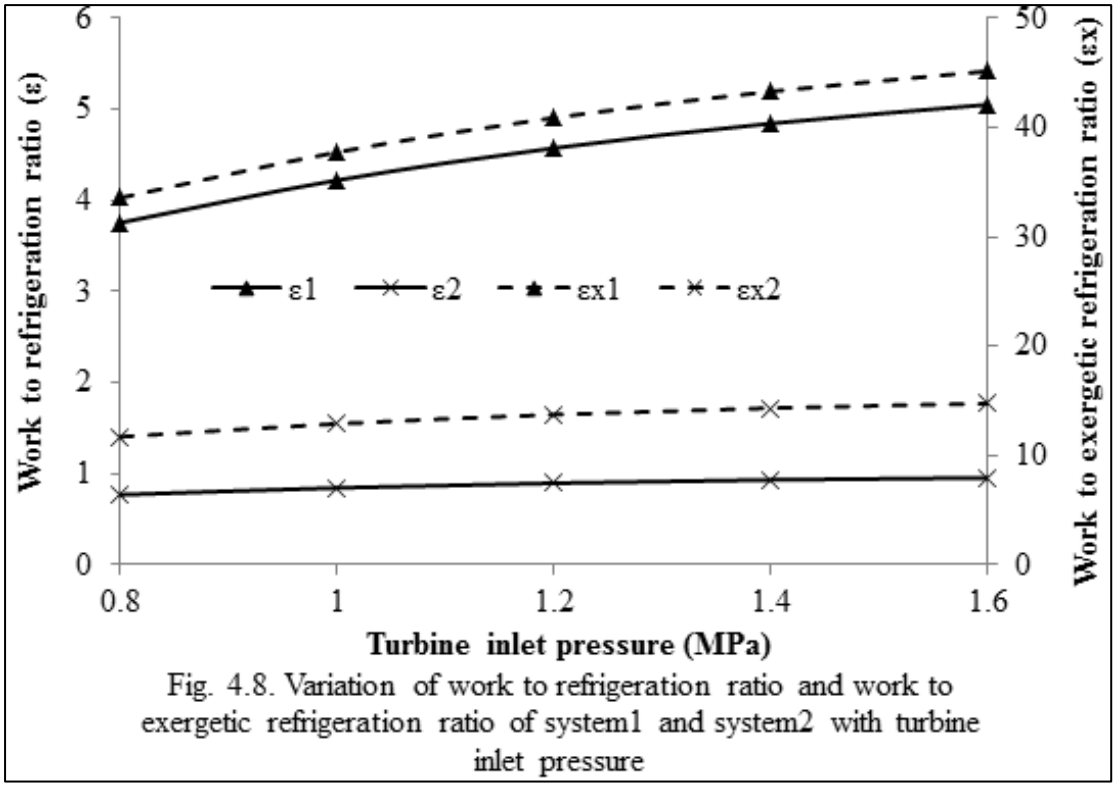

Fig. 4.8. Variation of work to refrigeration ratio and work to exergetic refrigeration ratio of system1 and system2 with turbine inlet pressure

The variation of work to refrigeration ratio (ε) and work to exergetic refrigeration ratio (ε_x) with turbine inlet pressure is shown in Fig. 4.8 for system1and system2. As can be seen from Fig. 4.8 that the work to refrigeration ratio (ε) and work to exergetic refrigeration ratio (ε_x) increases with the increase in turbine inlet pressure. This is due to the fact that the work output increases, ejector refrigeration output decreases and TPLAS refrigeration output remain same with increase in turbine inlet pressure.

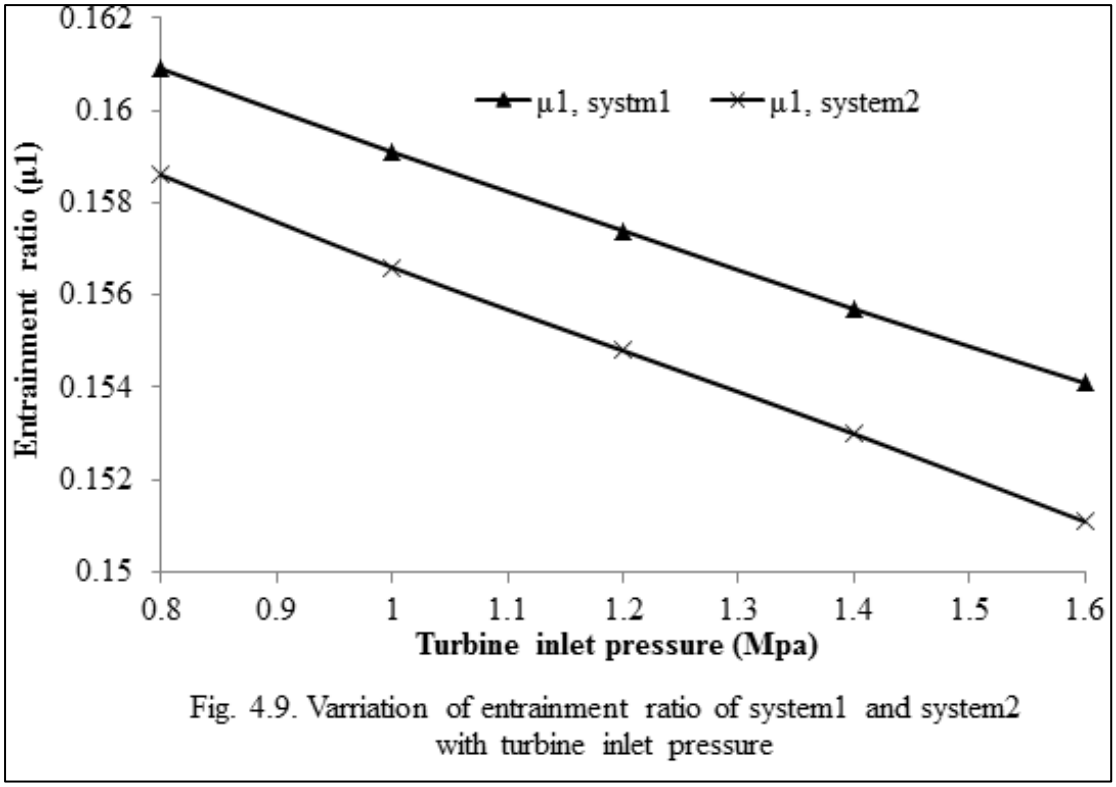

Fig. 4.9. Varriation of entrainment ratio of system1 and system2 with turbine inlet pressure

The change of entrainment ratio (μ_1) with turbine inlet pressure is shown in Fig. 4.9 for system1and system2. Increase in turbine inlet pressure brings about reduction of turbine extraction temperature. This low turbine extraction temperature stream (5) works as primary flow for ejector which lessens the primary stream velocity at the exit of ejector nozzle and results in reduction in entrainment of secondary vapor from the ejector evaporator. Therefore the entrainment ratio for system1 and system2 decreases with increase in turbine inlet pressure. As turbine inlet temperature for system1 is more than that of system2 therefore the entrainment ratio for system1 is higher than that of system2.

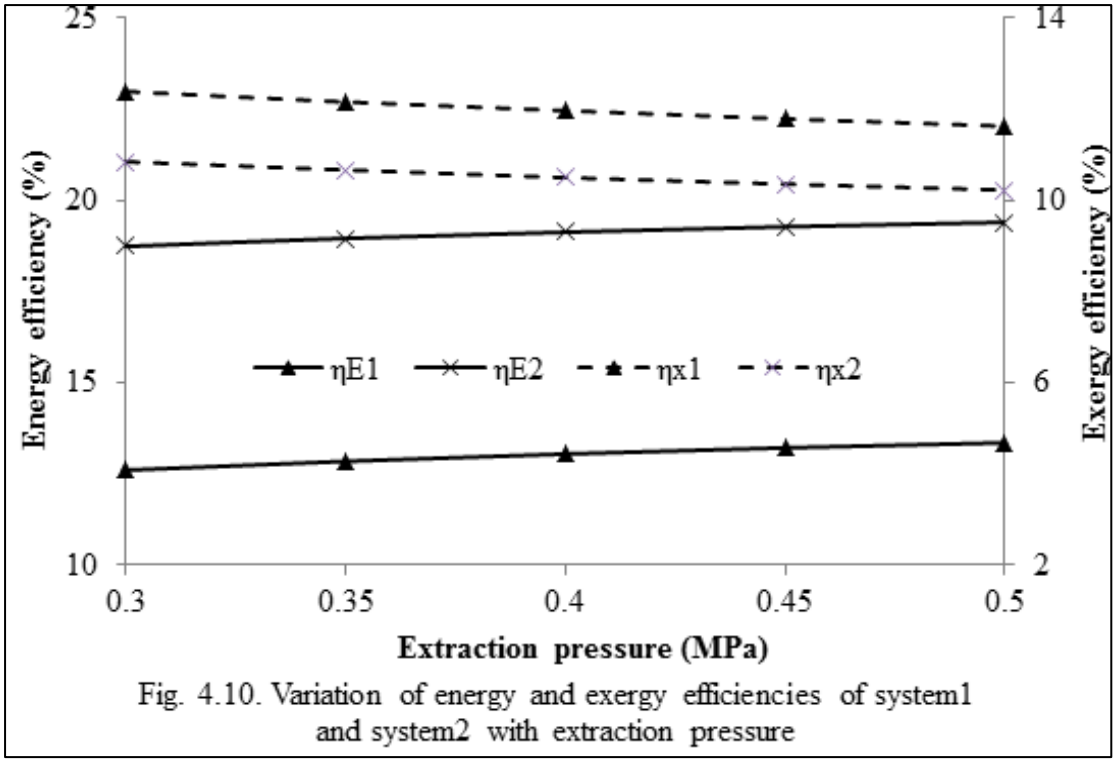

Fig. 4.10. Variation of energy and exergy efficiencies of system1 and system2 with extraction pressure

The change of energy and exergy efficiencies with extraction pressure for system1 and system2 is shown in Fig. 4.10. It is marked that work output diminishes, while ejector refrigeration output increases with the increase in extraction pressure. The net impact on energy efficiencies for both the systems is to increase with increase in extraction pressure. With increase in extraction pressure, exergy efficiencies for both of the systems decrease.

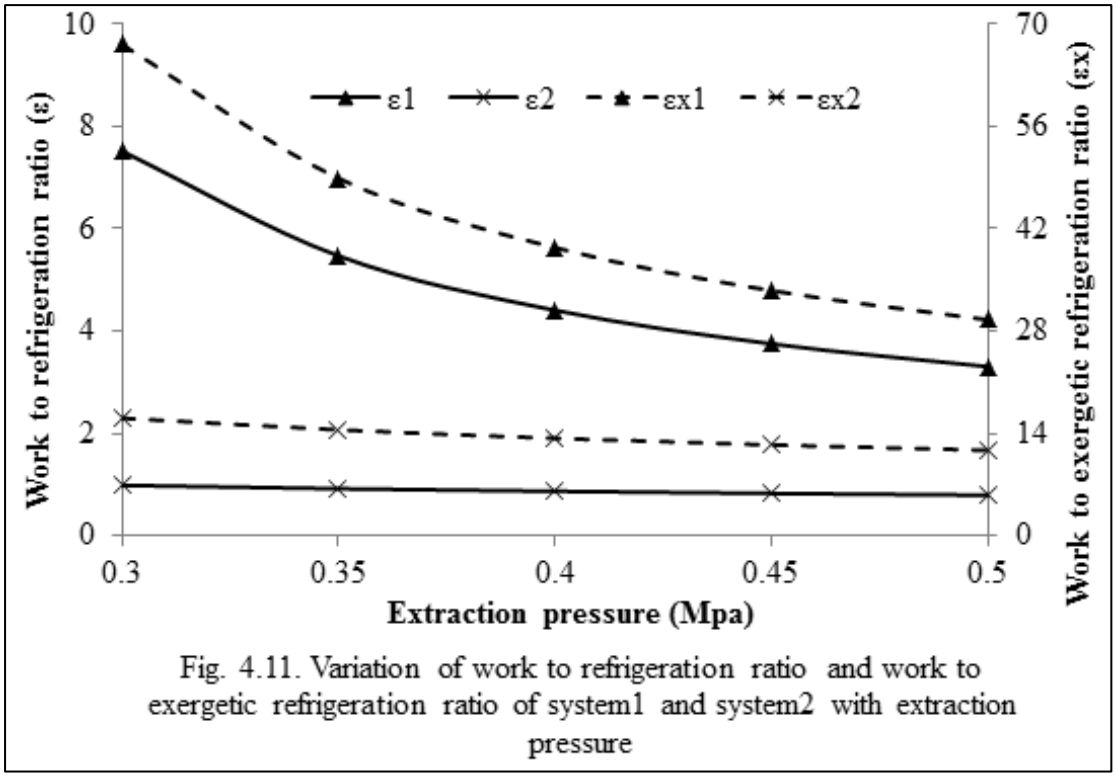

Fig. 4.11. Variation of work to refrigeration ratio and work to exergetic refrigeration ratio of system1 and system2 with extraction pressure

The variation of work to refrigeration ratio (ε) and work to exergetic refrigeration ratio (ε_x) with turbine extraction pressure is shown in Fig. 4.11 for system1 and system2. It is evident from the Fig. 4.11 that the ε and ε_x for both the systems deceases with increase in turbine extraction pressure. This is because of the way that work output decreases whereas ejector refrigeration output increases with increase in turbine extraction pressure as expressed previously.

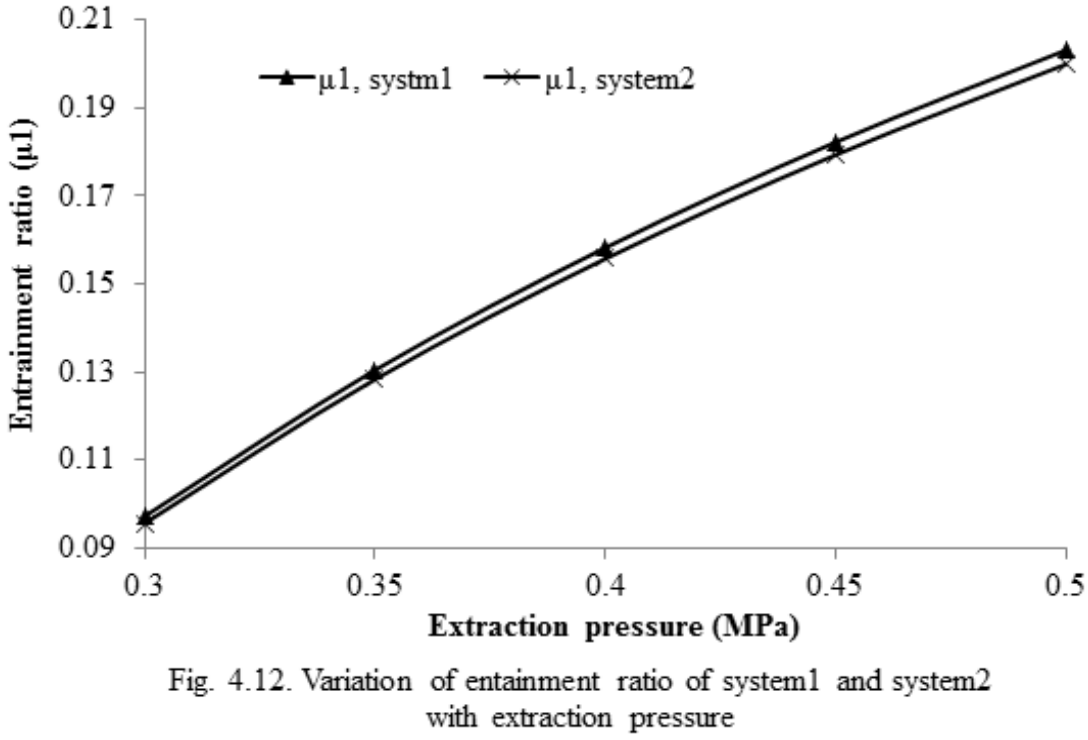

Fig. 4.12. Variation of entainment ratio of system1 and system2 with extraction pressure

Fig. 4.12 depicts the change of entrainment ratio (μ_1) with turbine extraction pressure for system1 and system2. The entrainment ratio for both the systems increases with increase in extraction pressure.

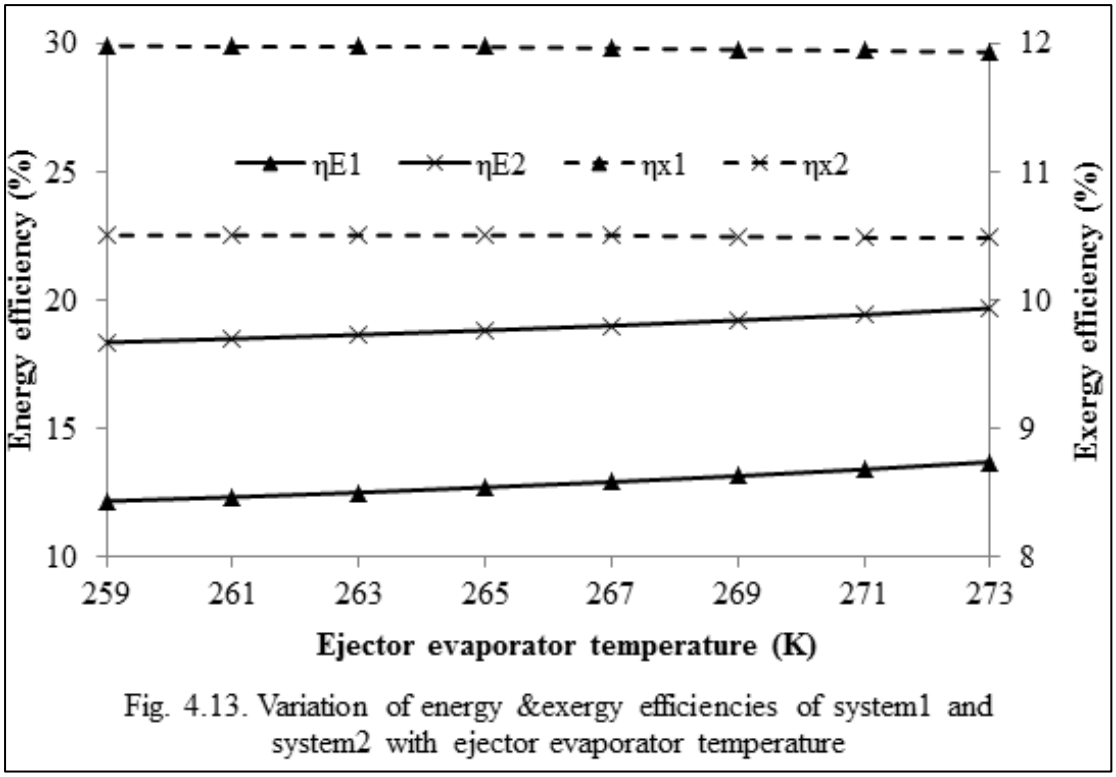

Fig. 4.13. Variation of energy &exergy efficiencies of system1 and system2 with ejector evaporator temperature

The change of energy and exergy efficiencies with ejector evaporator temperature for both the systems is shown in Fig. 4.13**.** The increase in ejector evaporator temperature results in increase of ejector refrigeration output (Qe1) without having any impact on the work output. The combined result is increase in energy efficiencies of both the systems. The exergy efficiency for both the systems vary insignificantly because amount of the variation of exergy associated with the ejector refrigeration outputs is considerably less than the energy associated with the ejector refrigeration output.

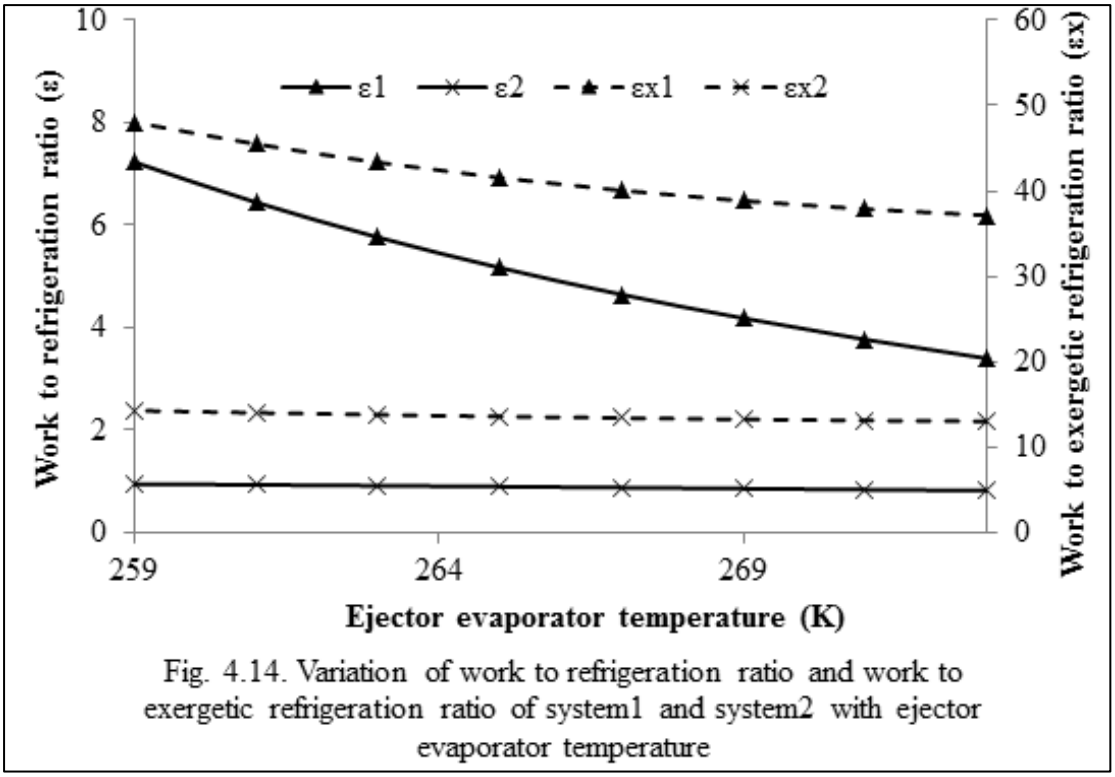

Fig. 4.14. Variation of work to refrigeration ratio and work to exergetic refrigeration ratio of system1 and system2 with ejector evaporator temperature

The variation of work to refrigeration ratio (ε) and work to exergetic refrigeration ratio (ε_x) with ejector evaporator temperature for both the systems is shown in Fig. 4.14. It is apparent from the Fig. 4.14 that the ε and ε_x for both the systems deceases with increase in evaporator temperature. This is due to the fact that work output and TPLAS refrigeration output remains constant whereas ejector refrigeration output increases with increase in evaporator temperature as mentioned above. Work to refrigeration ratio (ε) and work to exergetic refrigeration ratio (ε_x) at the same ejector evaporator temperature for system1 is higher than that of system2 because of the enhancement of refrigeration output ($Q_{e1}+Q_{e2}$) & exergetic refrigeration output ($E_{e1}+E_{e2}$).

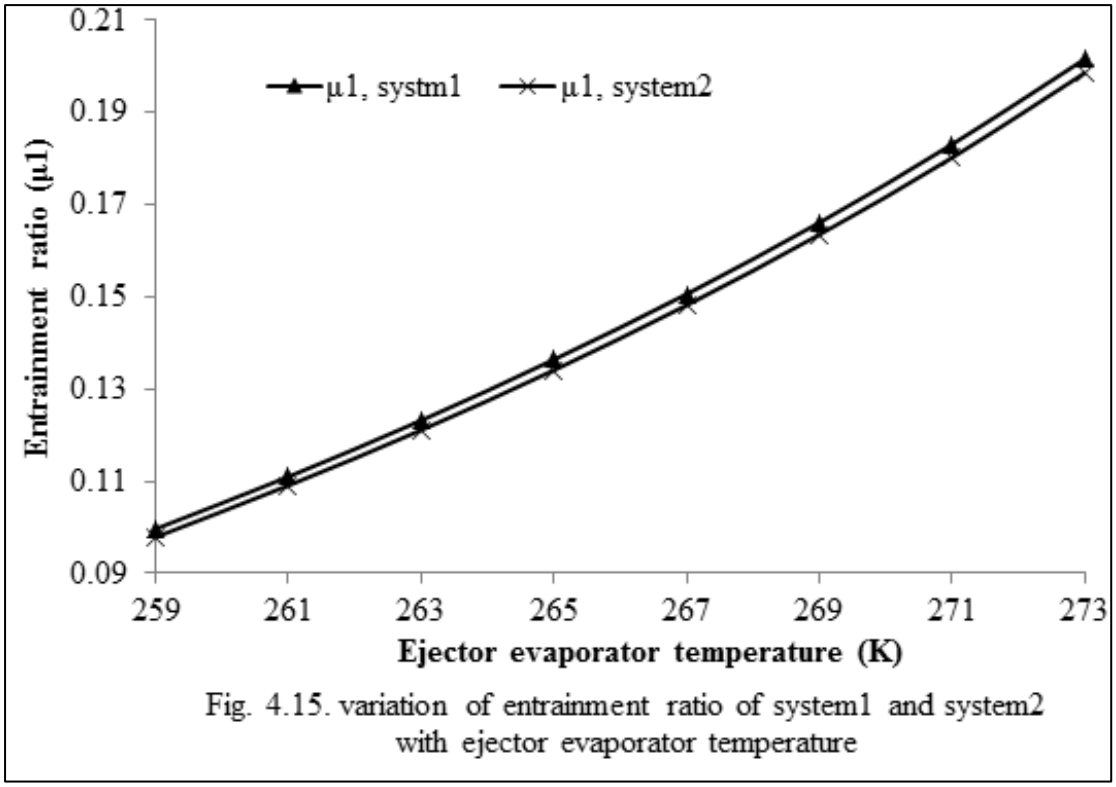

Fig. 4.15. variation of entrainment ratio of system1 and system2 with ejector evaporator temperature

Fig. 4.15 depicts the change of entrainment ratio (μ_1) with ejector evaporator temperature for system1 and system2. With increase in ejector evaporator temperature the entrainment ratio for system1 and system2 increases.

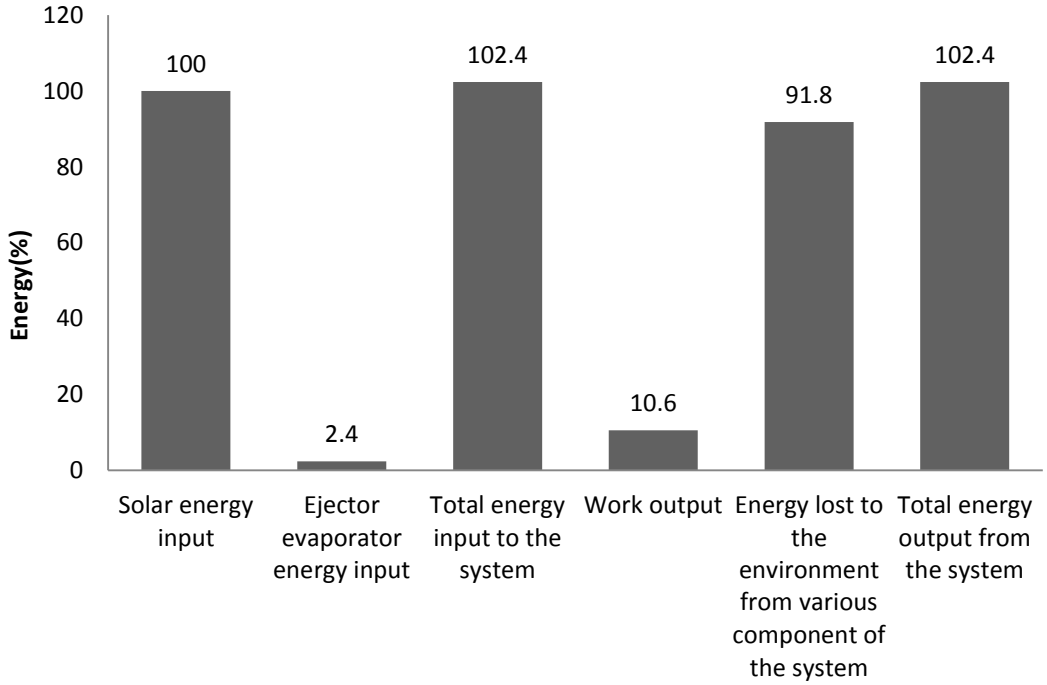

Fig. 4.16 Energy distribution for system1

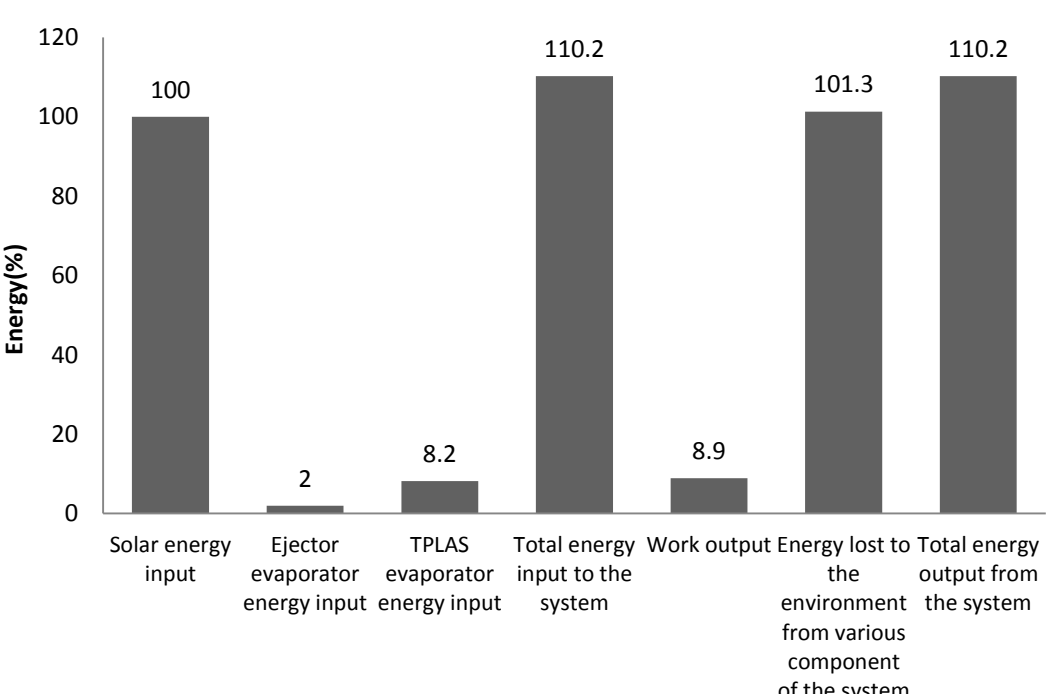

Fig. 4.17 Energy distribution for system2

Fig. 4.16 and 4.17 shows the energy distribution for the system1 and system2. The sum of the energy input at the solar field (100%) and at the evaporator

(2.4%) in the form of cooling is equal to 102.4%. The sum of the energy output is equal to the work output (10.6%) and energy lost to the environment (91.8%) through various components of the system1 which is equal to the total energy input to the system1 [146]. Similarly for the system2, the sum of the energy input at the solar field (100%), at the ejector evaporator (2%) and at TPLAS evaporator (8.2%) in the form of cooling is equal to 110.2%. The sum of the energy output is equal to the work output (8.9%) and energy lost to the environment (101.3%) through various components of the system2 which is equal to the total energy input to the system2.

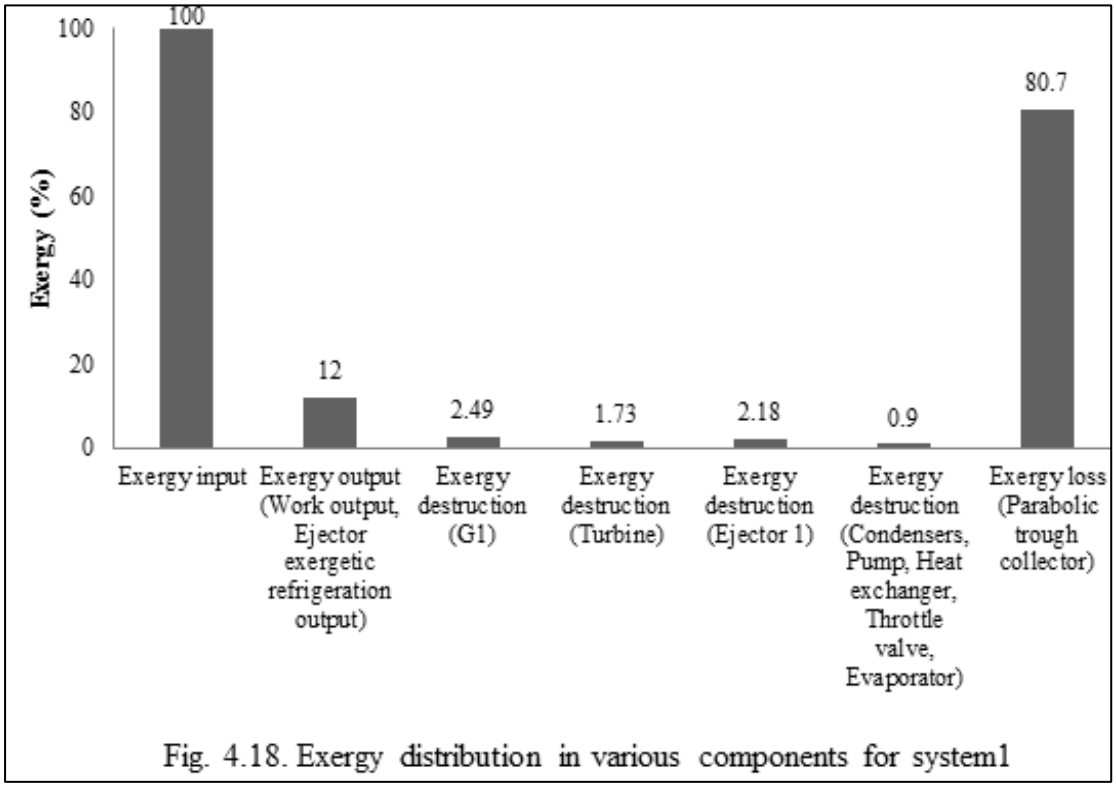

Fig. 4.18. Exergy distribution in various components for system1

Fig. 4.18 and 4.19 shows the distribution of exergy for system1 and system2. It is observed that out of total exergy input to the system1 around 12.0% is available as useful exergy output (work output and ejector exergetic refrigeration output) and 88.0% of the exergy loss/destruct to the environment and in various components of the system. Out of total exergy input to the system2 around 10.5% is available as useful exergy output (work output, ejector exergetic refrigeration output and TPLAS

exergetic refrigeration output) and 89.5% of the exergy loss/destruct to the environment and in various components of the system.

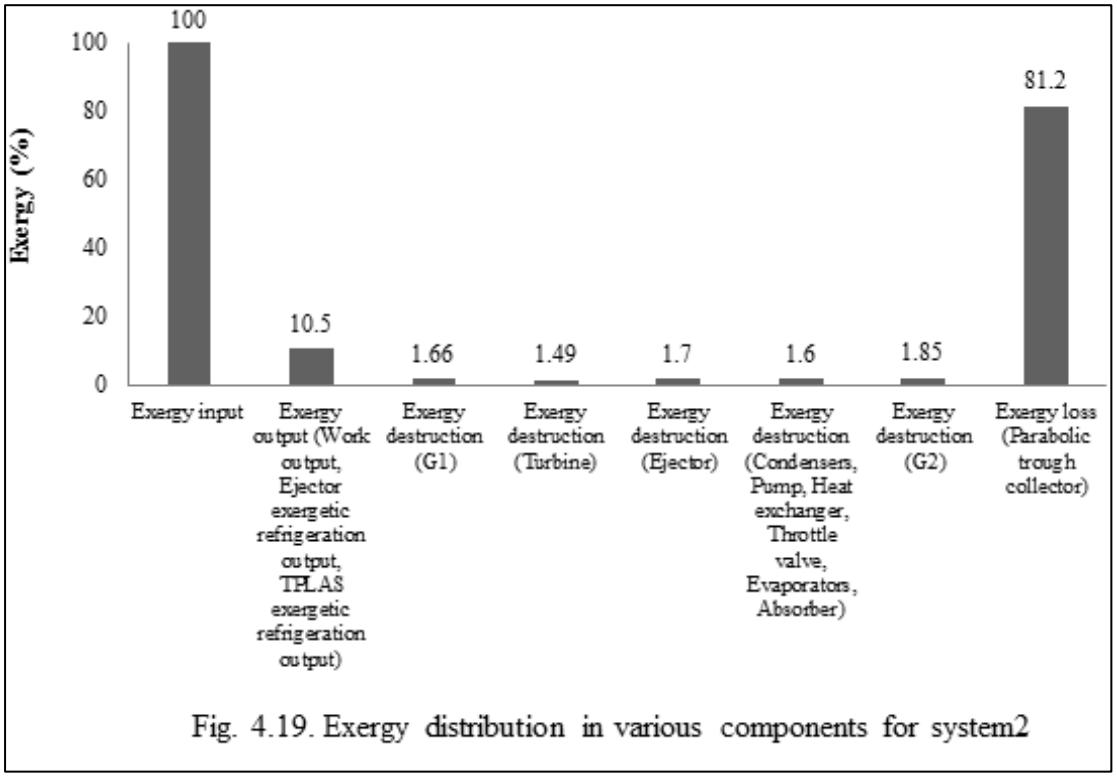

Fig. 4.19. Exergy distribution in various components for system2

4.5 Summary:

The proposed system produces power and refrigeration output at different temperatures simultaneously. Thermodynamic investigation was directed to explore the impact of various design parameters for example SBR, turbine inlet pressure, turbine extraction pressure, and ejector evaporator temperature on the performance of proposed system (system 2) and also compared with the performance of ejector organic Rankine cycle (system 1). The main conclusions from this analysis can be outlined as follows:

- It is clear that the system2 has higher refrigeration output, exergetic refrigeration output, and energy efficiency than that of the system1for the same energy input.

- The different thermodynamic parameters like SBR, turbine inlet pressure, turbine extraction pressure, and ejector evaporator temperature, in their operating range, have noteworthy impact on the work output, refrigeration output, work to refrigeration ratio, work to exergetic refrigeration ratio and entrainment ratio of the proposed system.
- The energy efficiency for system1 increases from 12.0% to 13.9% and for system2 increases from 18.2% to 19.8%, whereas exergy efficiency increases from 10.7% to 13.0% and 9.4% to 11.3% for system1 and system2 respectively with turbine inlet pressure vary from 0.8 MPa to 1.6 MPa.
- The system2 has higher energy efficiency as compared to the system1 but exergy efficiency is lower for the same input parameters.
- The exergy efficiency for system1 and system2 decreases slightly with increase in extraction pressure and ejector evaporator temperature for the same input parameters.
- The energy efficiency for system1 and system2 increases slightly with increase in extraction pressure and ejector evaporator temperature for the same input parameters.

CHAPTER 5

COMBINED ORGANIC RANKINE CYCLE WITH DOUBLE EJECTOR

5.1 Introduction:

PTC field based ejector organic Rankine cycle (EORC) and double ejector organic Rankine cycle (DEORC) is proposed for improving overall energy conversion efficiency. In EORC cooling is produce at single temperature while in DEORC cooling is produce at two different temperatures. The cycle has been investigates from the viewpoints of both first law and second law of thermodynamics and the impact of working parameters on the performance of the cycle is also observed. The refrigerant R141b is used as working fluid and Therminol VP1 as heat transfer fluid. Thermal storage tanks are also used to store the thermal energy from the Sun which provides the continuous net power output during insufficient solar radiation.

5.2 Working of proposed cycle:

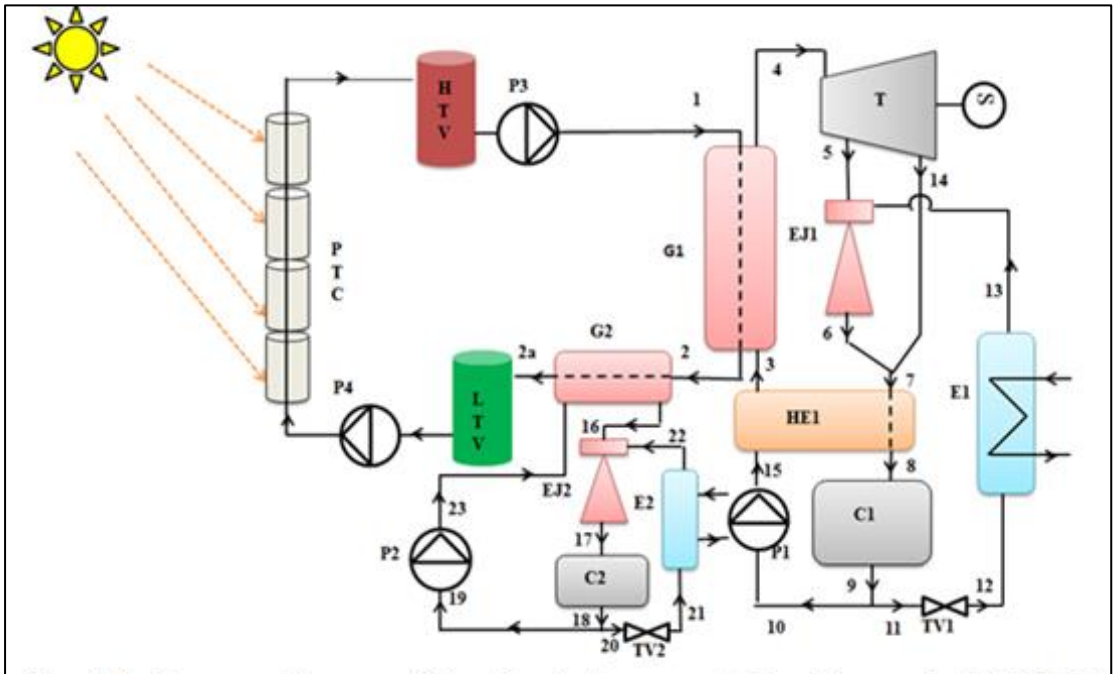

Fig. 5.1. Process diagram of double ejector organic Rankine cycle (DEORC)

The DEORC as shown in Fig. 5.1 consists of parabolic trough collector (PTC) solar field, high temperature vessel, low temperature vessel, pumps, heat recovery vapor generator, turbine, ejector, condenser, throttle valve, evaporator and heat exchanger. Solar energy is used to heat the heat transfer fluid Therminol VP1 (1) with the help of PTC field. Heat transfer fluid (HTF) enters the heat recovery vapor generator (G_1) which is used to superheat the high pressure refrigerant and leaves at (2), which again enters into the heat recovery vapor generator (G_2) to vaporize the refrigerant and return back to the PTC solar field. Superheated refrigerant vapor (4) expands in the turbine. After expansion up to the extraction pressure, refrigerant vapors are extracted (5) from turbine at extraction pressure and then it flows into the ejector nozzle, entrains secondary vapor (13) from the evaporator (E_1) and mixes in mixing chamber of the ejector (EJ_1). The ejector exit stream (6) mixes with the turbine exhaust (14) and is cooled (7-8) in the heat exchanger (HE) by rejecting heat to the refrigerant leaving from the pump (P_1) which is preheated (15-3). The refrigerant leaving from heat exchanger (8) is condensed in the condenser (C1) and converts into saturated liquid (9). The saturated liquid (9) from condenser is divided into two parts. One part (11) enters the throttle valve (TV1) and other part (10) into pump (P1). The saturated liquid (10) with the help of pump (P1) is delivered into the heat exchanger (15). The preheated refrigerant (3) leaving from heat exchanger (HE1) enters the heat recovery vapor generator (G1) in which refrigerant is heated and converted into superheated vapor (4). The saturated liquid (11) is expanded in the throttle valve (TV1) upto the evaporator pressure (12). The refrigerant (12) enters into the evaporator (E1) and produce the cooling effect by evaporation of refrigerant (12-13). The refrigerant vapour (16) flows into the ejector nozzle and entrains secondary vapor (22) from the evaporator (E2) mixes in mixing chamber of the ejector. The ejector (EJ2) exit stream (17) is condensed in the condenser (C2) and converted into the saturated liquid (18). Saturated liquid (18) is divided into two parts. One part (20) enters the throttle valve (TV2) and other part (19) into pump (P2). The saturated liquid (19) with the help of pump (P2) is delivered into the heat recovery vapor generator (G2) and converts into saturated vapor (16). The saturated liquid (20) is expanded in the throttle valve (TV2) upto the evaporator pressure (21). The refrigerant (21) enters into the evaporator (E2) and produce the cooling effect by

evaporation of refrigerant (21-22). The system description of ejector organic Rankine cycle (EORC) is same as DEORC and shown in Fig. 4.1.

Fig. 5.2 and Fig. 5.3 illustrate the T-s diagram of EORC and DEORC respectively.

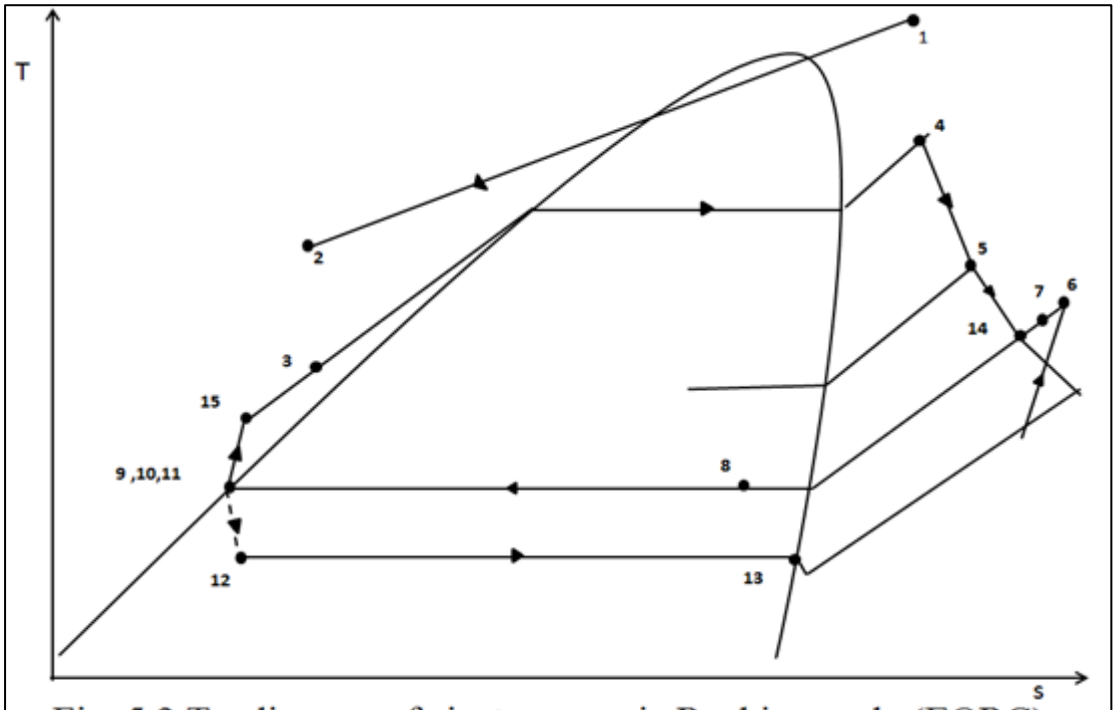

Fig. 5.2 T-s diagram of ejector organic Rankine cycle (EORC)

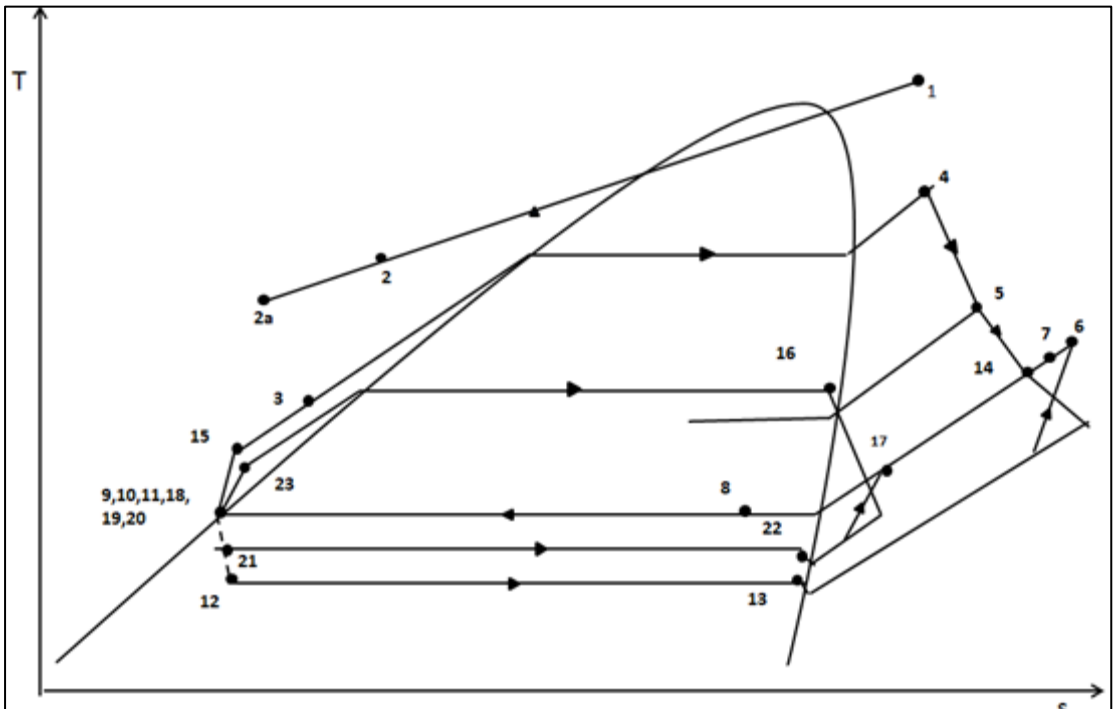

Fig. 5.3 T-s diagram of double ejector organic Rankine cycle (DEORC)

For the thermodynamic analysis, the parameters considered for the operation of EORC and DEORC are depicted in Table 5.1.

Table 5.1: Main parameters considered for the analysis of EORC and DEORC [127-130].

Atmospheric Temperature (^{0}C)	25
Atmospheric pressure (bar)	1.0135
Turbine inlet Temperature (^{0}C)	150
Pressure at the inlet of the turbine (bar)	6
Turbine extraction pressure (bar)	2.4
Extraction ratio	0.3
Turbine isentropic efficiency (%)	85
Pump isentropic efficiency (%)	70
Condenser temperature (^{0}C)	30
Evaporator (E_1) temperature (^{0}C)	-5
Evaporator (E_2) temperature (^{0}C)	0
Effectiveness of the heat exchanger	0.75
Aperture area (m^2)	10000
Solar beam radiation (kWm^{-2})	0.60
HTF temperature inlet to HRVG (^{o}C)	160
HTF temperature exit to HRVG (^{o}C)	90
HRVG efficiency (%)	100
Efficiency of the nozzle (%)	90
Mixing efficiency (%)	85
Efficiency of the diffuser (%)	85

5.3 First and second law analysis of proposed cycle:

5.3.1 1st law analysis for DEORC

Solar energy received from the Sun:

$$\dot{Q}_{Solar} = G_b A_p \tag{5.1}$$

Solar beam radiation

$G_b = I \cos\theta$

I = Direct normal irradiance (Wm^{-2}),

A_p = Aperture area (m^2),

θ =Incidence angle.

Heat gain in the PTC field for DEORC

$$\dot{Q}_{gain} = \dot{m}(h_1 - h_{2a}) = \eta_{E,\ PTC}\, G_b A_p = \dot{m}_4 (h_4 - h_3) + \dot{m}_{16} (h_{16} - h_{23}) \tag{5.2}$$

where $\eta_{E,\ PTC}$ = First law efficiency of PTC field

$$\eta_{E,\ PTC} = a - b\left[\frac{T_m - T_0}{G_b}\right] - cG_b\left[\frac{T_m - T_0}{G_b}\right]^2 \tag{5.3}$$

a = optical efficiency = 0.7, b = first order loss coefficient = 0.1, c = second order loss coefficient = 0, $T_m = \{(T_i+T_o)/2\}$ = mean temperature of heat transfer fluid (HTF).

The first law efficiency ($\eta_{E,\ DEORC}$) of the DEORC can be characterized as the proportion of the net power output ($\dot{W}_{net}$) and cooling output in both the evaporators ($\dot{Q}_{e_1}$ & $\dot{Q}_{e_2}$) to the solar energy input ($\dot{Q}_{Solar}$).

$$\eta_{E,\ DEORC} = \frac{\text{Energy output}}{\text{Solar energy input}} = \frac{(\dot{W}_{net} + \dot{Q}_{e_1} + \dot{Q}_{e_2})}{\dot{Q}_{Solar}} \tag{5.4}$$

Turbine work:

$$\dot{W}_T = \dot{m}_4(h_4 - h_5) + \dot{m}_4(1 - R)(h_5 - h_{14}) \tag{5.5}$$

Extraction ratio:

$$R = \dot{m}_5/\dot{m}_4 \tag{5.6}$$

Pump work:

$$\dot{W}_P = \dot{m}_4(h_{15} - h_{10}) \quad (5.7)$$

Net power output:

$$\dot{W}_{net} = \dot{W}_T - \dot{W}_P \quad (5.8)$$

Cooling output in evaporator (E_1):

$$\dot{Q}_{e_1} = \dot{m}_5\mu_1(h_{13} - h_{12}) \quad (5.9)$$

Cooling output in evaporator (E_2):

$$\dot{Q}_{e_2} = \dot{m}_{16}\mu_2(h_{22} - h_{21}) \quad (5.10)$$

Cooling to power ratio (ρ) for EORC:

$$\rho\ (\text{EORC}) = \frac{\dot{Q}_{e_1}}{\dot{W}_{net}} \quad (5.11)$$

Cooling to power ratio (ρ) for DEORC:

$$\rho\ (\text{DEORC}) = \frac{\dot{Q}_{e_1} + \dot{Q}_{e_2}}{\dot{W}_{net}} \quad (5.12)$$

Entrainment ratio:

Ejector (EJ_1) –

$$\mu_1 = \dot{m}_{13}/\dot{m}_5 \quad (5.13)$$

Ejector (EJ_2) –

$$\mu_2 = \dot{m}_{22}/\dot{m}_{16} \quad (5.14)$$

5.3.2 Second law analysis for DEORC

Exergy analysis is based on second law approach. Exergy might be characterized as the greatest conceivable reversible work obtainable in conveying the condition of the system to the dead state.

Second law efficiency of PTC field is given as

$$\eta_{X,\ PTC} = \{\dot{m}(h_1 - h_{2a}) - T_0(s_1 - s_{2a})\}/G_b A_p \psi \tag{5.15}$$

Maximum useful work obtainable from sun radiation (ψ) is calculated from Petela [144] formula that is given as

$$\psi = 1 - \frac{4}{3}\frac{T_0}{T_{solar}} + \frac{1}{3}\left(\frac{T_0}{T_{solar}}\right)^4 \tag{5.16}$$

The second law efficiency ($\eta_{X,\ DEORC}$) of DEORC may be reported as

$$\eta_{X,\ DEORC} = \frac{\text{Exergy output}}{\text{Exergy input}} = \frac{\left(\dot{W}_{net} + \dot{X}_{e_1} + \dot{X}_{e_2}\right)}{\dot{X}_{Solar}} \tag{5.17}$$

where, $\dot{X}_{Solar}$ is exergy input associate with solar radiation falling on PTC field, $\dot{X}_{e_1}$ is the exergy associate with cooling output in the evaporator (E_1) and $\dot{X}_{e_2}$ is the exergy associate with cooling output in the evaporator (E_2),

$$\dot{X}_{e_1} = \dot{m}_{13}[(h_{12} - h_{13}) - T_0(s_{12} - s_{13})] \tag{5.18}$$

$$\dot{X}_{e_2} = \dot{m}_{22}[(h_{21} - h_{22}) - T_0(s_{21} - s_{22})] \tag{5.19}$$

$$\dot{X}_{Solar} = G_b A_p \psi \tag{5.20}$$

5.4 Result and discussion:

The first and second law analyses is conducted for EORC and DEORC, their results are compared by varying working parameters such as turbine inlet temperature (TIT) and turbine inlet pressure (TIP) at different extraction ratio on the **performance** of the cycle.

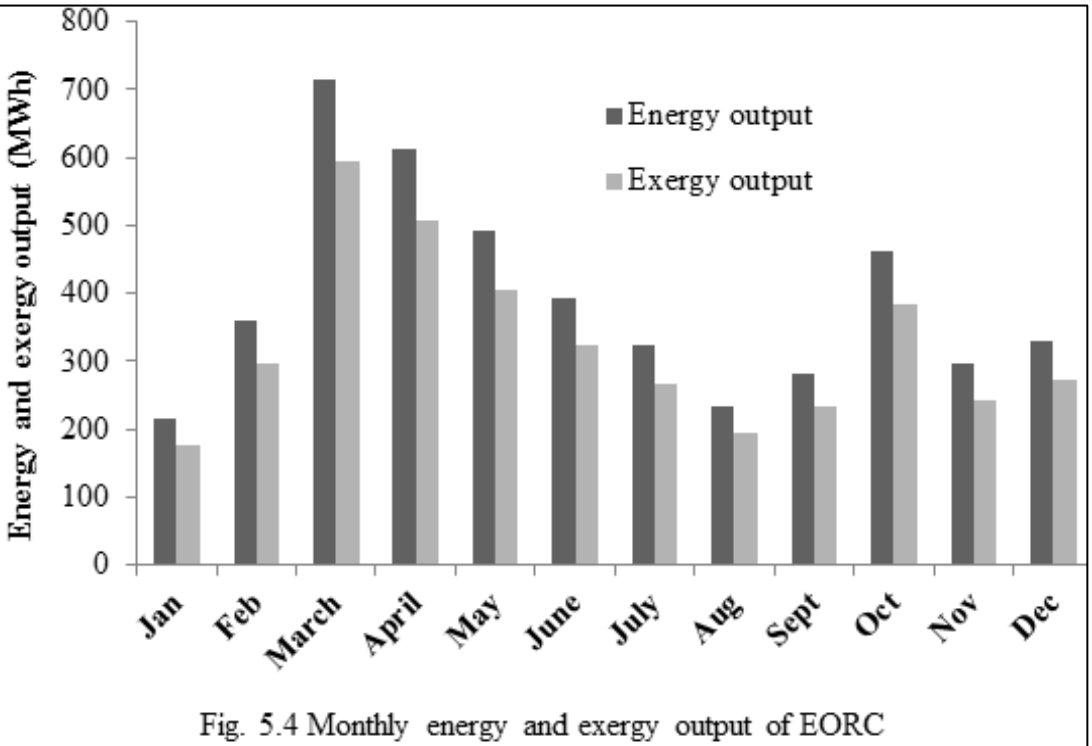

Fig. 5.4 Monthly energy and exergy output of EORC

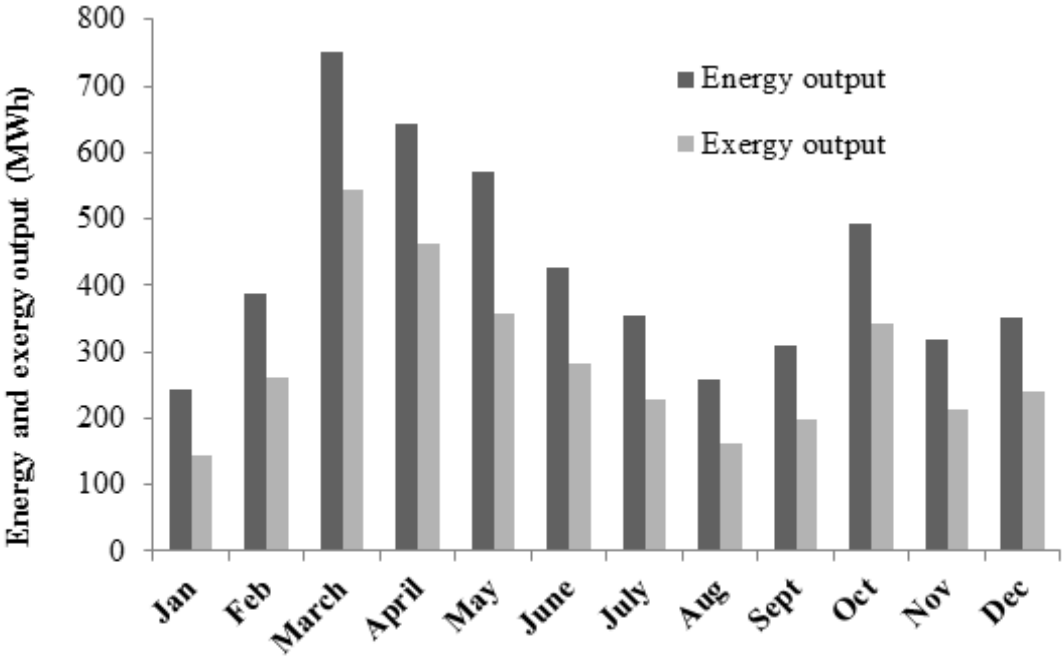

Fig. 5.5 Monthly energy and exergy output of DEORC

Fig. 5.4 and Fig. 5.5 show the monthly energy and exergy output of EORC and DEORC. It is observed that due to higher SBR in the month of March, April, May and October the energy and exergy output is higher while in the remaining months the energy and exergy output obtained is lower due to low value of SBR. The highest energy output (715.53 MWh) and exergy output (593.8 MWh) obtained in the month of March while lowest energy output (214.74 MWh) and exergy output (176.57 MWh) in the month of January in EORC. The maximum energy output in the month of March is 749.95 MWh and maximum exergy output 544.38 MWh while least energy output 244.07 MWh and exergy output is 142.82 MWh registered in the month of January in DEORC. The annual average energy output of EORC and DEORC is 4710.57 MWh and 5104.97 MWh respectively while annual average exergy output of EORC and DEORC is 3893.86 MWh and 3436.27 MWh respectively. It is concluded from Fig. 5.4 and Fig. 5.5 that yearly average energy output increases while average exergy output decreases with the addition of ejector refrigeration system in the EORC.

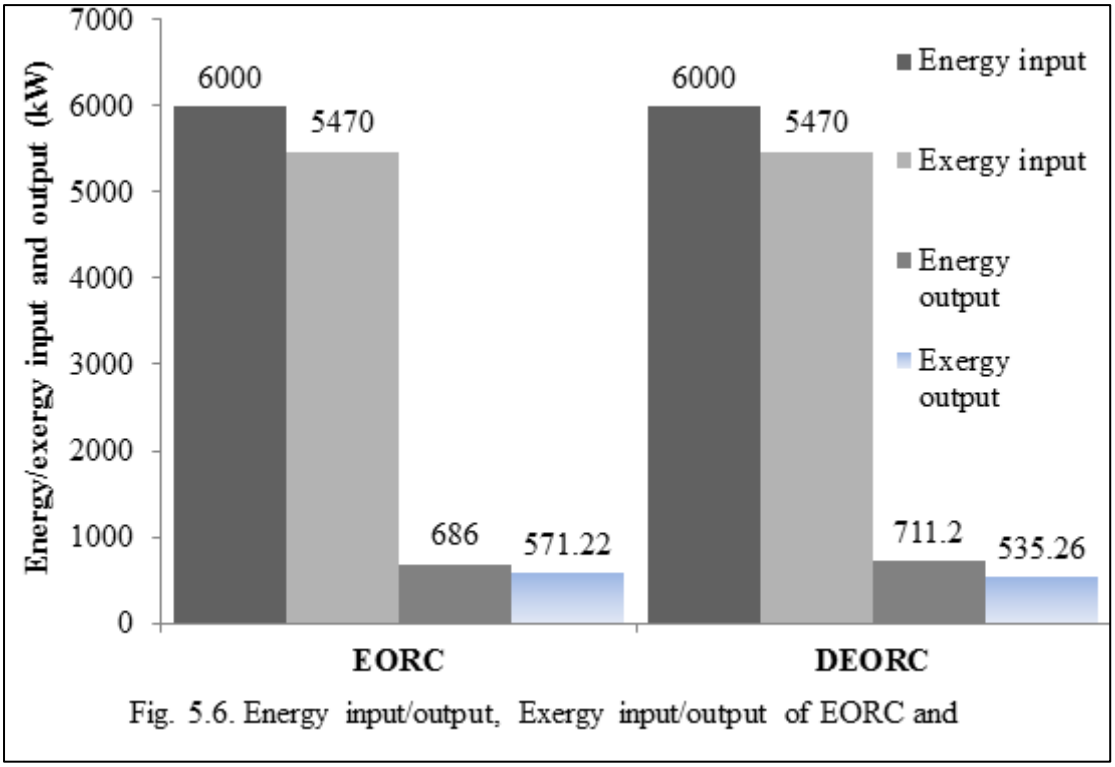

Fig. 5.6. Energy input/output, Exergy input/output of EORC and

Fig. 5.6 shows the energy input/output and exergy input/output in EORC and DEORC at input thermodynamic parameters as shown in Table 5.1. In EORC the total useful energy output of the cycle ($\dot{W}_{net} + \dot{Q}_{e_1}$) is 686 kW and the exergy output ($\dot{W}_{net} + \dot{X}_{e_1}$) is 571.22 kW is observed. In DEORC the total energy output ($\dot{W}_{net} + \dot{Q}_{e_1} + \dot{Q}_{e_2}$) is 711.2 kW and the exergy output ($\dot{W}_{net} + \dot{X}_{e_1} + \dot{X}_{e_2}$) is 535.26 is observed. It is clear that energy output in DEORC is higher than EORC.

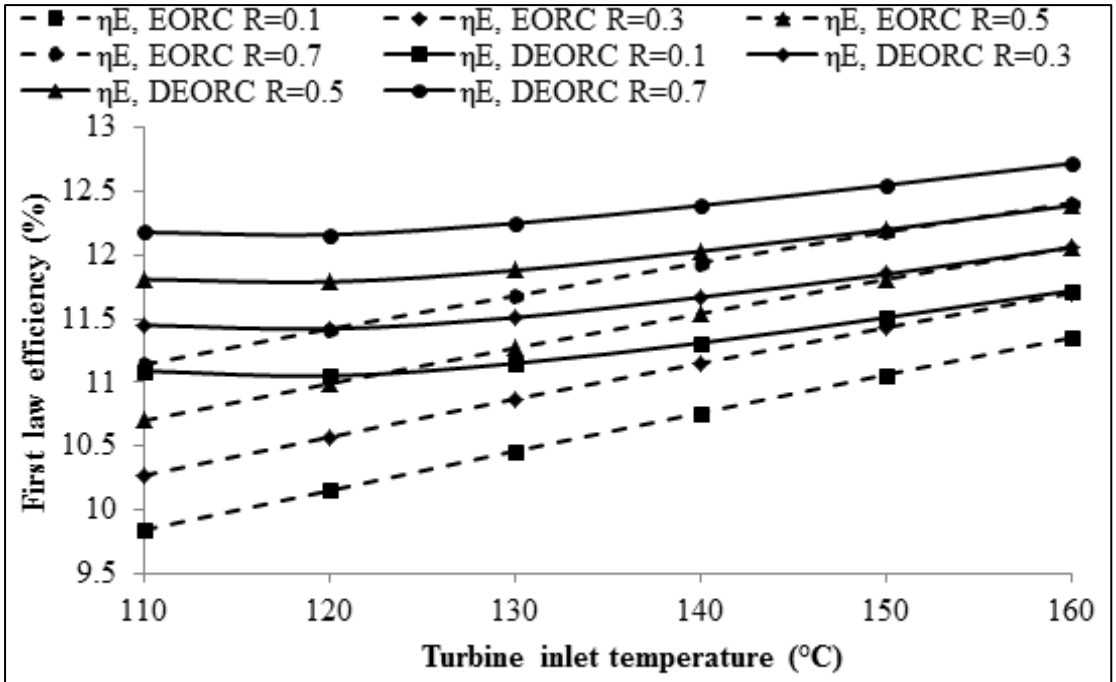

Fig. 5.7. Variation of First law efficiency with turbine inlet temperature at different extration ratio

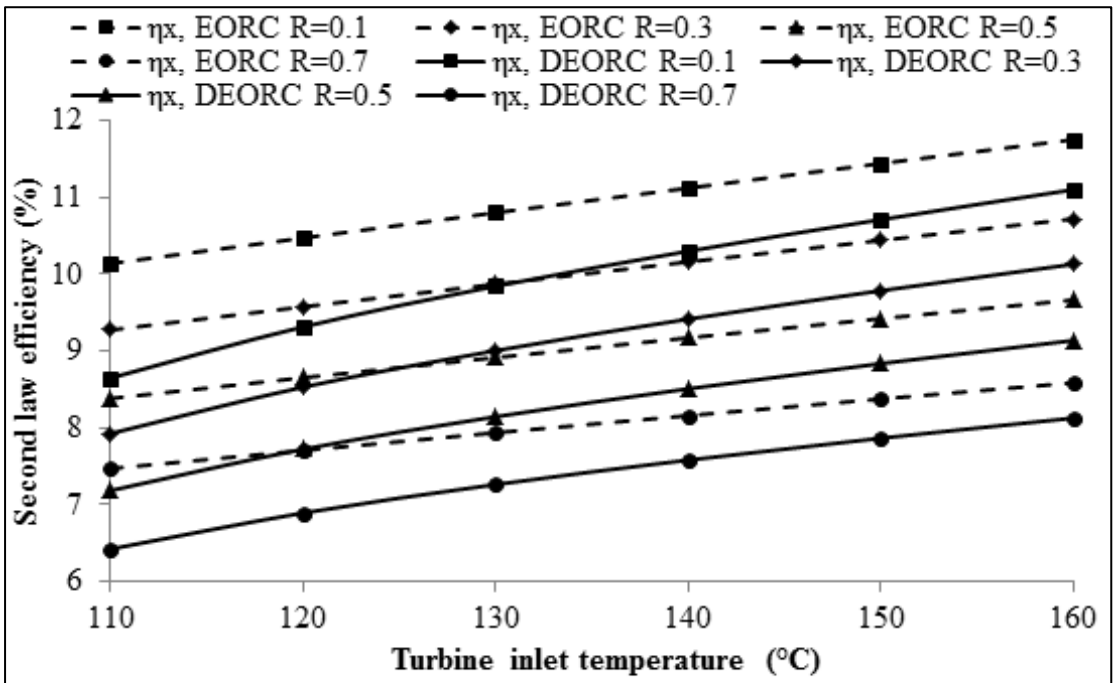

Fig. 5.8 Variation of second law efficiency with turbine inlet temperature at different extration ratio

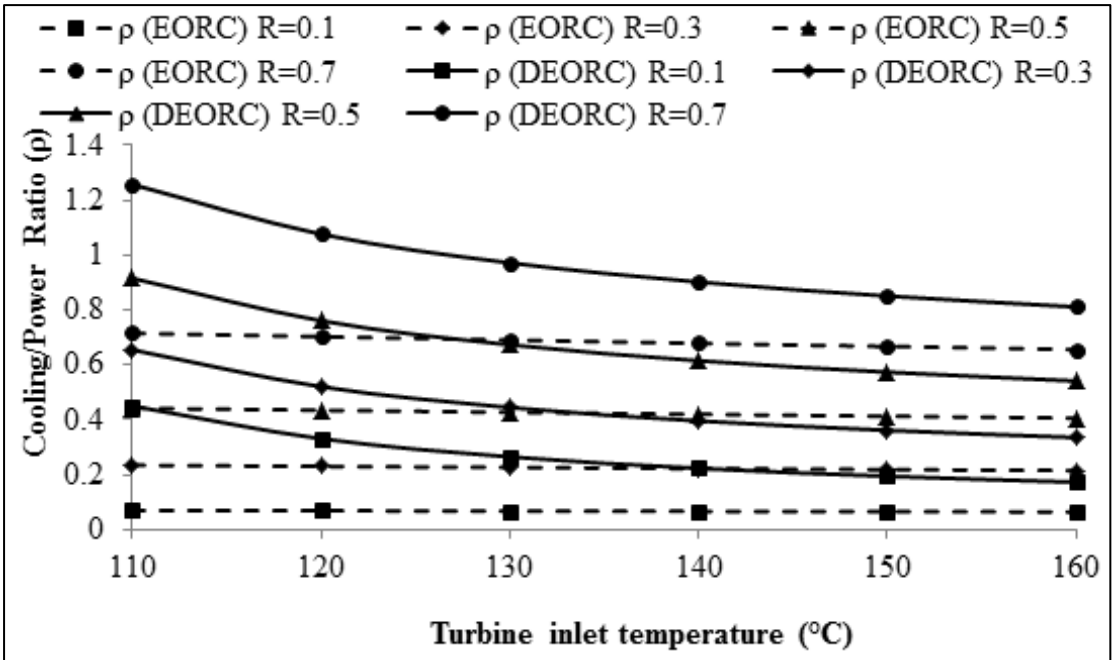

Fig. 5.9 Variation of Cooling/Power ratio with turbine inlet temperature at different extration ratio

Fig. 5.7, 5.8, and 5.9 demonstrates the impact of TIT on 1st law efficiency, 2nd law efficiency and cooling/power ratio at different extraction ratio in EORC and DEORC. With the increase in turbine inlet temperature, the rate of increase of net power output is higher than rate of increase of cooling output, the cooling to power ratio decreases. 1st law and 2nd law efficiencies increases with increase in turbine inlet temperature.

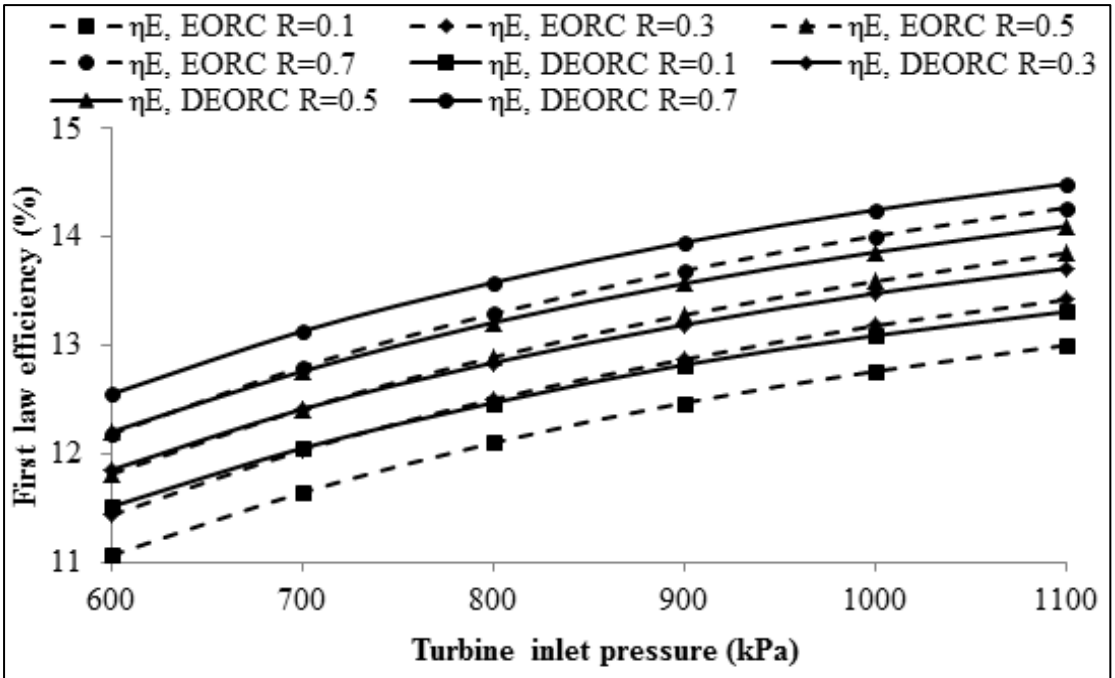

Fig. 5.10. Variation of First law efficiency with turbine inlet pressure at different extration ratio

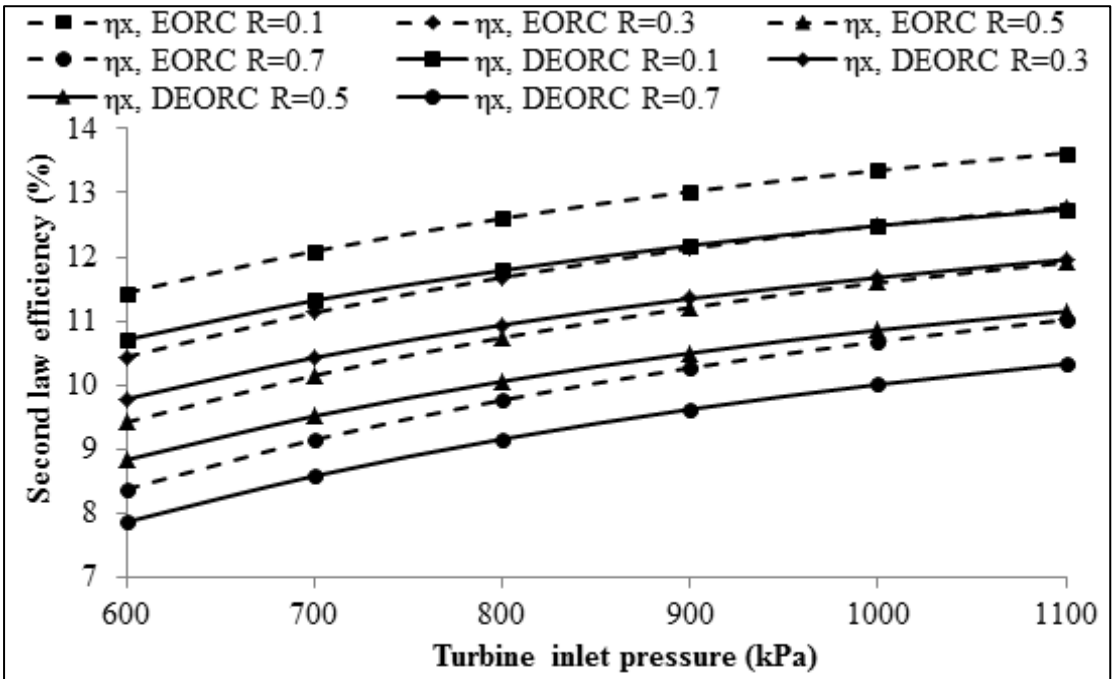

Fig. 5.11. Variation of Second law efficiency with turbine inlet pressure at different extration ratio

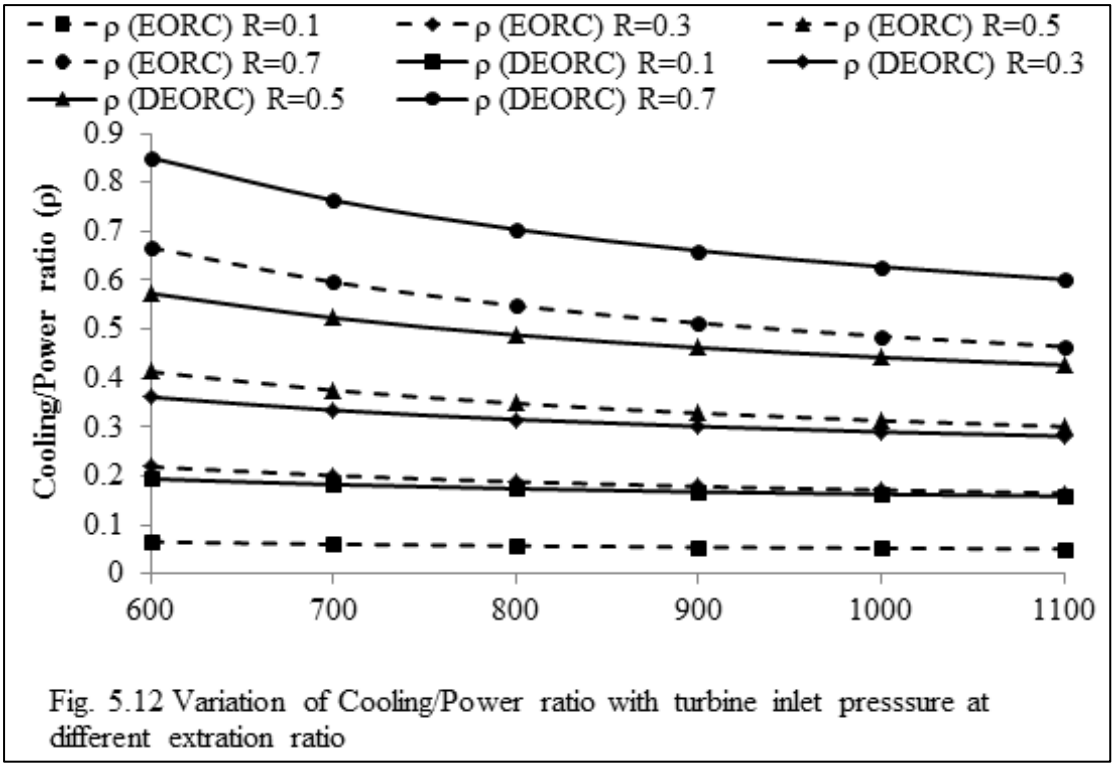

Fig. 5.12 Variation of Cooling/Power ratio with turbine inlet presssure at different extration ratio

Fig. 5.10, 5.11, and 5.12 demonstrates the impact of variation of turbine inlet pressure (TIP) on first law efficiency, second law efficiency and cooling to power ratio at different extraction ratio. As the turbine inlet pressure increases, the net power output increases and cooling output diminishes for EORC and DEORC. The rate of increase in net power output is more prominent than rate of diminishing in cooling output brings about in increase in first law efficiency and decrease in cooling to power ratio for EORC and DEORC with increase in turbine inlet pressure. A similar pattern for exergy efficiency observed with increase in turbine inlet pressure as shown in Figure 10. With the increase in extraction ratio at the same turbine inlet pressure, the net power output decreases and cooling output increases. Since the rate of increase in cooling output is higher than the rate of decrease in net power output. The cooling to power ratio and first law efficiency increases while second law efficiency decreases as the extraction ratio increases. Fig. 5.10, 5.11, and 5.12 indicate that first law efficiency and cooling to power ratio is higher and second law efficiency is lower for DEORC than EORC at the same working conditions.

Table 5.2 shows the energy distribution of the EORC and DEORC. The sum of the energy input at the solar field from the Sun (100%) and at the evaporator E_1 (2.05%) in the form of cooling is equal to 102.05% in EORC. The sum of the energy output is equal to the work output (9.38%) and energy lost to the environment (92.67%) through PTC field and condenser which is equal to the total energy input to the EORC [146]. In DEORC the sum of the energy input at the solar field from the Sun (100%), and at both the evaporators (3.15%) in the form of cooling is equal to 103.15%. The sum of the energy output is equal to the work output (8.71%) and energy lost to the environment (94.44%) through PTC field and condenser which is equal to the total energy input to the DEORC.

Table 5.2: Energy distribution of the EORC and DEORC

	Ejector organic Rankine cycle (EORC)		**Double ejector organic Rankine cycle (DEORC)**	
	Amount (kW)	**% of solar energy input**	**Amount (kW)**	**% of solar energy input**
Solar energy input	**6000**	**100**	**6000**	**100**
Evaporator energy input	123.1	2.05	188.7	3.15
Total energy input to the system	**6123.1**	**102.05**	**6188.7**	**103.15**
Net power output	562.9	9.38	522.53	8.71
Energy lost to the environment from various component of the system	5560.2	92.67	5666.17	94.44
Total energy output from the system	**6123.1**	**102.05**	**6188.7**	**103.15**

Table 5.3 shows the distribution of exergy in EORC and DEORC. The total exergy output in DEORC is 535.26 kW as compared to exergy output of 571.22 kW in EORC.

Table 5.3: The distribution of exergy in EORC and DEORC

	EORC		**DEORC**	
	Amount (kW)	**% of exergy**	**Amount (kW)**	**% of exergy**
Exergy input	5470.00	100.00	5470.00	100.00
Exergy output	571.22	10.44	535.26	9.785
Exergy destruction/ losses				
Generator	218.50	3.99	212.84	3.89
Turbine	81.46	1.49	75.68	1.38
Ejector	87.23	1.59	110.19	2.02
Condenser	60.44	1.10	63.75	1.165
Pump	9.36	0.17	9.19	0.168
Heat exchanger	10.77	0.20	10.00	0.183
Throttle valve	1.65	0.03	2.24	0.041
Evaporator	4.85	0.09	5.92	0.108
Parabolic trough collector	4424.52	80.90	4444.93	81.26
Total Exergy destruction/loss	4898.78	89.56	4934.74	90.215

5.5 Summary:

Thermodynamic analysis of PTC based EORC & DEORC using R141b as working fluid and Therminol VP1 as heat transfer fluid presented. The main conclusions from this analysis can be outlined as follows:

- With the increase in inlet temperature of turbine (110^0C - 160^0C), the 1st and 2nd law efficiency of EORC and DEORC increases while cooling to power ratio decreases.
- With the increase in the inlet pressure of turbine (600 kPa - 1100 kPa), the 1st and 2nd law efficiency of EORC and DEORC increases whereas cooling to power ratio decreases.
- The 1st law efficiency and cooling to power ratio is higher in DEORC as compared to EORC at the same working condition.
- In EORC the maximum energy output (715.53 MWh) and the maximum exergy output (593.8 MWh) obtained in the month of March while minimum energy output (214.74 MWh) and minimum exergy output (176.57 MWh) in the month of January. The annual average energy output of EORC is 4710.57 MWh while annual average exergy output of EORC is 3436.27 MWh.
- In DEORC the highest energy output (749.95 MWh) and exergy output (544.38 MWh) is registered in the month of March while least energy output (244.07 MWh) and exergy output (142.82 MWh) registered in the month of January respectively. The annual average energy output of DEORC is 5104.97 MWh while annual average exergy output of DEORC is 3436.27 MWh respectively.
- With the addition of ejector in EORC the first law efficiency increases from 11.43% to 11.85% while second law efficiency decreases from 10.44% to 9.785% at input thermodynamic parameters as shown in Table 5.1.

CHAPTER 6

CONCLUSION AND RECOMMENDATION FOR FUTURE

6.1 Conclusions

In this thesis the detailed energy and exergy analysis of a solar operated ejector cooling and power cycle, combined power and ejector system employed with a triple pressure level absorption system, and double ejector organic Rankine cycle have been presented. Based on the theoretical studies and investigations, the major outcomes of the present work are summarized below:

- Addition of ejector refrigeration cycle with ORC produces power and cooling simultaneously.
- Integration of a triple pressure level absorption cycle with ejector cooling and power cycle produces cooling at two different temperatures along power simultaneously.
- It can be seen that out of total energy input to the system1 and the system2 around 13.0% is available as useful energy output (work output - 10.6% and ejector refrigeration output - 2.4%) and around 19.1% is available as useful energy output (work output – 8.9%, ejector refrigeration output -- 2% and TPLAS refrigeration output – 8.2%) respectively.
- It is observed that out of total exergy input (100%) to the system1 12.0% is available as useful exergy output (work output – 11.7% and ejector exergetic refrigeration output – 0.3%) and 88.0% of the exergy loss/destruct to the environment and in various components of the system. Out of total exergy input (100%) to the system2, 10.5% is available as useful exergy output (work output – 9.76, ejector exergetic refrigeration output – 0.26% and TPLAS exergetic refrigeration output – 0.48%) and 89.5% of the exergy is lost to the environment.

- Combined double ejector organic Rankine cycle produces power and cooling at two different temperatures simultaneously.
- With the addition of ejector in EORC the first law efficiency increases from 11.43% to 11.85% while second law efficiency decreases from 10.44% to 9.785% due to the addition of more number of components in the system.
- Performance of the system relies on the refrigerant utilized and working conditions.
- At high turbine expansion ratio (τ), the performance of R290 and R152a is better other than that of other refrigerants (R134a, R717).
- At high compression ratio (λ), the performance of R717 and R134a shows good results.
- At high driving pressure ratio (σ), R290 and R134a give better performance.
- Parametric examination demonstrates that turbine inlet pressure, evaporator temperature, condenser temperature, extraction ratio, and solar beam radiation have critical impact on the 1^{st} law (energy) efficiency and 2^{nd} law (exergy) efficiency of the proposed multi-generation thermodynamic cycles.
- This will lead to a well-developed and accepted low temperature energy sources operated multi-generation thermodynamic systems to serve the humanity.
- Results demonstrate that greatest irreversibility happens in the solar collector followed by the HRVG, ejector and condenser.

The methodology used in the present research work will guide researcher, engineers, decision makers, educators and designers in the evaluation of existing real systems and design of future energy systems.

6.2 Recommendation for future

In order to harness the solar thermal potential in efficient and cost effective manner, a thermo-economic analysis which combines the basic principle of economics and second law of thermodynamics is needed to include in the analysis of multi-generation thermodynamic cycles considered in the present research work. Exergy analysis has been systematically applied to estimate the performance of proposed solar operated multi-generation thermodynamic cycles. Presence of thermo-economic analysis of the proposed cycles have a two fold benefits for the researcher and private sectors employers in the way that analysis shows the directions how the solar operated combined power and cooling systems commissioned in an effective and economically viable fashion. Therefore the future scope of the present research work is very much recommended for the cost analysis of all proposed solar operated multi-generation thermodynamic cycles such as ejector cooling and power cycle, combined power and ejector system employed with a triple pressure level absorption system, and double ejector organic Rankine cycle.

REFERENCES

[1] Kalkan, N., Young, E.A. and Celiktas, A., 2012, "Solar Thermal Air Conditioning Technology Reducing the Foot Print of Solar Thermal Air Conditioning," Renewable and Sustainable Energy Reviews, **16**, pp. 6352–6383.

[2] Solar Heat for Industrial Processes; IEA-ETSAP and IRENA 2015.

[3] Assilzadeh, F., Kalogirou, S.A., Ali, Y. and Sopian, K., 2005, "Simulation and Optimization of a Li-Br Solar Absorption Cooling System with Evacuated Tube Collectors," Renewable Energy, **30**, pp. 1143-1159.

[4] Solar Radiation Energy over India. Indian Meteorological Department and Ministry of New and Renewable Energy, 2008, Govt. of India.

[5] Duffie, J.A. and Beckman, W.A., 1980, "Solar Engineering of Thermal Processes," 2nd edition, John Wiley Publication: New York.

[6] Chun, W., Oh, S.J., Lim, S.H. and Chen, K., 2012, "Maximum Efficiency of Solar Energy Conversion," International Journal of Energy Research; **36(8)**, pp. 928-934.

[7] Jeter, S.M., 1981, "Maximum Conversion Efficiency for the Utilization of Direct Solar Radiation," Solar Energy, **36(3)**, pp. 231–236.

[8] Pingzhen, M., Wei, L. and Guoliang, X., 2006, "Analytical and Numerical Investigation of the Solar Chimney Power Plant Systems, International Journal of Energy Resources, **30 (11)**, pp. 861–873.

[9] Flueckiger, S.M., Iverson, B.D., Garimella, S.V. and Pacheco, J.E., 2014, "System-Level Simulation of a Solar Power Tower Plant with Thermo Cline Thermal Energy Storage," Applied Energy, **113**, pp. 86–96.

[10] Abdulateef, J.M., Sopian, K., Alghoul, M.A. and Sulaiman, M.Y., 2009, "Review on Solar-Driven Ejector Refrigeration Technologies," Renewable and Sustainable Energy Reviews, **13**, pp. 1338-1349.

[11] Zheng, H.F., Liang Y.H. and Huang L.Y., 2012, "Analysis of Entrainment Ratio about Solar Ejector Refrigeration System," Energy Procedia, **16**, pp. 516-521.

[12] Horlock, J.H., 1987, "Cogeneration-Combined Heat and Power (CHP) e Thermodynamics and Fluid Mechanics Series," Pergamon, Oxford.

[13] F. Kreith and J.F. Kereider, 1978, “Principles of Solar Engineering,” Mcgraw-Hill, New York.

[14] Kalogirou S.A., 2004, “Solar Thermal Collectors and Applications,” Progress in Energy and Combustion Science, **30**, pp. 231-295.

[15] Xu, C., Wang, Z., Li, X. and Sun, F., 2011, “Energy and Exergy Analysis of Solar Power Tower Plants,” Applied Thermal engineering, 2011, **31**, pp. 3904-3913.

[16] Garcia, A.F., Zarza, E., Valenzuela, L. and Perez, M., 2010, “Parabolic Trough Solar Collectors and Their Applications,” Renewable and Sustainable Energy Reviews, **14(7)**, pp.1695-1721.

[17] Garcia, I.L., Alvarez, J.L. and Blanco D., 2011, “Performance Model for Parabolic Trough Solar Thermal Power Plants with Thermal Storage: Comparison to Operating Plant Data,” Solar Energy, **85**, pp. 2443-2460.

[18] Montes M.J., Rovira A., Munoz M. and Martinez-Val J.M., 2011, “Performance Analysis of an Integrated Solar Combined Cycle Using Direct Steam Generation in Parabolic Trough Collectors,” Applied Energy, **85**, pp. 2443-2460.

[19] Alkhamis, A.L. and Sherif S.A., 1997, “Feasibility Study of a Solar Assisted Heating/Cooling System for an Aquatic Center in Hot and Humid Climates,” International Journal of Energy Resources, **21**, pp. 823-839.

[20] Wu, S.Y., Xiao, L., Cao, Y. and Li, Y.R., 2010, “A Parabolic Dish/AMTEC Solar Thermal Power System and its Performance Evaluation,” Applied Energy, **87**, pp. 452-462.

[21] Goswami, D.Y., 2015, “Principles of Solar Engineering,” Third edition, CRC Press.

[22] Kearney, D.W. and Price, H.W., 1992, “Solar Thermal Plants-LUZ Concepts (current status of the SEGS plants),” Proceedings of the Second Renewable Energy Congress, Reading UK, **2**, pp. 582-588.

[23] Grase, W. Solar PACES Annual Report, DLR Germany, 1995.

[24] Mokheimer, E.M.A., Dabwan, Y.N., Habib, M.A., Said, S.A.M. and Al-Sulaiman, F.A., 2014, “Techno-Economic Performance Analysis of Parabolic Trough Collector in Dhahran, Saudi Arbia,” Energy Conversion and Management, **86**, pp. 622-633.

[25] Barbero, R., Rovira, A., Montes, M.J. and Val, J.M.M., 2016, "A New Approach for the Prediction of Thermal Efficiency in Solar Receivers," Energy Conversion and Management, **123**, pp. 498-511.

[26] Tyagi, S.K., Wang, S., Singhal, M.K., Kaushik, S.C. and Park, S.R., 2007, "Exergy Analysis and Parametric Study of Concentrating Type Solar Collectors," International Journal of Thermal Sciences, **46**, pp. 1304-1310.

[27] Padilla, R.V., Fontalvo, A., Demirkaya, G., Mrtinez, A. and Quiroga, A.G., 2014, "Exergy Analysis of Parabolic Trough Solar Receiver," Applied Thermal Engineering, **67**, pp. 579-586.

[28] Denholm, P. and Hand, M., 2011, "Grid Flexibility and Storage Required to Achieve Very High Penetration of Variable Renewable Electricity," Energy Policy **39(18)**, pp. 17–30.

[29] Denholm, P., Ela, E., Kirby, B. and Milligan M., 2010, "The Role of Energy Storage with Renewable Electricity Generation," NREL/TP-6A2-47187, National Renewable Energy Laboratory.

[30] Sioshansi, R. and Denholm, P., 2010, "The Value of Concentrating Solar Power and Thermal Energy Storage," NREL-TP-6A2-45833, National Renewable Energy Laboratory.

[31] Barlev, D., Vidu, R. and Stroeve, P., 2011, "Innovation in Concentrated Solar Power," Solar Energy Materials and Solar Cells, **95**, pp. 2703–2725.

[32] Burgaleta, J.I., Arias, S. and Ramirez, D., "Gemasolar: the first tower thermosolar commercial plant with molten salt storage," In: Proceedings of Solar PACES 2011, Granada (Spain), 20-23September 2011.

[33] Herrmann, U., Kelly, B. and Price, H., 2004, "Two Tank Molten Salt Storage for Parabolic Trough Solar Power Plants," Energy, **29**, pp. 883-893.

[34] Tzivanidis, C., Bellos, E. and Antonopoulos K.A., 2016, "Energetic and Financial Investigation of a Stand-Alone Solar-Thermal Organic Rankine Cycle Power Plant," Energy Conversion and Management, **126**, pp. 421-433.

[35] Price, H., Lupfert, E. and Kearney D., 2002, "Advances in Parabolic Trough Solar Power Technology," ASME J. Solar Energy Engineering, **124 (2)**, pp. 109-125.

[36] Montes, M.J., Abanades, A. and Martinez-Val, J.M., 2010, "Thermofluidynamic Model and Comparative Analysis Parabolic Trough Collectors Using Oil, Water/Steam or Molten Salt as Heat Transfer Fluids," ASME J. Solar Energy Engineering, **132**, pp. 021001-021007.

[37] Hung, T.C., Shai, T.Y. and Wang, S.K., 1997, "A Review of Organic Rankine Cycles (ORCs) for the Recovery of Low Grade Waste Heat," Applied Energy, **6**, pp. 661-667.

[38] Tchanche, B.F., Lambrinos, G., Frangoudakis, A. and Papadakis G., 2011, "Low Grade Heat Conversion into Power Using Organic Rankine Cycles – A Review of Various Applications," Renewable Sustainable Energy Reviews, **15**, pp. 3963-3979.

[39] Saitoh, T., Yamada, N. and Wakashima, S., 2004, "Solar Rankine Cycle System Using Scroll Expander," Journal of Energy and Engineering, **2**, pp. 708-718.

[40] Kane, M., Larrain, D., Favrat, D. and Allani, Y., 2003, "Small Hybrid Solar Power System," Energy, **28**, pp. 1427-1443.

[41] Yagoub, W., Doherty, P. and Riffat, S.B., 2006, "Solar Energy Gas Driven Micro-CHP System for an Office," Applied Thermal Engineering, **26,** pp. 1604-1610.

[42] Prigmore, D. and Barber, R., 1975, "Cooling with the Suns Heat: Design Considerations and Test Data for a Rankine Cycle Prototype," Solar Energy, **17**, pp. 185-192.

[43] Wei, D., Lu, X., Lu, Z. and Gu, J., 2007, "Performance Analysis and Optimization of Organic Rankine Cycle (ORC) for Waste Heat Recovery," Energy Conversion and Management, **48**, pp. 1113–1119.

[44] Zhang, J.H., Zhang, W.F., Hou, G.L. and Fang, F., 2012, "Dynamic Modeling and Multivariable Control of Organic Rankine Cycles in Waste Heat Utilizing Processes," Computers & Mathematics with Applications, **64(5)**, pp. 908–921.

[45] Roy, J.P., Mishra, M.K. and Misra, A., 2010, "Parametric Optimization and Performance Analysis of a Waste Heat Recovery System Using Organic Rankine Cycle," Energy, **35(12)**, pp. 5049–5062.

[46] Yamamoto, T., Furuhata, T., Arai, N., and Mori, K., 2001, "Design and Testing of the Organic Rankine Cycle," Energy, **26,** pp.239–51.

[47] Madhawa Hettiarachchi, H.D., Golubovic, M., Worek, W.M. and Ikegami Y., 2007, "Optimum Design Criteria for an Organic Rankine Cycle Using Low-Temperature Geothermal Heat Sources," Energy, **32(9)**, pp. 1698–1706.

[48] Nguyen, V.M., Doherty, P.S. and Riffat, S.B., 2001, "Development of a Prototype Low-Temperature Rankine Cycle Electricity Generation System," Applied Thermal Engineering, **21**, pp. 169–181.

[49] Drescher, U. and Bruggemann, D., 2007, "Fluid Selection for the Organic Rankine Cycle (ORC) in Biomass Power and Heat Plants," Applied Thermal Engineering, **27**, pp. 223–228.

[50] Quoilin, S., 2007, "Experimental Study and Modeling of a Low Temperature Rankine Cycle for Small Scale Cogeneration," Thesis, University of Liege.

[51] Hung, T.C., 2001, "Waste Heat Recovery of Organic Rankine Cycle Using Dry Fluids," Energy Conversion and Management, **42**, pp. 539-553.

[52] Tchanche, B.F., Quoilin, S., Declaye, S., Papadakis, G. and Lemort V., "Economic Optimization of Small Scale Organic Rankine Cycles," In: 23rd International conference on efficiency, cost, optimization, simulation and environmental impact of energy systems (ECOS), Lausanne, Switzerland, June 14–17, 2010.

[53] Wali, E., 1980, "Working Fluids for Solar Rankine Cycle Cooling Systems," Energy, **5**, pp. 631–639.

[54] Maizza, V. and Maizza, A., 1996, "Working Fluids in Non-Steady Flows for Waste Energy Recovery Systems," Applied Thermal Energy, **16(7)**, pp. 579–590.

[55] Badr, O., Probert, S.D. and O'Callaghan, P.W., 1985, "Selecting a Working Fuid for a Rankine Cycle Engine," Applied Energy, **21(1)**, pp. 1–42.

[56] Badr, O., O'Callaghan, P.W. and Probert, S.D., 1985, "Thermodynamic and Thermos-Physical Properties of Organic Working fluids for Rankine Cycle Engines," Applied Energy, **19(1)**, pp. 1–40.

[57] Maizza, V. and Maizza, A., 2001, "Unconventional Working fluids in Organic Rankine Cycles for Waste Energy Recovery Systems," Applied Thermal Engineering, **21** pp. 381–390.

[58] Liu, B., Chien, K. and Wang, C., 2004, "Effect of Working fluids on Organic Rankine Cycle for Waste Heat Recovery," Energy, **29**, pp. 1207–1217.

[59] Saleh, B., Koglbauer, G., Wendland, M. and Fischer, J., 2007, "Working Fluids for Low Temperature Organic Rankine Cycle," Energy, **32**, pp. 1210–1221.

[60] Tchanche, B.F., Papadakis, G., Lambrinos, G. and Frangoudakis, A., 2009, "Fluid Selection for a Low Temperature Solar Organic Rankine Cycle," Applied Thermal Engineering, **29**, pp. 2468–76.

[61] Wang, X.D. and Zhao, L., 2009, "Analysis of Zeotropic Mixtures used in Low-Temperature Solar Rankine Cycles for Power Generation," Solar Energy, **83**, pp. 605-613.

[62] Lakew, A.A. and Bolland, O., 2010, "Working Fluids for Low-Temperature Heat Source," Applied Thermal Engineering, **30**, pp. 1262-1268.

[63] Chen, H., Goswami, D.Y. and Stefanakos, E.K., "A Review of Thermodynamic Cycles and Working fluids for the Conversion of Low Grade Heat," Renewable and Sustainable Energy Reviews, **14**, pp. 3059–3067.

[64] Papadopoulos, A.I., Stijepovic, M. and Linke, P., 2010, "On the Systematic Design and Selection of Optimal Working fluids for Organic Rankine Cycles," Applied Thermal Engineering, **30**, pp. 760–769.

[65] Gupta, M.K. and Kaushik, S.C., 2010, "Exergy Analysis and Investigation for Various Feed Water Heaters of Direct Steam Generation Solar-Thermal Power Plant," Renewable Energy, **35**, pp. 1228-1235.

[66] Kaska, O., 2014, "Energy and Exergy Analysis of an Organic Rankine for Power Generation from Waste Heat Recovery in Steel Industry," Energy Conversion and Management, **77**, pp. 108-117.

[67] Jung, H.C., Krumdieck, S. and Vranjes, T., 2014, "Feasibility Assessment of Refinery Waste Heat-To-Power Conversion Using an Organic Rankine Cycle," Energy Conversion and Management, **77** pp. 396-407.

[68] Deethayat, T., Kiatsiriroat, T. and Thawonngamyingsakul, C., 2015, "Performance Analysis of an Organic Rankine Cycle With Internal Heat Exchanger Having Zeotropic Working Fluid," Case Studies in Thermal Engineering, **6** pp. 155–161.

[69] Mohammad, U., Imran, M., Lee, D.H. and Park, B.S., 2015, "Design and Experimental Investigation of a 1 kW Organic Rankine Cycle System Using R245fa as Working Fluid for Low Grade Waste Heat Recovery from Steam," Energy Conversion and Management, **103**, pp. 1089-1100.

[70] Yuandan, W.U., Yadong, Z. and Lijun, Y., 2016, "Thermal and Economic Performance Analysis of Zeotropic Mixture for Organic Rankine Cycles," Applied Thermal Engineering, **96**, pp. 57–63.

[71] Dong, B., Xu, G., Luo, X., Zhuang, L. and Quan, Y., 2017, "Potential of Low Temperature Organic Rankine Cycle with Zeotropic Mixtures as Working Fluids," Energy Procedia, **105** pp. 1489-1494.

[72] Li, L., Ge, Y.T. and Tassou, S.A., 2017, "Experimental Study on a Small-Scale R245fa Organic Rankine Cycle System for Low-Grade Thermal Energy Recovery," Energy Procedia, **105**, pp. 1827-1832.

[73] Wang, H., Li, H., Wang, L. and Bu, X., 2017, "Thermodynamic Analysis of Organic Rankine Cycle with Hydrofluoroethers as Working Fluids." Energy Procedia, **105**, pp. 1889-1894.

[74] Keenan, H., Neumann, E.P. and Lustwerk, F., 1950, "An Investigation of Ejector Design by Analysis and Experiment," ASME Journal of Applied Mechanics, **72**, pp. 299–309.

[75] Huang, B.J., Chang, J.M., Wang, C.P. and Petrenko, V.A., 1999, "A 1-D Analysis of Ejector Performance," International Journal of Refrigeration, **22(5)**, pp. 354–364.

[76] Ouzzane, M. and Aidoun, Z., 2003, "Model Development and Numerical Procedure for Detailed Ejector Analysis and Design," Applied Thermal Engineering, **23**, pp. 2337–2351.

[77] Munday, J.T. and Bagster, D.F., 1977, "A New Ejector Theory Applied to Steam Jet Refrigeration," Industrial Engineering Chemical Process Research and Development, **16(4)**, pp. 442 – 449.

[78] Bowrey, R.G., Dang, V.B. and Sergeant, G.D., 1986, "An Energy Model to Minimize Energy Consumption in a Low–Temperature Operation, Steam Ejector – Cooling System," Journal of the Institution of Energy Sources, **45**, pp. 45- 48.

[79] Bevilacqua, P., 1991, "Mechanical Refrigeration Using an Ejector–Injector to Transfer the Working Fluid from the Evaporator to the Condenser," International Journal of Refrigeration, **14**, pp. 137-139.

[80] Sun, Da-Wen, 1996, "Variable Geometry Ejectors and Their Applications in Ejector Refrigeration Systems," Energy, **21(10)**, pp. 919-929.

[81] Sun, Da-Wen, 1997, "Experimental investigation of the performance characteristics of a steam jet refrigeration system," Energy Sources, **19(4)**, pp. 349-367.

[82] Sun, Da-Wen, 1997, "Solar Powered Combined Ejector-Vapour Compression Cycle for Air Conditioning and Refrigeration," Energy Conversion and Management, **38(5)**, pp. 479-491.

[83] Sun, Da-Wen, 1999, "Comparative Study of the Performance of an Ejector Refrigeration Cycle Operating with Various Refrigerants," Energy Conversion and Management, **40**, pp. 873-884.

[84] Cizungu, K., Mani, A. and Groll, M., 2001, "Performance Comparison of Vapour Jet Refrigeration System with Environment Friendly Working Fluids," Applied Thermal Engineering, **21**, pp. 585-598.

[85] Selvaraju, A. and Mani, A., 2004, "Analysis of a Vapour Ejector Refrigeration System with Environment Friendly Refrigerants," International Journal of Thermal Sciences, **43**, pp. 915-921.

[86] Dahmani, A., Aidoun, Z. and Galanis, N., 2011, "Optimum Design of Ejector Refrigeration Systems with Environmentally Benign Fluids" International Journal of Thermal Sciences, **50**, pp. 1562-1572.

[87] Yapici, R., 2007, "Experimental Investigation of Performance of Vapor Ejector Refrigeration System Using Refrigerant R123," Energy Conversion and Management, **49**, pp. 953– 961.

[88] Li, D. and Groll, E.A., 2005, "Transcritical CO2 Refrigeration Cycle with Ejector-Expansion Device," International Journal of Refrigeration, **28**, pp. 766–773.

[89] Yapici, R. and Yetisen, 2007, "Experimental Study on Ejector Refrigeration System Powered by Low Grade Heat," Energy Conversion and Management, **48**, pp. 1560–1568.

[90] Pianthong, K., Seehanam, W., Behnia, M., Sriveerakul, T. and Aphornratana, S., 2007, "Investigation and Improvement of Ejector Refrigeration System Using Computational Fluid Dynamics Technique," Energy Conversion and Management, **48**, pp. 2556–2564.

[91] Sankarlal, T., Mani, A., 2007, "Experimental Investigation on Ejector Refrigeration System with Ammonia," Renewable Energy, **32**, pp. 1403–1413.

[92] Pridasawas, W. and Lundqvist, P., 2004, "An Exergy Analysis of a Solar-Driven Ejector Refrigeration System," Solar Energy, **76**, pp. 369-379.

[93] Chen, X., Omer, S., Worall, M. and Riffat, S., 2013, "Recent Developments in Ejector Refrigeration Technologies," Renewable Sustainable Energy Reviews, **19**, pp. 629–651.

[94] Besagni, G., Mereu, R. and Inzoli, F., 2016, "Ejector Refrigeration: A Comprehensive Review," Renewable Sustainable Energy Reviews, **53**, pp. 373–407.

[95] Elbel, S. and Lawrence, N., 2016, "Review of Recent Developments in Advanced Ejector Technology," International Journal of Refrigeration," **62** pp. 1–18.

[96] Ibarra-Bahena, J. and Romero, R.J., 2014, "Performance of Different Experimental Absorber Designs in Absorption Heat Pump Cycle Technologies: A Review," Energies, **7**, pp. 751–766.

[97] Gomri, R., and Hakimi, R., 2008, "Second Law Analysis of Double Effect Vapour Absorption Cooler System," Energy Conversion and Management, **49**, pp. 3343–3348.

[98] Shwartz, I., and Shitzer, A., 1997, Solar Absorption System for Space Cooling and Heating," ASHARE Journal, **19(11)**, pp. 51-54.

[99] Sun, D.W., 1997, "Computer Simulation and Optimization of Ammonia-Water Absorption Refrigeration System," Energy Sources, **19(7)**, pp.677-690.

[100] Sun, D.W., 1997, "Thermodynamics Design Data an Optimum Design Maps for Absorption Refrigeration System," Applied Thermal Engineering, **17(3)**, pp. 211-221.

[101] Sun, D.W., 1998, "Comparison of the Performance of NH3-H2O, NH3-LiNO3 and NH3-NaSCN Absorption Refrigeration Systems," Energy Conversion and Management, **39**, pp. 357–368.

[102] Atmaca, I. and Yigit, A., 2003, "Simulation of Solar Powered Absorption Cooling System," Renewable Energy, **28**, pp. 1277-1293.

[103] Khaliq, A. and Kumar, R., 2007, "Exergetic Analysis of Solar Powered Absorption Refrigeration System Using LiBr-H2O and NH3-H2O as Working Fluids," International Journal of Exergy, **4(1)**, pp. 1-18.

[104] Gong, S. and Goni Boulama, K., 2015, "Advanced Exergy Analysis of an Absorption Cooling Machine: Effects of the Difference between the Condensation and Absorption Temperatures," International Journal of Refrigeration, **59**, pp. 224-234.

[105] Manu, S., Prasad T.B., Chandrashekar, T.K. and Nagendra, 2012, "Theoretical Model of Absorber for Miniature LiBr-H2O Vapor Absorption Refrigeration System," International Journal of Modern Engineering Research, **2(2)**, pp. 010–017.

[106] Giannetti, N., Rocchetti, A., Lubis, A., Saito, K. and Yamaguchi, S., 2016, "Entropy Parameters for Falling Film Absorber Optimization," Applied Thermal Engineering, **93**, pp. 750-762.

[107] Yildiz, A. and Ali Ersoz, Mustafa., 2013, "Energy and Exergy Analyses of the Diffusion Absorption Refrigeration System," Energy, **60**, pp. 407–415.

[108] Zhang, L., Wang, Y., Fu, Y., Xing, L. and Jin, L., 2015, "Numerical Simulation of H2O/LiBr Falling Film Absorption Process," Energy Procedia, **75**, pp. 3119–3126.

[109] Modi, B., Mudgal, A. and Patel, B., 2017, "Energy and Exergy Investigation of Small Capacity Single Effect Lithium Bromide Absorption Refrigeration System," Energy Procedia, **109**, pp. 203-210.

[110] Xu, F., Goswami, D. Y., and Bhagwat, S.S., 2000, "A Combined Power Cooling Cycle," Energy, **25**, pp. 233-246.

[111] Padilla, R.V., Demirkaya, G., Goswami, D.Y., Stefanakos, E. and Rahman, M.M., 2010. "Analysis of Power and Cooling Cogeneration Using Ammonia–Water Mixture," Energy, **35(12)**, pp. 4649-4657.

[112] Hasan, A.A., Goswami, D.Y. and Vijayraghvan S., 2002, "First and Second Law Analysis of a New Power and Refrigeration Thermodynamic Cycle using a Solar Heat Source," Solar Energy, **73 (5)**, pp. 385-393.

[113] Tamm, G., Goswami, D.Y., Lu, S., and Hassan, A.A., 2004, "Theoretical and Experimental Investigation of an Ammonia–Water Power and Refrigeration Thermodynamic Cycle," Solar Energy, **76**, pp. 217-228.

[114] Vidal, A., Best, R., Rivero, R., and Cervantes, J., 2006, "Analysis of a Combined Power and Refrigeration Cycle by the Exergy Method," Energy, **31 (15)**, pp. 3401-3414.

[115] Zhang, N., Cai, R. and Lior, N., 2004, "A Novel Ammonia–Water Cycle for Power and Refrigeration Cogeneration," In: Proceedings of the ASME advanced energy systems division, pp. 183-196.

[116] Liu, M. and Zhang, N., 2007, "Proposal and Analysis of a Novel Ammonia–Water Cycle for Power and Refrigeration Cogeneration," Energy, **32(6)**, pp. 961-970.

[117] Zheng, D., Chen, B., Qi, Y. and Jin, H., 2006, "Thermodynamic Analysis of a Novel Absorption Power/Cooling Combined-Cycle," Applied Energy, **83**, pp. 311–323.

[118] Zhang, N. and Lior, N., 2007, "Development of a Novel Combined Absorption Cycle for Power Generation and Refrigeration," ASME Journal of Energy Resources Technology, **129**, pp. 254-265.

[119] Zhang, N. and Lior, N., 2007, "Methodology for Thermal Design of Novel Combined Refrigeration/ Power Binary Fluid Systems," International Journal of Refrigeration, **30**, pp. 1072-1085.

[120] Wang, J.F., Dai, Y.P. and Gao, L., 2008, "Parametric Analysis and Optimization for a Combined Power and Refrigeration Cycle," Applied Energy, **85** pp. 1071-1085.

[121] Wang, J., Zhao, P. and Dai, Y., 2016, "Thermodynamic Analysis of a New Combined Cooling and Power System Using Ammonia–Water mixture," Energy Conversion and Management, **117**, pp. 335-342.

[122] Alexis, G.K., 2007, "Performance Parameters for the Design of a Combined Refrigeration and Electrical Power Cogeneration System," International Journal of Refrigeration, **30**, pp. 1097–1103.

[123] Zheng, B. and Weng, Y.W., 2010, "A Combined Power and Ejector Refrigeration Cycle for Low Temperature Heat Sources," Solar Energy, **12 (5)**, pp. 784-791.

[124] Rashidi, M.M., Beg, O.A. and Aghagoli, A., 2012, "Utilization of Waste Heat in Combined Power and Ejector Refrigeration for a Solar Energy Source," International Journal of Appl. Math and Mech., **8(17)**, pp.1-16.

[125] Habibzadeh, A., Rashidi M. M., and Galanis, N., 2013, "Analysis of a Combined Power and Ejector-Refrigeration Cycle using Low Temperature Heat," Energy Conversion and Management, **65**, pp. 381-391.

[126] Chen, X., Su,Y., Omer, S. and Riffat, S., 2015, "Theoretical Investigations on Combined Power and Ejector Cooling System Powered by Low-Grade Energy Source," International Journal of Low-Carbon Technologies Advance Access, pp. 01-10.

[127] Wang, J., Dai, Y. and Sun, Z., 2009, "A Theoretical Study on a Novel Combined Power and Ejector Refrigeration Cycle," International Journal of Refrigeration, **32**, pp. 1186-1194.

[128] Dai, Y., Wang, J. and Gao, L., 2009, "Exergy Analysis, Parametric Analysis and Optimization for a Novel Combined Power and Ejector Refrigeration Cycle," Applied Thermal Engineering, **29**, pp. 1983-1990.

[129] Agrawal, B.K. and Karimi, M.N., 2013, "Parametric, Exergy and Energy Analysis of Low Grade Energy and Ejector Refrigeration Cycle," International Journal of Sustainable Building Technology and Urban Development, **4(2)**, pp. 170-176.

[130] Khaliq A., 2017, "Energetic and Exergetic Performance Investigation of a Solar Based Integrated System for Cogeneration of Power and Cooling," Applied thermal Engineering, **112**, PP. 1305-1316.

[131] Wang, J., Chen, G. and Jiang, H., 1998, "Study on a Solar Driven Ejector-Absorption Cycle," International Journal of Energy Research, **22**, pp. 733-739.

[132] Goktum, S., 1999, "Optimal Performance of a Combined Absorption and Ejector Refrigerator," Energy Conversion and Management, **40**, pp. 51-58.

[133] Eames, I.W. and Wu, S., 2000, "A Theoretical Study of an Innovative Ejector Powered Absorption-Recompression Cycle Refrigerator," International Journal of Refrigeration, **23**, pp. 475-484.

[134] Luvy, A., Jelinek, M. and Borde, I., 2002, "Numerical Study on the Design Parameters of a Jet Ejector for Absorption System," Applied Energy, **72**, pp. 467-478.

[135] Sozen, A. and Ozalp, M., 2003, "Performance Improvement of Absorption Refrigeration System Using Triple Pressure," Applied thermal Engineering, **23**, pp. 1577-1593.

[136] Sozen, A., Ozalp, M. and Arcaklioglu, E., 2004, "Prospectus for Utilization of Solar Driven Ejector-Absorption Cooling System in Turkey," Applied thermal Engineering, **24**, pp. 1019-1035.

[137] Alexis, G.K., 2014, "Thermodynamic Analysis of Ejector-Absorption Refrigeration Cycle Using Second Thermodynamic Law," International Journal of Exergy, **14(2)**, pp. 179-190.

[138] Hong, D., Chen, G., Tang, L. and He Y., 2011, "A Novel Ejector-Absorption Combined Refrigeration Cycle," International Journal of refrigeration, **34**, pp. 1596-1603.

[139] Verda, C., Ventas, R., Lecuona, A. and Lopez, R., 2014, "Single Effect Refrigeration Cycle Boosted with an Ejector-Adiabatic Absorber Using a Single Solution Pump," International Journal of refrigeration, **38**, pp. 22-29.

[140] NIST Standard Reference Database 23, 1998, NIST Thermodynamic and Transport Properties of Refrigerants and Refrigerants Mixtures REFPROP, Version 6.01.

[141] Xu, C., Wang, Z., Li, X., and Sun, F., 2011, "Energy and Exergy Analysis of Solar Power Tower Plants" Applied Thermal Engineering, **31,** pp. 3904-3913.

[142] Yao, Z.H., Wang, Z.F., Lu, Z.W., and Wei, X.D., 2009, "Modeling and Simulation of the Pioneer 1MW Solar Thermal Central Receiver System in China," Renewable Energy, **34**, pp. 2437-2446.

[143] Li, X., Kong, W.Q., Wang, Z.F., Chang, C. and Bai F.W., 2010, "Thermal Model and Thermodynamic Performance of Molten Salt Cavity Receiver," Renewable Energy, **35**, pp. 981-988.

[144] Petela, R., 2003, "Exergy of Undiluted Thermal Radiation," Solar Energy, **74(6)**, pp. 469-488.

[145] Bejan, A., 2002, "Fundamentals of Exergy Analysis, Entropy Generation Minimization and the Generation of Flow Architecture," International Journal of Energy Research, **26**, pp. 545-565.

[146] Aphornratana, S. and Eames, I. W., 1995, "Thermodynamic analysis of absorption refrigeration cycles using the second law of thermodynamics method," International Journal of Refrigeration, **18(4)**, pp. 244-252.

[147] Khaliq A., Agrawal, B.K. and Kumar, R., 2012, "First and second law investigation of waste heat based combined power and ejector-absorption refrigeration cycle," International Journal of Refrigeration, **35(1)**, pp. 88-97.

[148]

PUBLICATIONS

[1] D.K. Gupta, R. Kumar, N. Kumar, "First and Second Law Analysis of Solar Operated Combined Rankine and Ejector Refrigeration Cycle", **International Journal of Applied Solar Energy**, Vol. 50 (2), 2014, pp. 113-121.

[2] D.K. Gupta, R. Kumar, N. Kumar, "Thermodynamic Evaluation of PTC based Organic Rankine Cycle for Power & Cooling", **European Journal of Engineering Research and Science**, Vol. 2, No. 1, January 2017.

[3] D.K. Gupta, R. Kumar, "Thermodynamic Analysis of PTC Field Based Power and Ejector Refrigeration System", AES-ATEMA 29th Int. Conference (Toronto, CANADA: July 04 - 08, 2016) pp. 163 - 168.

[4] D.K. Gupta, R. Kumar, "Exergetic Analysis of Combined Power and Ejector Refrigeration Cycle using Solar Energy as Heat Source", Global Sci-Tech, Vol. 7 (4), 2015, pp. 181-185.

[5] D.K. Gupta, R. Kumar, "Thermodynamics Analysis of a Solar Operated Combined Power and Ejector Cooling Cycle with Environmentally Benign Fluids", Journal of Basic and Applied Engineering Research, Vol. 2 (12), 2015, pp. 1009-1012.